The Hong Kong Polytechnic University

Department of Mechanical Engineering

Heat Transfer Characteristics of Impinging Premixed Flame Jet with Induced Swirl

By

HUANG Xiao-qun

A thesis submitted in partial fulfillment of the requirements for the degree of

MASTER OF PHILOSOPHY

in

MECHANICAL ENGINEERING

March 2006

CERTIFICATE OF ORIGINALITY

I hereby declare that this thesis is my own work and that, to the best of my knowledge and belief, it reproduces no material previously published or written, nor material which has been accepted for the award of any other degree or diploma, except where due acknowledgement has been made in the text.

__________________________ (Signed)

____HUANG Xiao Qun_____ (Name of student)

ABSTRACT

The premixed gas-fired impinging flame jets are widely used for domestic and industrial applications because of their advantages in offering high heat transfer rate, rapid combustion process and lower emission of air pollutants. In addition, they are of simple construction, convenient and safe to use, and very suitable for low Reynolds number and low pressure applications.

The heat transfer characteristics of impinging flame jets have been investigated by many researchers. There have been several methods applied successfully to enhance their flammable limits for the production of stable and reliable flame, and hence enhance their heat transfer performance. For example, swirl has been successfully adopted in industrial combustors utilizing turbulent diffusion flame jets to extend the flammable limits as well as to improve the combustion efficiency, to enhance the heating performance and to reduce the pollution emissions. The use of swirl appears to be a rather promising method, but the application of swirl to the small-scale domestic and industrial appliances utilizing premixed gas-fired impinging flame jets at low Reynolds numbers has not yet been investigated.

The present study had been conducted to fill this gap by studying the heat transfer from a small-scale premixed butane/air circular impinging flame jet with induced

swirl to a horizontally placed copper impingement plate. It was essentially an experimental study, and the major parameters affecting the impingement heat transfer including: Reynolds number of the air/fuel jet, Swirl number of the air/fuel jet, nozzle-to-plate distance and equivalence ratio of the air/fuel mixture, had been fully investigated. Butane gas was used as the gaseous fuel for the present investigation, as it is one of the major gaseous fuels used in Hong Kong.

The first part of the present study was to confirm the feasibility of introducing swirl to a gas-fired premixed circular flame jet operating at low Reynolds numbers and low pressure. After reviewing the relevant literature, there were several approaches considered. The ability of each of these approaches to produce the swirling flame was examined. It was decided that the swirl is better induced by mixing and balancing the axial and tangential flows of working fluids into the conical chamber of the burner, where the tangential flow is admitted into the burner through two symmetrical tangential inlets. It had been confirmed from this part of study that it is feasible to apply the laminar premixed gas-fired swirling impinging flame jets under quite a wide range of operation conditions.

The second part of the present study was to investigate the thermal characteristics of the swirling impinging flame jets. Two experimental setups, namely I and II, had been used to produce the swirling flame jets, in which different methods were applied to mix and distribute the air and fuel streams into the burner. For the entire heat transfer characteristics study, the local heat flux distributions on the impingement plate under different operating conditions were measured and compared. The total heat flux on the impingement surface was obtained by integrating the local heat flux along the whole impingement area, from which the area-averaged-heat-flux was then determined.

In the experimental setup I, the air and fuel streams were admitted into the burner via the tangential and axial inlets, respectively. Thus, ratio between the tangential flow and axial flow which determines the Swirl number is directly linked to the equivalence ratio (i.e. air/fuel ratio). This approach enables a rather high swirl intensity to be obtained, but effects of the Swirl number and equivalence ratio on the heat transfer performance of the swirling impinging flame can not be separately identified. The method used to calculate the Swirl number is referred as the "Geometric Swirl Number Calculation Method", where the Swirl number is calculated directly from the tangential and axial flow rates.

In the experimental setup II, the air and fuel were premixed and the air/fuel mixture was divided into two separate streams, which were then supplied to the burner via the axial and tangential inlets. Each of these two streams can be adjusted and measured by a flow meter. In this approach, the Swirl number can be determined with the aid of the photographs obtained by applying the "Smoke Flow Visualization Technique". This approach enables the production of a very stable swirling impinging flame having rather good thermal performance. In addition, effects of Swirl number and equivalence ratio can be individually identified, but a rather low swirl intensity can only be generated with this approach.

Experimental results obtained from both experimental setups I and II were discussed and compared with each other, as well as with the findings obtained from the previous work on non-swirling flame jets.

In the final part of the present study, semi-analytical non-dimensional equations had been developed with the aid of the present experimental results and the multiple regression method in Matlab 7.0. These equations provide quick but accurate predictions of the convective heat transfer coefficient, both local and area-averaged, between the swirling impinging flame jet and the impingement plate. The predictions obtained from these equations had been compared with the findings obtained from similar impinging flame jets without swirl induced, which were reported in literature.

LIST OF PUBLICATIONS

1. **X.Q. Huang**, C.W. Leung and C.K. Chan, "Heat transfer of premixed butane/air impinging circular flame jet with induced swirl", The 7^{th} Asia-Pacific International Symposium on Combustion and Energy Utilization, Paper number: B3 – 315, December 2004, Hong Kong.

2. **X.Q. Huang**, C.W. Leung and C.K. Chan, "Heat transfer of premixed butane/air impinging circular flame jet with induced swirl", HKIE Transactions, Vol. 12, No. 3, pp. 21 – 24, 2005.

3. **X.Q. Huang**, C.W. Leung and C.K. Chan, "Effect of swirl intensity on the heat performance of a premixed circular impinging flame jet with swirl induced", Proceedings of ASME Summer Heat Transfer Conference, Paper number: HT2005 – 72750, San Francisco, USA, 2005.

4. **X.Q. Huang**, C.W. Leung, C.K. Chan and S.D. Probert, "Thermal characteristics of a premixed impinging laminar flame jet with induced swirl", Applied Energy, Vol. 83, Issue 4, pp. 299 – 412, 2006.

5. **X.Q. Huang**, C.W. Leung and C.K. Chan, “Heat transfer characteristics of a premixed butane/air impinging flame jet with swirl induced”, Int. J. Heat Mass Transfer, Under Review, June 2005.

ACKNOLEDGEMENTS

My sincere thanks should firstly go to my supervisors, Professor C.W. Leung and Dr. C.K. Chan. Thanks for choosing me two years ago, thanks for your kind help through these two years, thanks for your patience and tolerance when it seemed hard for me to move on. The thesis work with your continuous guidance and support has deepened and broadened my view towards research on combustion and heat transfer. I will definitely benefit a lot from such training in my career.

Special thanks should also be given to the technicians in the Department of Mechanical Engineering. The experiments wouldn't have been completed successfully without your professional work. My great appreciation for Dr. Tse: thank you for your patience and wonderful ideas in the laboratory work. I learned so much from your talent.

Finally, my beloved family and friends, you are so great gifts from God. I couldn't even have gone this far without all of you here.

Thanks for those mornings and nights, thanks for the red balloon shining down, thanks for smiles in people's eyes, thanks for hope on children's face… Thanks, days in Hong Kong. Thank you and goodbye!

TABLE OF CONTENTS

Content **Page**

LIST OF FIGURES

NOMENCLATURE

SYMBOL	DEFINITION (UNIT)
A	Throat area (mm^2)
A_t	Flow area of the air tube to induce tangential air-flow (mm^2)
C_p	Specific heat of fluid (J/kgK)
d	Diameter of nozzle exit (mm)
h	Local heat transfer coefficient (kW/m^2K)
h_f	Enthalpy of the flame (J/kg)
h_w	Enthalpy of the gas on the wall (J/kg)
H	Nozzle-to-plate distance (mm)
k	Thermal conductivity (kW/mK)
Le	Lewis number
$\dot{m}$	Fluid mass flow rate (kg/s)
M	Molecular weight (kg/mol)
Nu	Nusselt number
Pr	Prandtl number
$\dot{q}$	Local heat flux (kW/m^2)
$\dot{Q}$	Total heat flux (kW)
r	Radial distance from stagnation point (mm)

r_o	Radius of axial tube through which the tangential air is introduced (mm)
R	Throat diameter (mm)
Re	Reynolds number
S	Swirl number
T	Temperature (K)
u	Velocity of mixture (m/s)
U	Axial velocity component at the nozzle exit (m/s)
W	Tangential velocity component at the nozzle exit (m/s)
Y	Mole fraction of components
β	Volumetric expansion coefficient [23]
Φ	Equivalence ratio
μ	Dynamic viscosity (kg/ms)
θ	Inclined angle of the smoke flow at the nozzle exit (^{o})
ρ	Gas density (kg/m^2)

SUPERSCRIPTS	**DEFINITION**
−	Area-averaged value
~	Weighed mean value

SUBSCRIPTS	**DEFINITION**
f	Flame
i	Composition items
max	Local maximum
mix	Air/fuel mixture
p	Impingement plate
stoic	At the stoichiometric condition
t	Tangential component
w	Wall
θ	Axial component

CHAPTER 1
INTRODUCTION

1.1 BACKGROUND

Gas-fired impinging flame jet is an effective means of localized heating, which has been widely used for both industrial and domestic purposes because of the rapid heat transfer rate and the convenience to apply. For industrial applications, it is used to melt scrap metals, shape glasses, heat-treat metal bars, and etc. Gaseous fuel burners are also playing a more and more important role in domestic cooking and heating appliances. Thus, it is necessary to perform a thorough investigation into the heat transfer of the impinging flame, which includes the flame structure, the heat transfer mechanisms and characteristics.

There are two basic idealized types of flame jets: premixed and non-premixed (diffusion), which are schematically illustrated in Figure 1.1. For premixed flames, fuel is previously mixed with the oxidizer (usually air) before combustion at the burner exit. For non-premixed flames, the oxidizer (again, usually air) diffuses into the fuel stream to sustain a continuous combustion.

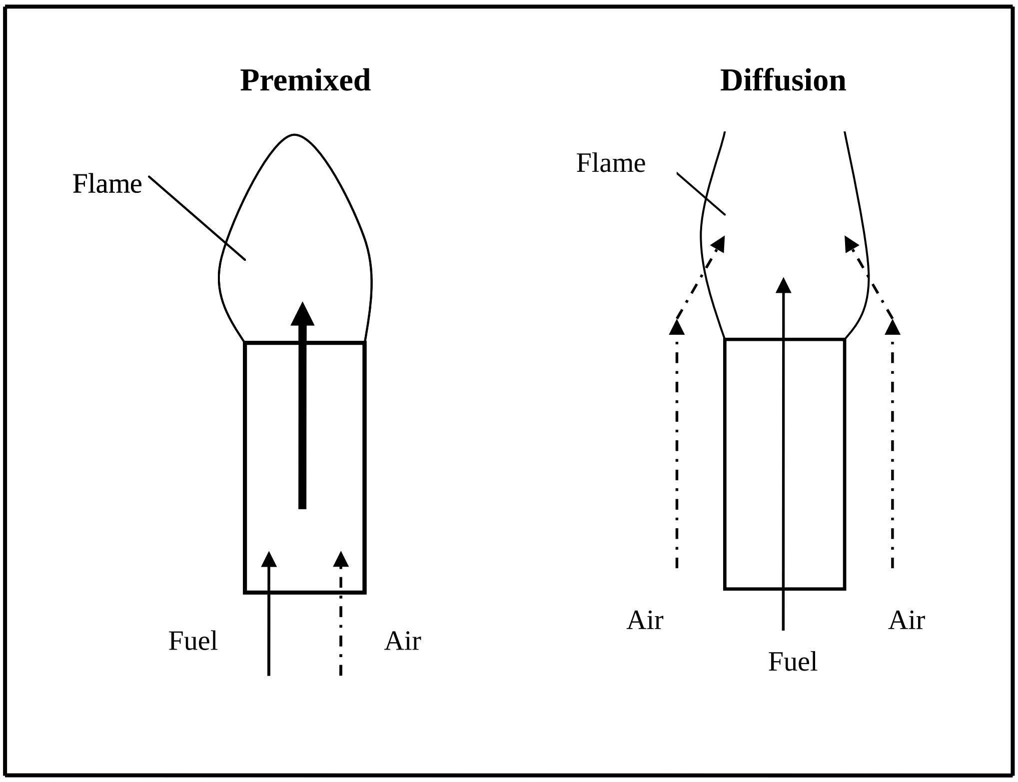

Figure 1.1 Schematics of the two operation modes of flame jet

The present study is concentrated on premixed flame jets since they are commonly adopted for small-scale gas-fired domestic, commercial and light-industrial applications. However, even though they are used in almost every household in modern cities, information is not yet available to facilitate their best utilization. It is significant to improve the burner's heating performance so as to reduce the energy consumption, which is supposed to depend on several important parameters such as geometry and configuration of the burner system including the nozzle-to-plate distance, and the flow conditions including Reynolds number, the chemical properties of the fuel, the arrangement of the mixing including equivalence ratio.

Research efforts on the enhancement of the heating efficiency as well as stability of the premixed impinging flame jets have been ever increased. The main principle of combustion stabilization is to create a region where the local velocity is equal to the flame propagation velocity. This can be achieved either by using a stabilizer in the form of a bluff body or by inducing swirl.

Swirl has been applied to non-reacting tube flows for many years as an effective way to enhance the heat transfer rate between the decaying internal flow and its adjacent tube wall [1 and 2]. When applying to laminar impinging jets, it is an effective way to enhance the thermal performance of the impinging flow, because swirl encourages recirculation, thereby decreases the transport coefficient [3]. It has also been proven to be able to enhance the air/fuel mixing, stabilize the flame and hence extend the flammable limits, consequently, the combustion efficiency is increased and the pollutant emissions reduced [4, 5 and 6]. Currently, most of the applications of swirling-flow concerning with large-scale industrial burners, such as aircraft gas turbines are usually operating in diffusion mode. However, studies on the introduction of swirl to the gas-fired domestic burners have rarely been reported. Neither its feasibility has been ascertained nor its thermal characteristics explored.

The schematics of both non-swirling and swirling impinging jets are shown in Figure 1.2 [7].

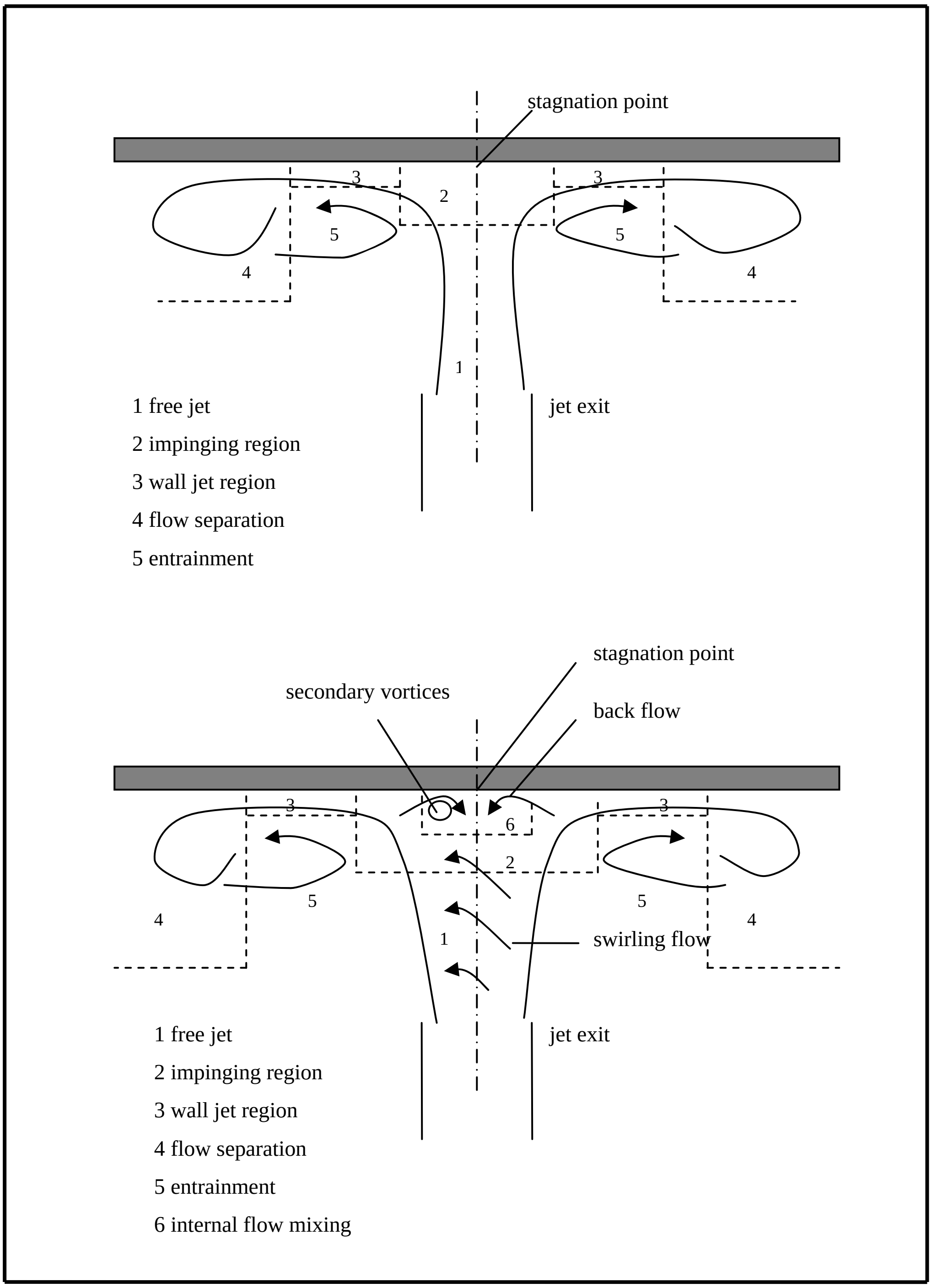

Figure 1.2 Developed flows for non-swirling and swirling impinging jets

Heat transfer from a premixed flame jet to the impingement surface is a complicated problem still under investigation. The thermal and flow characteristics become even more complex when swirl is to be introduced. Many parameters have been proven to have significant influence on the thermal performance in previous research on non-swirling impinging flame jets. These parameters include equivalence ratio and Reynolds number of the air/fuel mixture as well as their mixing condition [8 – 12, 13 and 14]. Considering the research on swirling jets, the method of inducing swirl, the strength of the swirl and the burner configurations also have strong effects on the combustion and heat transfer of the swirling flame in addition to the parameters as mentioned previously [7, 15, 16].

In order to achieve an optimal burner design, utilizing a small-scale gas-fired premixed impinging flame jet with induced swirl, for better heating performance and energy saving, effort is necessary on the full investigation of such impinging flame jet system operating at low pressure and low Reynolds numbers.

1.2 RESEARCH OBJECTIVES

The present study mainly focuses on experimental investigation of the heat transfer characteristics of premixed butane/air circular impinging flame jets with swirl induced operating at low inlet Reynolds numbers and low pressure. Effects of the important parameters affecting the thermal characteristics of the impinging flame jet as well as the heat transfer between the flame and the impingement plate are investigated. The entire research project can be divided into the following specific tasks:

1. To investigate the feasibility of inducing swirl to a small-scale gas-fired impinging circular flame jet. The techniques used to generate a swirling flame and the methods applied to measure the strength of the generated swirling flame, will be investigated.

2. To investigate the heat transfer characteristics of the premixed butane/air impinging circular flame jet with swirl induced. To determine the effects of the major parameters on the thermal performance of the flame jet system. The interaction between the flame jet system with the important experimental conditions including equivalence ratio of the air/fuel mixture, Reynolds number of the air/fuel jet, the nozzle-to-plate distance and the swirling intensity, will also be investigated.

3. To develop a non-dimensional equation by using the multiple regression method with the aid of the experimental results obtained. The developed equation is for the prediction of the heat transfer coefficient of the impinging flame jet system with swirl induced.

4. To compare the heat transfer characteristics of the premixed butane/air impinging circular flame jets, with and without swirl induced. Such comparison will provide a bench mark for the swirling flame jet.

1.3 THESIS STRUCTURE

This thesis mainly contains nine chapters. The 1st chapter provides a brief introduction of the background and the objectives of the present study. The 2nd chapter gives an intensive review of the investigations of heat transfer characteristics of the premixed impinging flame jets, as well as the previous research work on swirling flame combustion, both theoretical and experimental.

Then the methodology applied in the current study is introduced. The methods of swirl generation are discussed in the 3rd chapter, which is followed by the description of the two experimental setups being used to determine the swirl number of an impinging flame jet with swirl induced. The 4th chapter mainly describes the setup of the experimental system to measure the heat transfer characteristics of the swirling flame system. It includes recording, collection and handling of the experimental data, and error analysis of the experiment. As there are two methods used to generate the swirling flame, this experimental study will be repeated twice, with each of them conducted with one of these two methods in generating the swirling flame.

The 5th and 6th chapters present the experimental results obtained from both setups, respectively, illustrating the effects of different parameters on the heat transfer characteristics of the impinging flame jet system with swirl induced.

The 7th chapter gives a comparison of the heat transfer characteristics of the swirling flames produced by the two experimental setups. They are also compared with the heat transfer characteristics of a premixed butane/air impinging circular flame jet without swirl induced.

In the 8th chapter, a non-dimensional equation has been developed by using the multiple regression method. The developed equation is for the prediction of the heat transfer coefficient of the impinging flame jet system with swirl induced.

Conclusions are then drawn in the 9th chapter based on the present investigation, with suggestions for future work being put forward.

CHAPTER 2
LITERATURE SURVEY

Research works have been carried out on the flow and thermal characteristics of impinging flame jets for many years. In this survey, the previous works, both theoretical and experimental, are reviewed to provide a fundamental understanding of the flame structure and the heat transfer characteristics of the premixed impinging flame jet, with and without swirl induced.

2.1 FLAME STRUCTURE

Relatively more information about premixed circular flame jets can be found in the literature as the topic has been studied for many years. Figure 2.1 demonstrates the schematics of the flow of an impinging flame jet. The flow structure is basically divided into three regions: free jet region, stagnation region and wall-jet region.

The free jet region consists of a potential core and a fully developed region. The potential core plays an important role in ignition and flame stability. The fluid in the potential core is not affected by contacting with the surrounding fluid, and has the same characteristics as the flow in the nozzle [17]. The jet flow in the fully developed region is of constant velocity profile. There are relatively more investigations, experimental and numerical, conducted to study this region.

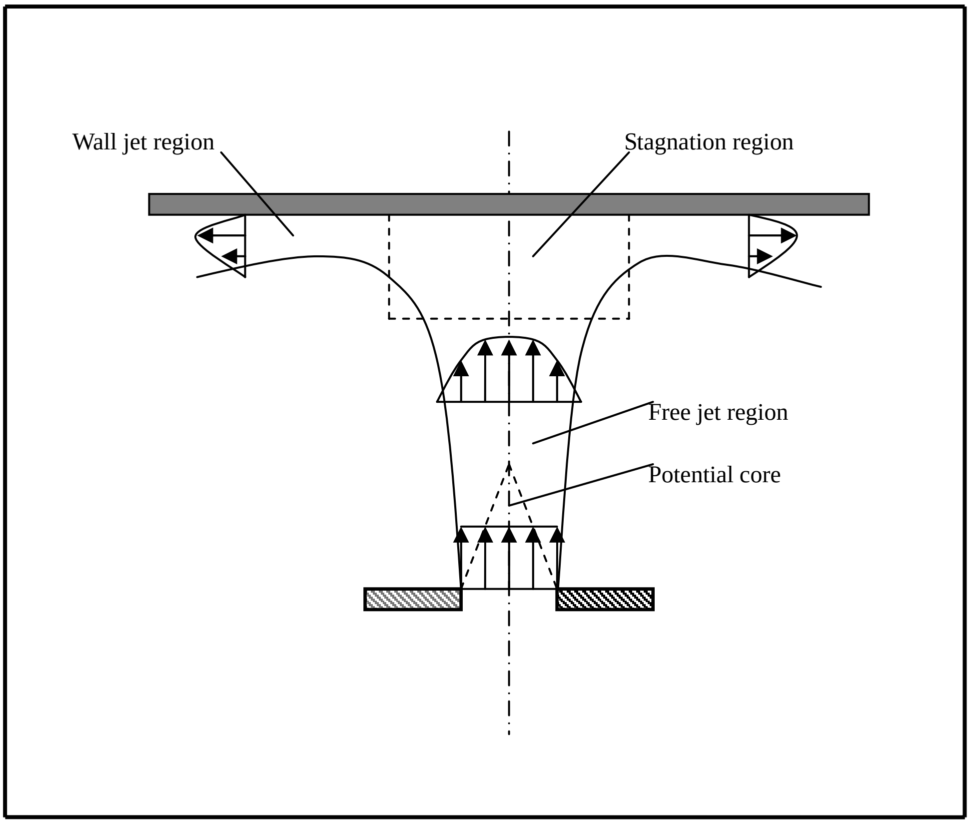

Figure 2.1   Flow characteristics of an impinging flame jet

The stagnation region is also known as the impingement region. It has been found to be an intensive combustion zone, in which the heat transfer rate is very high [18]. Yet the heat transfer mechanisms here are complicated not only because of the uncertainty of the impinging boundary layer, but also for the intensive combustion of the mixture.

The wall jet region has been considered as half of a free jet with an inner layer near the wall [19]. The temperatures in the zone are relatively low due to a fuel-lean combustion, with excess ambient air entrained [18 and 20].

The thermal and flow characteristics become more difficult to understand when swirl is induced to the impinging flame jet. It will change the flow pattern and hence influences the combustion process. Therefore the heat transfer characteristics of an impinging flame jet with swirl induced need further investigated.

The complicated flow characteristics of the swirling flame jet lead to the absence of a well described flame structure in the literature. The formation of an impinging swirling flame is even more difficult to be fully understood. Zhao et al. [15] carried out a numerical study of an open swirl-stabilized premixed flame. The weak swirl generates flow divergence to stabilize the flame at a distance above the burner exit. Figures 2.2 (a) and (b) illustrate the fuel burning velocity and the flame temperature distribution, which both indicate that combustion is taking place in a region which is locally normal to the centerline and close to the exit of the nozzle.

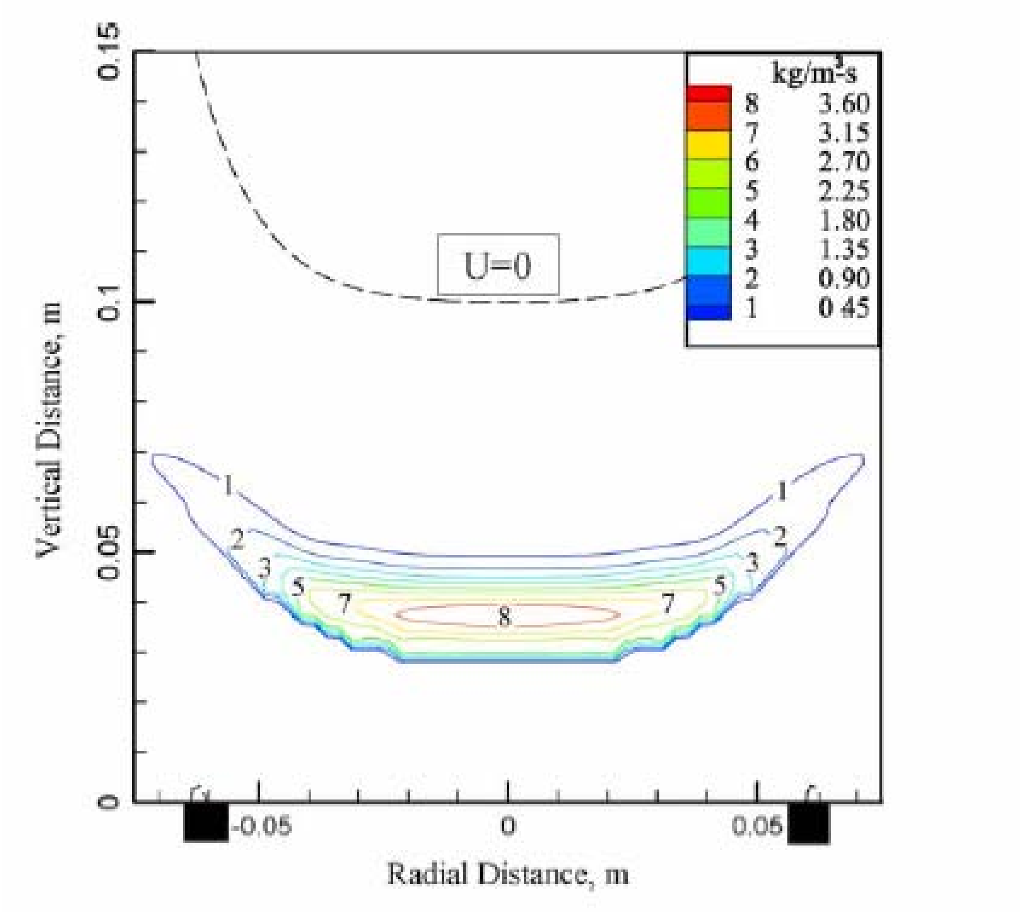

Figure 2.2 (a) Distribution of fuel burning rate

(Zhao et al. [15])

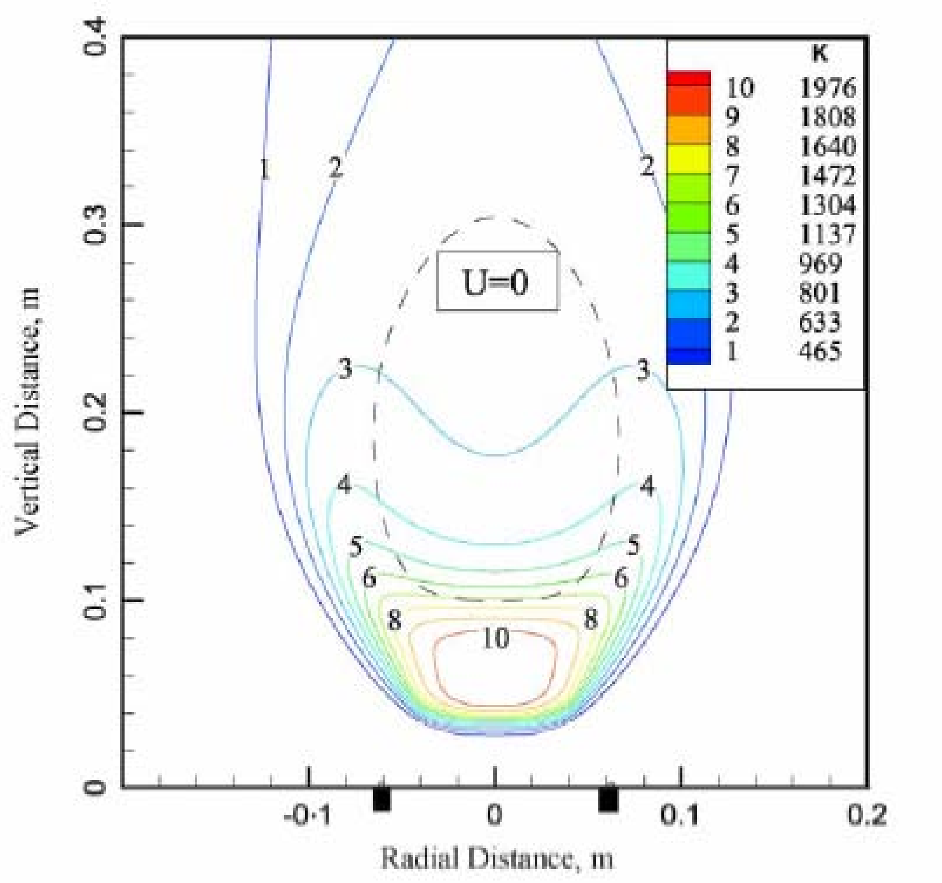

Figure 2.2 (b) Distribution of flame temperature in a simulated domain

(Zhao et al. [15])

2.2 HEAT TRANSFER MECHANISMS

There are several heat transfer mechanisms in the impinging flame jet system, among which forced convection, thermo-chemical-heat-release (TCHR), radiation and condensation have been verified, and will be discussed here. Yet the predominant mechanism varies with the experimental conditions. In the absence of information about the impinging flame jet with induced swirl at low Reynolds numbers, the impinging flame jet without swirl induced has usually been used as the foundation of its studies.

2.2.1 Forced Convection

In flame impingement without a furnace enclosure, forced convection is the predominant heat transfer mechanism. Convective heat transfer rates have been experimentally quantified by many investigators. The fraction of convection in the total heat transferred varies with the operating conditions. In the work of Hustad and Sonju [21] which was conducted to investigate the propane flames impinging normally to a submerged pipe, the convection heat transfer sums up to 80% of the total heat flux. It was also concluded that it is the intense convective heat transfer between the flame and the impingement surface that brings up the rapid heating technique.

2.2.2 Thermo-Chemical-Heat-Release (TCHR)

This mechanism refers to the exothermic release of energy from the burning gases. When temperature of the impinging flame is sufficiently high, effect of the Thermo-Chemical-Heat-Release (TCHR) which is featured with the recombination of atoms and the radicals, becomes important on the overall heat transfer. This process is also termed as chemical recombination or recombination [22]. Pyro-generation of the combustion products occurs when temperature exceeds 1800K. The atoms or radicals are then recombined into molecules when they are reaching the cool surface, and heat is thus released during the process [23 and 24].

In high temperature flame impingement, the combustion products diffuse along the boundary layer to the colder surface. It was found that this chemical process usually indicates two mechanisms: equilibrium and catalytic [25]. In the former type of process, the gaseous chemical reactions occur in the boundary layer. The reaction time is much less than the time required for the gases to diffuse to the surface. The latter one involves chemical diffusion reactions at a surface, where radical species are reacting with the surface materials. These two mechanisms can also be combined to provide another type of TCHR process, the mixed flow process. However, there are very few methods reported to measure TCHR directly.

2.2.3 Radiation

Radiation in a heating furnace should be taken into consideration because of the radiation heat transfer from the high temperature furnace walls. Radiation heat transfer can be measured directly by using radiometer. It has been concluded by Baukal et al. [26] that the heat transferred by radiation can be neglected for non-luminous flames, after comparing the results with impingement surfaces fabricated with different emissivities ranging from black body to highly polished surface. The largest difference in radiation heat transfer between the two extreme situations is only 9.8 %. In most of the studies on premixed impinging flames, the non-luminous radiation is assumed and therefore becomes negligible.

2.2.4 Condensation

Condensation occurs when temperature of the impingement surface is lower than the dew point temperature of the combustion gases. Energy will be released during the condensation process. The target surface temperature can be maintained at an appropriately high level above the dew point temperature of the combustion gases to prevent the vapor from condensing [27], thus, the contribution of condensation to the total heat transfer is usually not significant.

2.3 HEAT TRANSFER ENHANCEMENT BY INDUCED SWIRL

Swirl has been adopted as an effective way for many years to enhance heat transfer between a decaying internal flow and its adjacent tube wall. Dhir and Chang [28] studied the heat transfer enhancement using tangential injections. An average enhancement of 35 to 40 % in heat transfer rate is obtained on a constant pumping power basis.

Razgaitis and Holman [29] suggested several possible mechanisms to enhance the heat transfer in swirling tube flow. One of them is to enhance the recirculation zone at the center of the tube, which increases the effective axial Reynolds number by reducing the cross-sectional flow area. The increasing velocity produces larger temperature gradients and hence a higher heat transfer rate. They also suggested that even in a flow with low swirling intensity in which no recirculation is found, the axial velocity near the wall can be increased because of tangential injection. Another possible mechanism is the destabilizing distribution of angular momentum in the free vortex zone predicted from the Rayleigh criterion, which improves both the heat and momentum transfer. The third mechanism discussed by them is the thermal instability. A thermally stratified layer caused by the centrifugal force promotes mixing by pushing the cold fluid towards the wall and hot fluid towards the center when the tube wall is heated.

Shuja et al. [30] simulated the flow field of a confined swirling jet, which is impinging onto an adiabatic wall, and is able to show its velocity profiles and temperature distributions. However, there is no heat transfer processes discussed. Owsenek et al. [31] conducted a numerical study on the heat transfer of impinging axial jets with superimposed swirl. They observed a significant heat transfer enhancement of as high as 77 % at the swirl number of unity.

However, discussion on the heat transfer mechanisms of an impinging flame jet with swirl induced is hardly found in literature.

2.4 HEAT TRANSFER PREDICTION

The heat transfer of an impinging flame jet system can usually be predicted via the approaches as described in the following sections.

2.4.1 Numerical Simulation

Owsenek et al. [31] conducted a numerical simulation on the heat transfer of the impinging axial and radial air jets with superimposed swirl. The near-field and far-field flow structures and temperature fields are simulated by solving the unsteady Navier-Stokes and Energy Equations. The flow has been considered as laminar at the locations where it is either periodic or unsteady periodic. The surfaces, except the constant temperature impingement plate, are all assumed adiabatic. As Reynolds number is varied from 10 to 1000, the steady solutions become periodic and then chaotically unsteady. No attempt has been made to identify the transition points. Moreover, there is no investigation to study the swirling intensity performed.

The interaction between combustion and swirl increases the complexity of the flow and thermal characteristics. In the numerical simulation of an open swirl-stabilized premixed combustion carried out by Zhao et al. [15], the flow is considered to be two-dimensional, steady and incompressible, while the swirling velocity is assumed to uniformly distribute along the burner circumference. A standard k-ε turbulence model has been applied to perform the simulation. However, the reported numerical simulation needs to be validated against experimental data.

2.4.2 Semi-analytical Solution

There have been attempts to predict the convective heat transfer from impinging flame jet to a target plate [32, 33, 34, 35 and 36]. However, it may be immature at this stage to identify reliable analytical solutions because most of these attempts are based on assumptions, which have not been totally validated. Therefore, the semi-analytical method is usually preferred in performing the prediction. Baukal and Gebhart [37] reviewed the semi-analytical solutions for impinging flame jet heat transfer.

Sibulkin [36] obtained the solution for the heat transfer from a uniform flow to the stagnation point on the revolution body, at which it impinged on. Equation (2.1) is derived by numerically solving the laminar boundary layer equations around the impingement body generated by the flow, which is assumed to be incompressible, axisymmetric and low-speed.

$$\dot{q}_s = 0.763(\rho_f \mu_f \beta_s)^{0.5}(h_f - h_w)P_r^{-0.6} \qquad \text{......} (2.1)$$

In Equation (2.1), ρ_f , μ_f and h_f are respectively the density, dynamic viscosity and enthalpy of the flame attached to the boundary layer at the stagnation point, and h_w represents the enthalpy of gas clung to the wall. Whereas β_s is the radial velocity gradient at the stagnation point obtained by Van der Meer [32]:

$$\beta_s = \frac{4u}{\pi d} \qquad \text{......} (2.2)$$

In Equation (2.2), u is the average axial velocity and d is diameter of the nozzle exit.

Fay and Ridell [38] considered the influences of air flow and recombination of radicals (TCHR) on the heat transfer at the boundary layer of an impingement plate by applying the Sibulkin’s theory. The developed equation for the determination of stagnation point heat flux is as shown in Equation (2.3):

$$\dot{q}_s = 0.763\left(\frac{\rho_w \mu_w}{\rho_f \mu_f}\right)^{0.1} (\rho_f \mu_f \beta)^{0,5} (h_f - h_w) P_r^{-0.6} \left[1 + (L_e{}^b - 1)\frac{h_{f,D}}{h_f}\right] \quad \ldots\ldots (2.3)$$

In Equation (2.3):

$b = 0.52$ for equilibrium TCHR

$b = 0.63$ for catalytic TCHR

Besides,

Le = D/a (i.e. the Lewis number), ρ_w and μ_w are the gas properties of the target surface, and $h_{f,D}$ is the dissociation enthalpy.

When equilibrium TCHR occurs, the above equation can be further developed into Equation (2.4) [39]:

$$\dot{q} = 0.763\beta^{0.5} (\overline{\rho u})^{0.5} \mathrm{Pr}_f{}^{-0.6} \left[1 + (\overline{Le_H} - 1)\frac{\Delta h_{rH}}{\Delta h}\right]^{0.6} \overline{C_{Pe}} \cdot \Delta T \quad \ldots\ldots (2.4)$$

Dong et al. [12] performed the study of a single circular premixed impinging flame jet. They derived a semi-analytical solution of the heat transfer between the flame and the impingement plate, and compared with the results of Sibulkin. The correlation between Nusselt number and the non-dimensional influencing parameters has been given in Equation (2.5):

$$\overline{Nu} \cdot \Pr^{-0.4} = 0.159 \operatorname{Re}^{0.4745} \phi^{-0.382} (H/d)^{0.2908}, \begin{Bmatrix} 600 \le \operatorname{Re} \le 1500 \\ 0.7 \le \phi \le 1.2 \\ 1.0 \le H/d \le 8.0 \\ 0 \le r/d \le 6.5 \end{Bmatrix} \qquad \ldots\ldots (2.5)$$

2.5 HEAT TRANSFER AND TEMPERATURE MEASUREMENTS

Baukal and Gebhart [40] reviewed the measurement techniques on the experimental studies of impinging flame jet system. The configurations under investigation include normal and oblique impingement of the jet onto a plane surface or a hemi-nosed cylinder, and normal impingement of the jet onto a cylinder. The most basic measurement required is the total heat flux received by the impingement plate, and then the flame jet's temperature and velocity. The flame jet's velocity profile is especially significant in the study of the swirling flame, as it is needed for the calculation of the swirl number, as well as the investigation of the swirling flow pattern.

The total heat flux is the total amount of energy received by a unit surface area of the target plate. There are several methods applicable for its measurement. Among them, use of a water-cooled impingement plate operating at steady-state was adopted by Baukal [8] in an early experimental study. In his experiments, the entire target surface was internally cooled by multiple cooling circuits. After the steady-state conditions of the coolant had been reached, the heat flux was then calculated from the rate of sensible energy gain by the coolant. In the study of Dong et al. [9 – 12], the impingement surface was cooled at its back-side (non-flame-side) with a steady supply of water maintained at a constant temperature. The local heat flux transferred to the surface was recorded by a heat flux sensor mounted into the surface. The total heat flux was then obtained by integrating the local heat flux over the entire impingement surface area.

There are many previous works conducted with the use of five-wire thermocouples, with and without coatings to measure the burning gas temperature. Van der Meer et al. [32] selected a B-type thermocouple of Pt30%Rh / Pt-6%Rh alloys, which are coated with Yt_2O_3 / BeO, with a diameter of 0.05 – 0.18 mm. While in the study of Baukal [8], a B-type thermocouple of Pt30%Rh / Pt-6%Rh with a diameter of 0.23 – 0.79 mm was applied without coating. Corrections were made for the radiation and conduction heat losses [40, 41 and 42].

Gas velocity is important for the understanding of the flow patterns, as well as for comparison of the experimental data with results calculated from semi-analytical expressions. The most commonly used instrument for measuring velocity are Pitot tube, Hot-Wire Anemometry and Laser Doppler Anemometry (LDA). Among them, LDA has been widely used in recent research on swirl-stabilized combustors [43, 44 and 45].

Besides, flow visualization techniques are also commonly applied to the investigation of the flow field. Masri et al. [13] and Khezzar [46] used the laser-induced fluorescence technique to study the compositional structure and velocity fields of a turbulent diffusion flame. Mixing modes, temperature and composition distributions, and reacted fields were presented, which covered a wide range of Swirl number and Reynolds number.

2.6 BURNER CONFIGURATION

The heat transfer characteristics of single circular burner, single slot burner and multiple-ports impinging flame jet systems have been investigated by previous researchers [8 – 12, 13 and 14]. However, the introduction of swirl to the small-scale impinging flame jet system has been rarely reported. Most of the applications of swirl to combustion process concern with large-scale non-premixed industrial combustors operating under very high Reynolds numbers.

Syred and Beer [47] conducted a review of the recent progress in the applications of swirling-flow. The possible methods to produce a swirling-flow were summarized, with the major considerations in the thermal performance, flame stability and combustion behavior of the impinging flame jet systems. Guillaume and LaRue [48] created a swirling flow by drawing the entrained air through two channels, which were formed by two overlapping curved vanes surrounding the fuel jet. A swirling flame jet was produced without the use of a high-pressure air source.

In most of the previous works, induction of the vortex swirling flow is produced by the addition of tangential entrances or guided vanes. Chang and Dhir [2] applied six tangential injectors to produce a decaying swirl flow, which was used to study the turbulent flow field and the heat transfer performance of a tube heated uniformly from the wall. Schematic drawing of the burner system is shown in Figure 2.3.

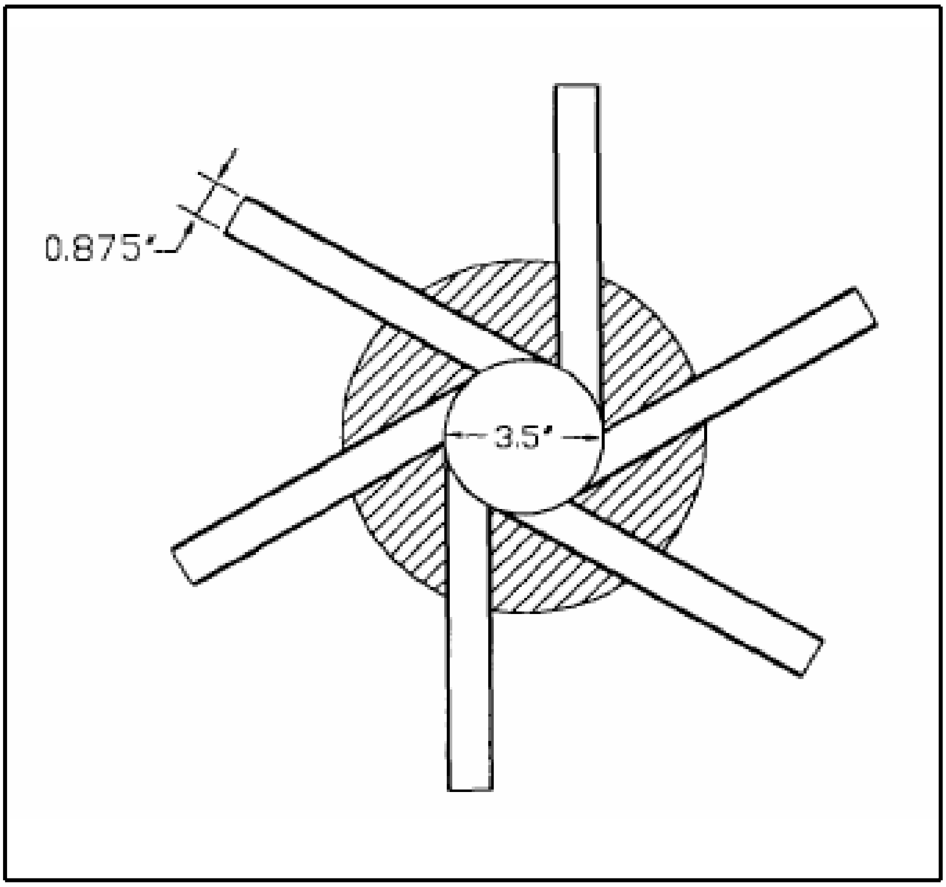

Figure 2.3 Tangential injectors to create swirling flow [Chang and Dhir, 1995]

Feikema et al. [5] applied a swirling flow to enhance the blowout limits of a non-premixed flame jet, which was produced with the aid of a nozzle having four tangential inlets in addition to the main axial flow. In their later study [6], the maximum co-axial air velocities achievable with and without swirl, were determined. It was suggested that flame stability can only be achieved when the velocity-to-diameter ratio of the fuel jet is within a critical value. Schematic drawing of the swirl burner used is presented in Figure 2.4.

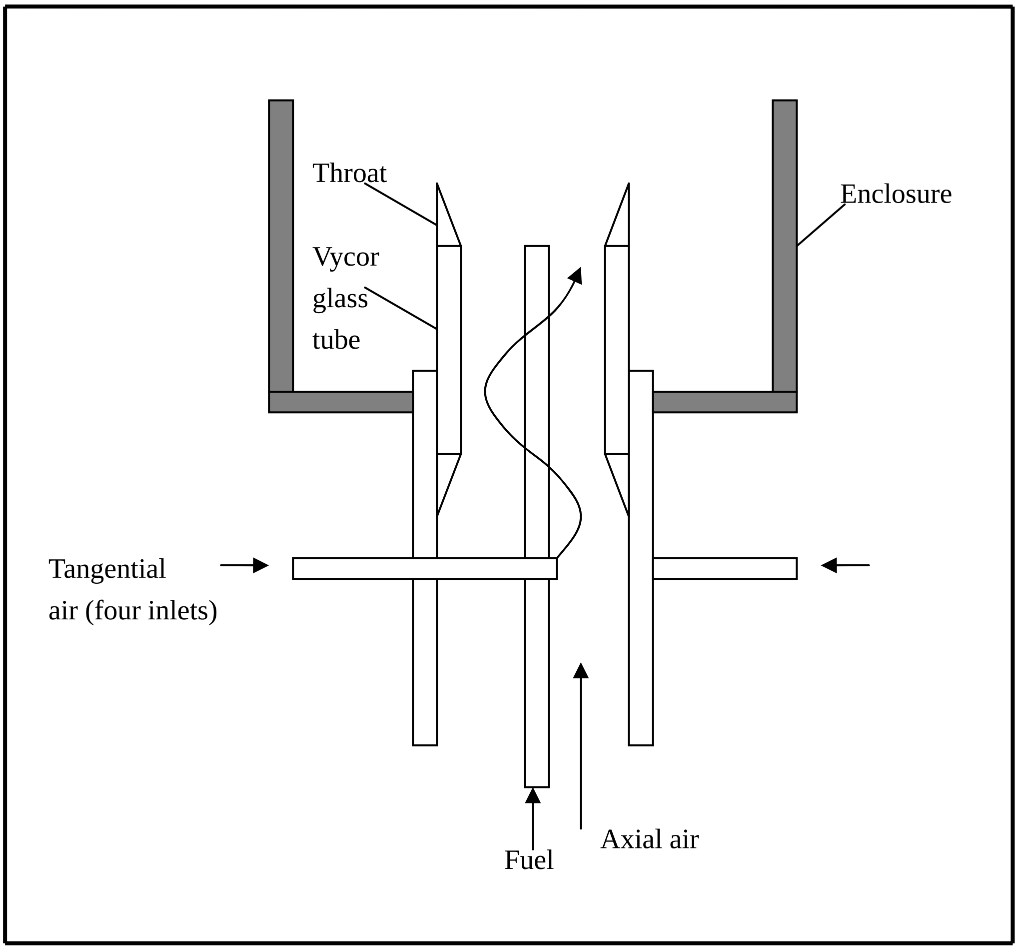

Figure 2.4 Burner provided with swirling flow [Feikema et al., 1990]

Chan et al. [49] applied weak swirls to stabilize premixed flames which were produced by a small amount of tangential injection, as shown in Figure 2.5. It was suggested that the flame can be maintained stable at the point where the local mass flux is balanced. Laser Doppler anemometry was applied to measure the velocity components to facilitate the calculation of swirl number.

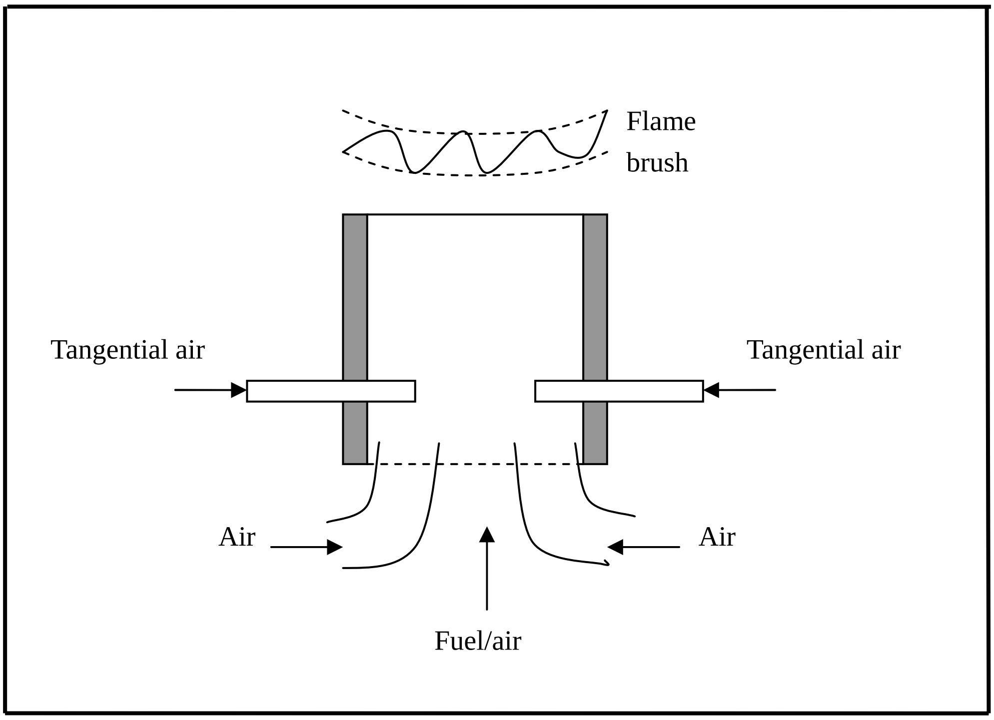

Figure 2.5 Burner provided with a weak swirl [Chan et al., 1992]

Noui-Mehidi et al. [49] studied the effect of apex angle of the nozzle on the swirling flow induced by tangential inlets between conical nozzles, and found that the use of conical configuration has advantages to enhance the swirl characteristics. The conical nozzle structures applied in their numerical work are presented in Figure 2.6.

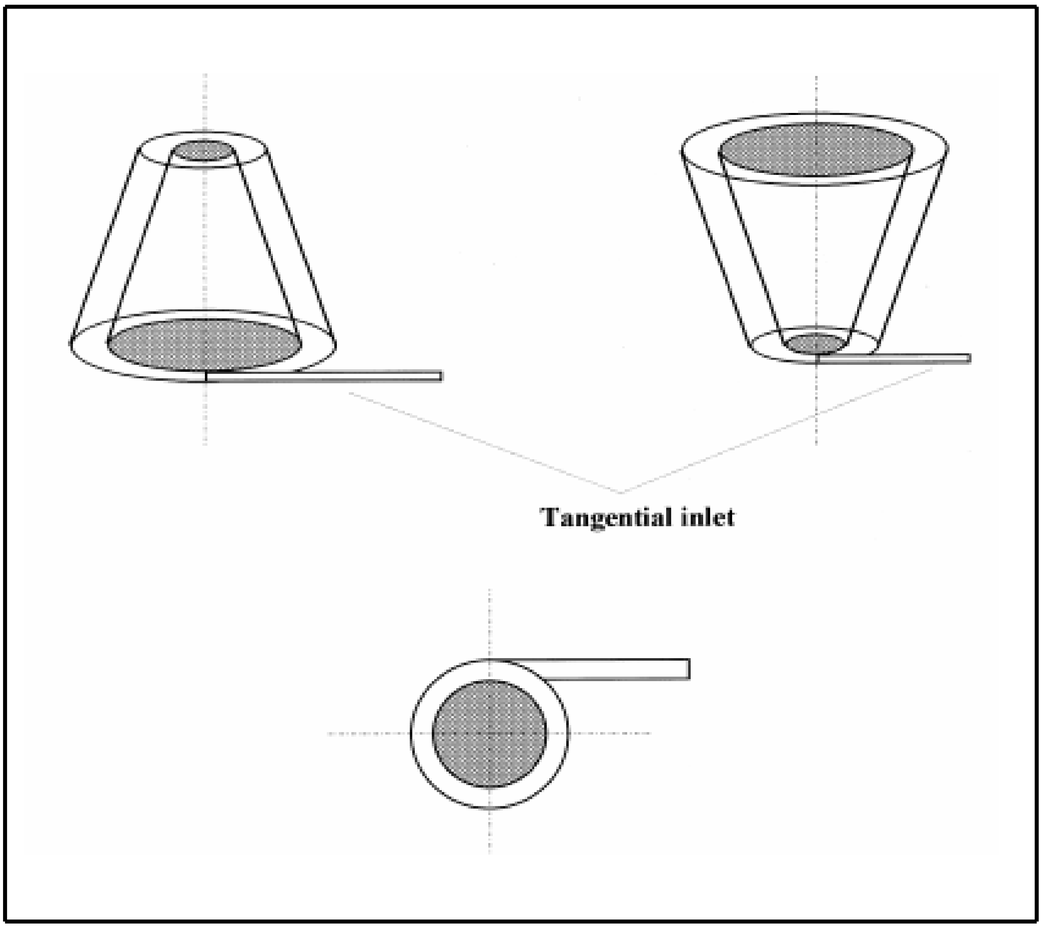

Figure 2.6 Conical nozzles used for numerical simulation

[Noui-Mehidi et al., 1999]

2.7 IMPINGEMENT SURFACE CONDITIONS

Most of the reported studies on the impingement surface condition have been focused on a stationary surface, which is the common situation in real-life applications. Baukal and Gebhart [51] fabricated the impingement plates with polished, untreated, and blackened surfaces to study the effect of surface emissivity. The heat flux received by the blackened and polished surfaces was the highest and lowest, respectively, and that received by the untreated surfaces is of value between them. Catalytic effects were also investigated by using alumina-coated (nearly non-catalytic), untreated, and platinum-coated (highly catalytic) impingement plate surfaces. The heat flux received by the platinum-coated surface is found to be the highest, whereas the heat flux received by the untreated surface is similar to that received by the alumina-coated surface.

Kilham et al. [52] performed a study on the effect of curvature radius of the impingement plate. The thermal resistance was first determined, thus, the heat transfer rate along the plate was controlled. However, there are yet very few literatures available on the effect of the curvature of the impingement plate surface.

Most of the attentions have been concentrated on the thermal characteristics of impingement plates with a flat surface. In the studies to investigate the heat transfer characteristics of impinging flame jet system conducted by Dong et al. [9 – 12], a highly polished copper plate had been adopted as the impingement target. Zhao et al. [53] fabricated the impingement plates with brass, bronze and stainless steel. It is found that with the use of a metal impingement plate of excellent thermal conductivity, a more rapid conduction and hence overall heat transfer through the plate can be achieved because of the very low thermal resistance encountered.

2.8 NOZZLE-TO-PLATE DISTANCE

Since the flame is impinging normally onto a flat polished copper plate in the present study, the geometry between the flame holder and the impingement surface is essentially decided by the nozzle-to-plate distance (H/d). It has been found that the nozzle-to-plate distance can significantly affect the impinging flame structure and thus the heat transfer characteristics, especially the Nusselt number [9 – 12]. Baukal et al. [51] found that the impingement heat transfer efficiency decreases with increasing nozzle-to-plate distance. Kataoka [54] and Viskanta [22] concluded that the optimum nozzle-to-plate distance corresponding to a maximum heat transfer performance coincides with the length of the potential core for isothermal jets. It was also suggested that the optimum nozzle-to-plate distance for a single circular flame jet is a function of Reynolds number and equivalence ratio, which have important effects on the burning velocity and the flame length.

Hargrave et al. [55] summarized the approximate nozzle-to-plate distances that correspond to maximum heat flux under different Reynolds numbers and equivalence ratios. It was concluded that the peak heat flux occurs when H/d = 2.5 for a circular flame jet operating under a Reynolds number of 2000. However, Van der Meer [32] found that the highest heat flux generated by a circular burner is obtained at H/d = 5 when the Reynolds number is varied from 1771 to 2700.

However, there are yet very few literature concerning with the applications of impinging circular flame jet with swirl induced. The vortex flow caused by the swirl may provide great impact on the flame length, configuration of the wall-jet zone and distribution of the high temperature combustion gas. This may change significantly the relationship between the thermal performance and the operation parameters of the impinging flame jet system.

2.9 FUEL TYPE

In the gas-fired flame jet studies, various gaseous fuels have been selected to produce the flame jet. Hydrocarbon fuel is most commonly used, which is oxidized by either air or pure oxygen. Use of different gaseous fuels will certainly result with different thermal characteristics of the impinging flame jet system as well as its pollutant emissions.

Beer et al. [56] conducted experimental work to compare the convective heat transfer characteristics of the flames produced by burning heavy fuel oil and coke oven gas. It was concluded that no remarkable difference is identified between the applications of these two fuels.

In the present study, butane gas is selected as the fuel. On the one hand, it is ideal for the purpose to generate a stable premixed flame. On the other hand, it is commonly used for domestic and light-industrial applications in Hong Kong, such that results obtained will have immediate significance to the local community.

2.10 OTHER MAJOR OPERATING PARAMETERS

In addition to the parameters as described in the above sections, there are other operating parameters believed to have significant influence on the thermal effect.

2.10.1 Equivalence Ratio

Equivalence ratio of the air/fuel mixture is a comparison of the stoichiometric air/fuel ratio to the actual one, i.e.

$$\phi = \frac{(A/F)_{stoic}}{(A/F)} \qquad \text{. . . . . . (2.6)}$$

Equivalence ratio is proven to have very significant effect on the heat transfer characteristics of an impinging flame jet system, and many research works have been conducted to explore its thermal effects.

It was concluded by Hargrave et al. [55] that a fuel/air mixture deviating from the stoichiometric condition will result in a decrease in the maximum rate of the heat transfer.

Premixed combustion is chosen in many applications, especially small-scale systems with low operating pressure, because it can provide very rapid combustion, high heat transfer rate and very low formation of soot. Equivalence ratio is of particular importance to premixed flame. In the study conducted by Kwok et al. [14 and 57] on the heat transfer characteristics of a single impinging circular flame jet, the peak heat flux occurs when the combustion is conducted at a slightly fuel-rich condition with the equivalence ratio varied between 1.0 and 1.1.

2.10.2 Reynolds Number

Reynolds number of the air/fuel jet is defined as:

$$R_e = \frac{ud}{\upsilon} \qquad \text{......} (2.7)$$

Reynolds number of a flame jet at the exit port determines the jet aerodynamics and hence becomes an important aspect of the heat transfer characteristics. Hargrave et al. [55] concluded that the peak heat flux in the flame increases with Reynolds number, but the axial extent of the flame's equilibrium region decreases with increasing Reynolds number. Dong et al. [9 – 12] carried out experimental studies on impinging flame jet systems operating under laminar and transitional flow conditions with Re < 2300, and the results are in good agreement with those proposed by Hargrave.

However, different results may be expected in the present study because of the addition of swirl to the impinging flame jet. The effects of equivalence ratio and Reynolds number on the heat transfer characteristics of the flame jet system may also be different for swirling and non-swirling flame jets, since the flame properties and flow characteristics may be changed significantly due to the induced swirl.

2.10.3 Swirl Number

The swirl number (S) of a flame jet with swirl induced had been defined by Claypole and Syred [59] as the ratio between the angular and axial momentum rates passing through the nozzle throat, divided by the nozzle throat radius (R) as shown in Equation (2.8):

$$S = \frac{\pi \ r_0 R}{A_t} \left(\frac{\dot{m}_t}{\dot{m}_\theta + \dot{m}_t} \right)^2 \qquad \ldots\ldots (2.8)$$

Quantity of the swirl number was calculated using the velocity profiles obtained by LDA / LDV. The same method has also been applied by other researchers. Chan et al. [49] studied the properties of a turbulent flame by measuring the velocity profile at the nozzle exit using a four-beam two-color LDA system. The swirl number calculated directly from the velocity values ranged from 0.07 – 0.18, indicating the production of a weak swirl.

Magnitude of the swirl number indicates the intensity of the swirling flow. In the study of Huang and El-genk [7], different swirling intensities were produced by solid inserts with different swirl angles. It was suggested that heat transfer to a heating object is first augmented with a larger swirl angle, and then decreases when the swirl angle is further increased.

2.11 SUMMARY OF LITERATURE SURVEY

Summarizing the above information on heat transfer characteristics of impinging flame jets, rather sufficient studies have been conducted on the non-swirling impinging flame jets to explore the influences of the major parameters on their thermal performance.

Concerning about the flame jets with swirl induced, swirl has been applied as an effective way to enhance the heat transfer rate between an internal tube flow and the tube wall, as well as to enhance the combustion efficiency in a chamber. It has also been shown that the blow-off limits can be extended by imposing swirl with appropriate intensity. However, the introduction of a weak swirl to small-scale, low Reynolds number, low pressure, domestic or light-industrial application, has rarely been reported. Neither the feasibility in applying a weak swirl has been investigated nor the heat transfer characteristics of an impinging flame jet with swirl induced been studied.

The present study aims to provide information to fill this gap by studying a circular impinging premixed flame jet with swirl induced. Heat transfer characteristics of the swirling impinging flame are investigated with the aid of the results reported by previous researchers to facilitate comparison.

2.12 RESEARCH METHODOLOGY

The present study on the heat transfer characteristics of premixed circular impinging flame jet with swirl induced essentially concern with experimental investigations, which are carried out to fulfill the following tasks.

(a) To investigate experimentally the feasibility of inducing swirl to a small-scale gas-fired impinging circular flame jet including the techniques used to generate a swirling flame and the methods applied to measure the strength of the generated swirling flame.

(b) To investigate the heat transfer characteristics of the premixed butane/air impinging circular flame jet with swirl induced. Effects of the major parameters on the thermal performance of the flame jet system under consideration: equivalence ratio of the air/fuel mixture, Reynolds number of the air/fuel jet, the nozzle-to-plate distance and the swirling intensity, will be investigated experimentally.

(c) To develop a non-dimensional equation by using the multiple regression method with the aid of the experimental results obtained. The developed equation is for the prediction of the heat transfer coefficient of the impinging flame jet system with swirl induced.

(d) To compare the heat transfer characteristics of the premixed butane/air impinging circular flame jets, with and without swirl induced. Such comparison will provide a benchmarking for the swirling flame jet.

CHAPTER 3
SWIRL GENERATION AND MEASUREMENT

In this chapter, the feasibility of several approaches in producing a stable swirling flow which have been proposed by previous researchers will be fully investigated. Design of the burner applied in the present study was based on the configuration of a Bunsen burner, a typical device to produce premixed flame, which causes less pressure drop by the flow and hence is able to provide a more flexible operating range.

It was concluded by Yilmaz et al. [16] that swirling flows can be classified into three groups: curved flow, rotating flow and vortex flow, according to the velocity profile characteristics, and these swirling flows are normally required to be produced with different methods. A curved flow can be generated by inserting twisted tapes or helical vanes. A rotating flow is usually generated by the application of a rotating tube. A vortex flow is also called a “decaying swirl flow”, which can be produced by drawing the flow through tangential inlets or guided vanes.

With regard to the experimental conditions under consideration, helical vane is first considered as the method of introducing swirl. As concluded by Huang and El-genk [7] in their heat transfer experiments of impinging air jet with induced swirl, the swirling jet is able to enhance significantly the local and average Nusselt numbers and hence the heat transfer at the impingement surface when it is compared to an impinging jet of the same geometry without swirl. The swirling flow is also able to improve the radial uniformity of heat transfer to the impingement surface. However, in the case when combustion is involved, the curved flow produced by inserting helical vanes scarcely contributes to the air/fuel mixing and combustion. In addition, the inserted vanes increase the flow resistance and hence the friction loss, which is disadvantageous for a flame jet operating with low inlet pressure.

3.1 ADDITIONAL TANGENTIAL FLOWS

As suggested by Yilmaz et al. [16], a swirling flow can be produced by drawing an additional tangential flow into the burner to react with the main axial flow. The resultant swirl intensity can be controlled by adjusting the ratio between the tangential and axial flows. This is the most common method adopted by many researchers in producing a stable swirling flow in their studies, and is suggested to be rather effective. However, the burners applied in the studies of heat transfer enhanced by inducing swirl, which have been reviewed in Chapter 2, are usually in large-scale for heavy-industrial applications. They are operating with turbulent flows with very high Reynolds numbers, and therefore are not suitable for the present investigation.

The concept of additional tangential flows to generate a swirling flow will be considered in the present study, but an appropriate scaling down of the burner for low Reynolds number and low pressure application is required. Therefore a much smaller flame holder was used in the present study. A nozzle with an inner diameter of 8.6 mm was purposely chosen to facilitate comparison with the previous work. However, it seems not practical to add tangential flow directly to a burner of such a small diameter. According to the suggestion of Noui-mehidi [50], a conical configuration has the advantage in producing a swirling flow. The schematic drawing of the burner used in the present study is shown in Figure 3.1, while its geometry as viewed from the bottom is shown in Figure 3.2.

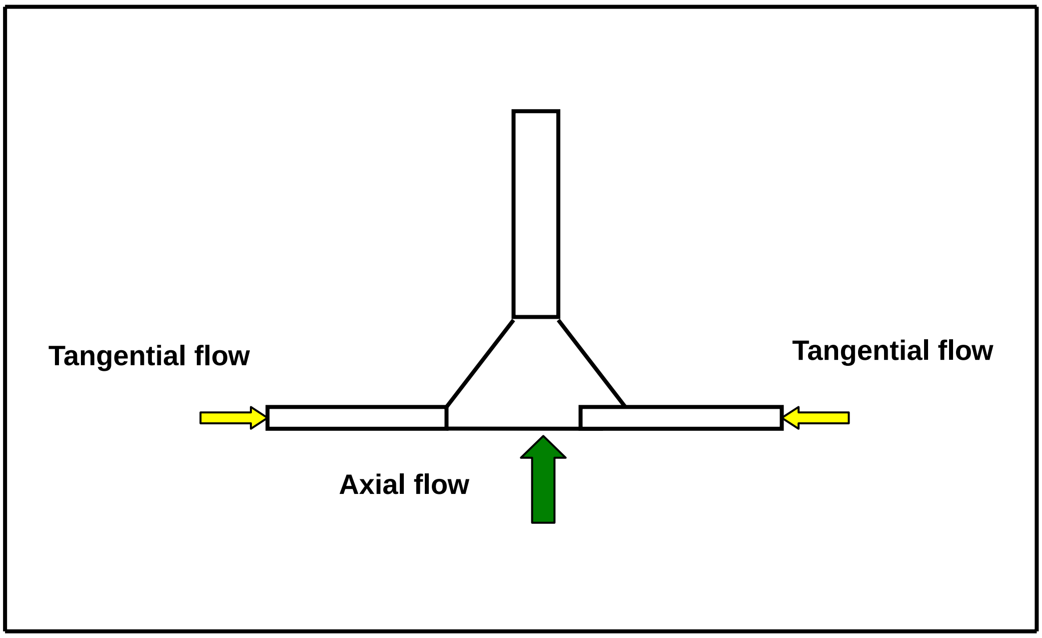

Figure 3.1 Schematics of the present burner system with swirl induced

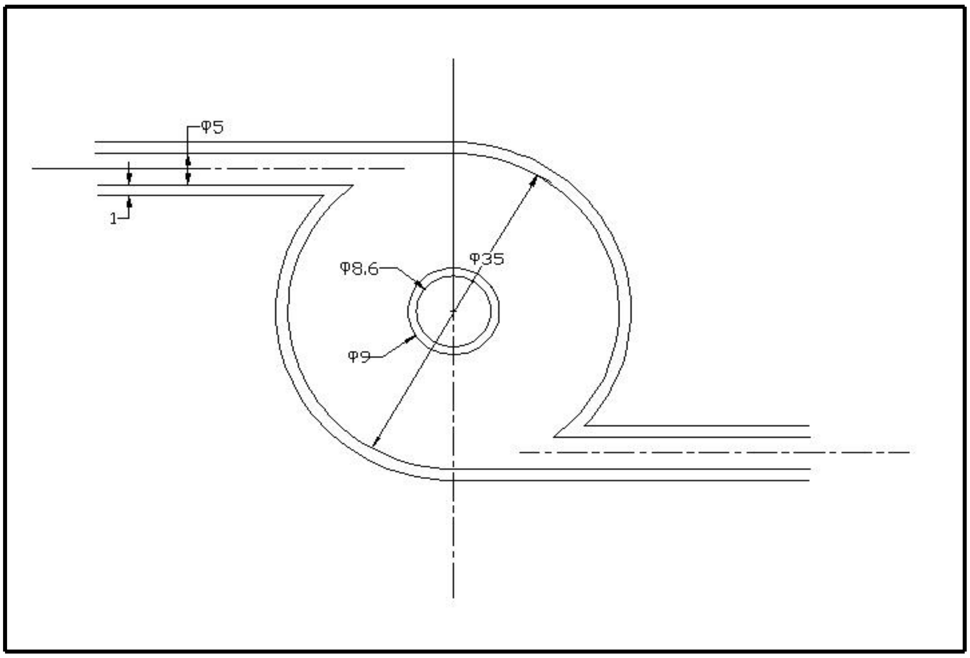

Figure 3.2 Bottom view of the present burner system with swirl induced

The flame holder is attached to a conical chamber to which two symmetrical tangential inlets are added to facilitate the production of a swirling flow. All components are made of copper. The length of the flame holder is 100 mm, with a wall thickness of 1 mm. The axial flow passes through a 200 mm cylindrical aluminum equalizing chamber, which is filled with stainless steel beads to well regulate the flow and to prevent the flame from flashing back. It then flows vertically through the flame holder. There are two tangential flows introduced into the conical chamber to facilitate the generation of the swirling flow. The swirl intensity can be adjusted via correctly proportioning between these two streams.

3.2 SWIRL NUMBER CALCULATION

The most commonly used parameter for the characterization of a swirling flow is the Swirl number (S), which can be determined analytically or experimentally.

3.2.1 Analytical Approach

As suggested by Claypore and Syred [59], Swirl number is the ratio between the rate of angular momentum and the rate of axial momentum, divided by the tangential inlet radius, as shown in Equation (3.1):

$$S = \frac{\pi\ r_0 R}{A_t}\left(\frac{\dot{m}_t}{\dot{m}_\theta + \dot{m}_t}\right)^2 \qquad \text{. . . . . . (3.1)}$$

It was suggested by Syred and Beer [47] that the Swirl number can be calculated from the experimentally measured velocity and static pressure profiles. Chan et al. [49] derived the following expression from Equation (3.1):

$$S = \frac{\int UWr^2 dr}{R\int\left(U^2 - \frac{W^2}{2}\right) r dr} \qquad \text{. . . . . . (3.2)}$$

In their study, Laser Doppler Anemometry was also applied to measure the flame velocity to facilitate the calculation of Swirl number with Equation (3.2).

Tangirala et al. [4] applied Equation (3.1) in their investigation of swirl-stabilized flames, and the Laser Doppler Anemometry had also been used for the measurement of actual velocity profile. The geometric Swirl numbers as calculated from Equation (3.1) were greater than the experimentally measured Swirl numbers with a maximum deviation of 50 %.

In the present study, both flow visualization technique and Equation (3.1) have been applied for the determination of Swirl number.

3.2.2 Smoke flow technique

Smoke-flow technique has been used to visualize the flow field of a premixed open flame jet with different swirling intensities, in which one of the tangential streams is used to mix with smoke generated from a smoke generator. The mixture of smoke and air/fuel flows along the nozzle. Laser is applied to illuminate the vicinity of the burner exit to facilitate a clear visualization of the swirling flow and a quantitative analysis of the flow field. The scheme of the illuminating system is shown in Figure 3.3. A digital camera (Sony P-10) is then used to take the photograph of the flow pattern of the smoke/butane/air mixture, which provides the inclined angle of the swirling flow. It can be used to calculate the swirl number in the absence of a detailed velocity profile.

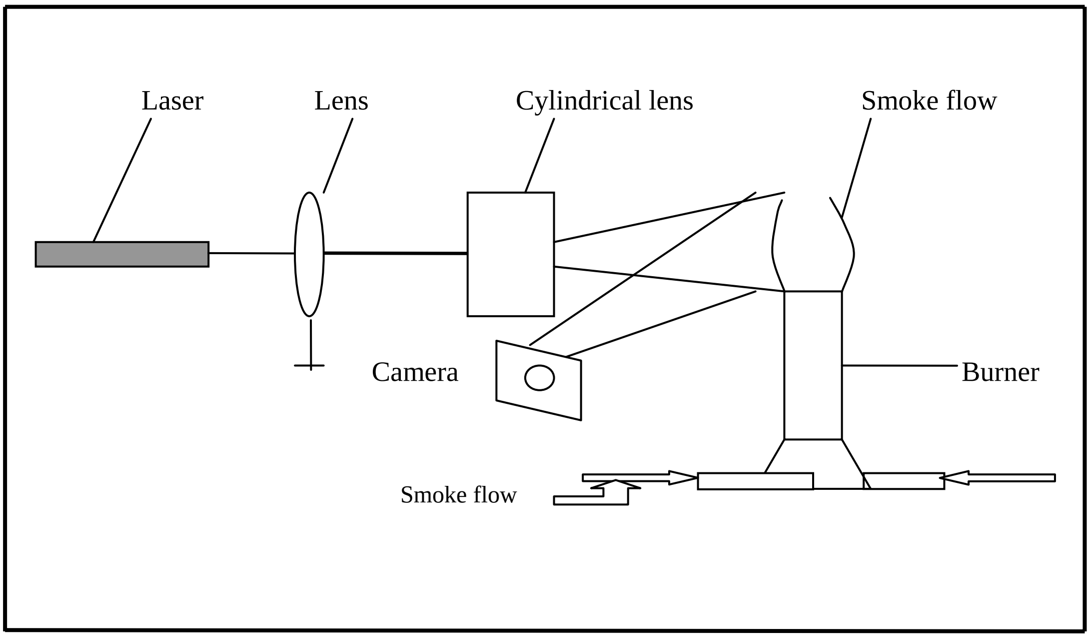

Figure 3.3 Illuminating system for smoke-flow visualization technique

Photographs of the flow pattern of the smoke/butane/air mixture taken under different operating conditions are indicated in Figure 3.4. The inclination angle of the flow deviated from the vertical axis (θ) is obtained directly on the photograph, with a maximum uncertainty of 1.5 º, which can be considered as rather accurate.

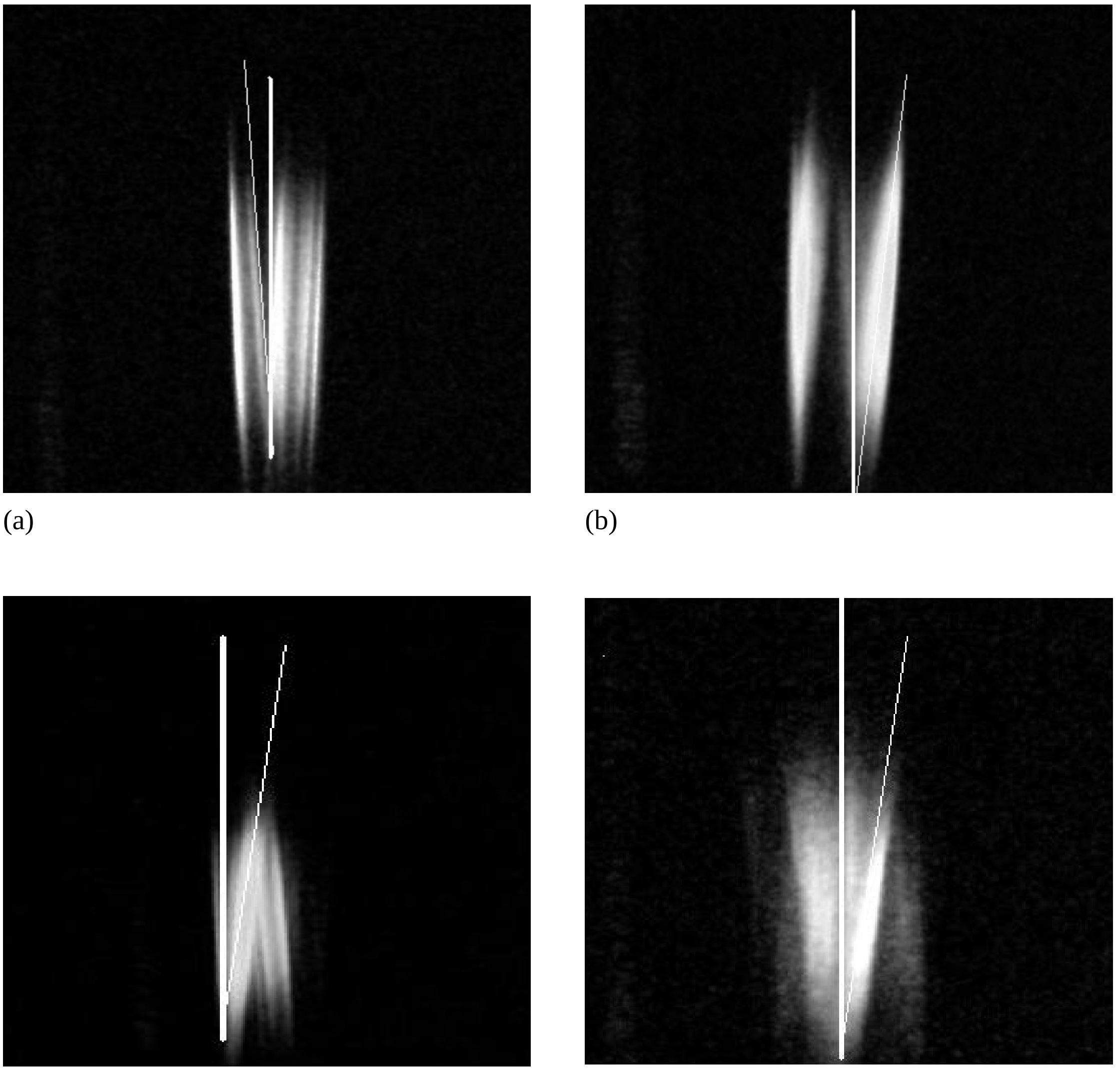

(a) (b) (c) (d)

Figure 3.4 Photographs obtained from smoke-flow visualization

(Re = 1200, Φ = 1, H/d = 2; (a) S = 0.075, (b) S = 0.109, (c) S = 0.144, (d) S = 0.171)

Due to the transient nature, the variation in local value and inclination of the velocity of the smoke/butane/air mixture at the nozzle exit, the axial component of the average velocity at the nozzle exit (U) is therefore measured instead of the swirling velocity itself. A rather reliable and accurate determination of the axial component of the average velocity of the smoke/butane/air mixture at the nozzle exit (U) can be obtained, with the aid of the measured flow rate and the Continuity Equation:

$$\rho UA = Constant \qquad \ldots\ldots (3.3)$$

The tangential component of the average velocity (*W*) of the smoke/butane/air mixture in Equation (3.2) can be obtained from the axial component of average velocity (U), with the aid of the inclination angle (θ), as shown in Figure 3.5.

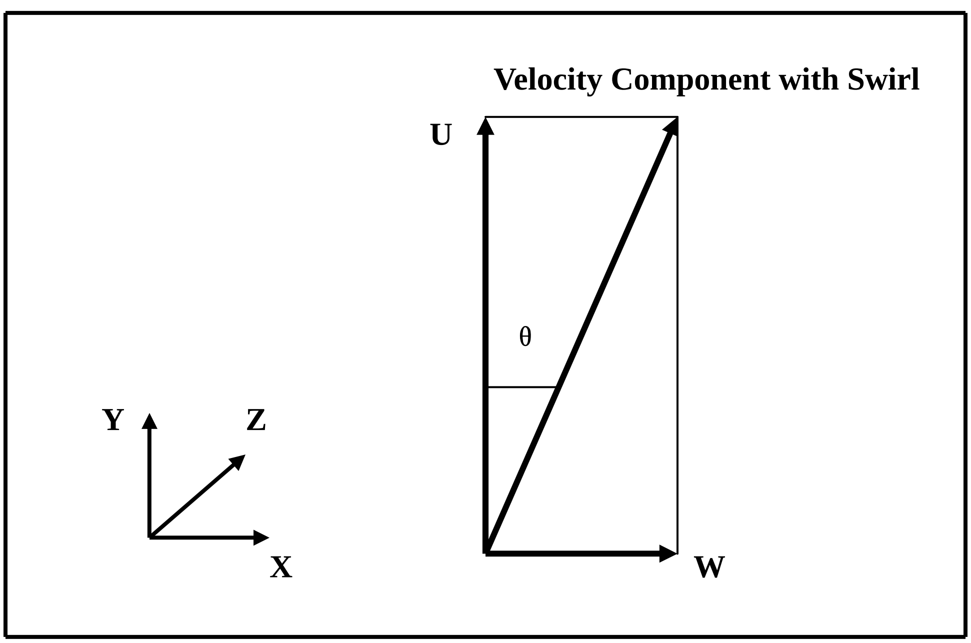

Figure 3.5 Velocity components at the nozzle exit

However, as indicated in Figure 3.6, the photograph obtained from the smoke flow technique becomes vague when the ratio between the tangential and axial components of the average velocity continues to increase and becomes too large. When the swirl intensity is further increased, the inclined angle can no longer be obtained clearly from the photograph. Thus, the smoke flow visualization technique is unable to produce reliable and accurate result under such situation, and it is the limitation of the technique.

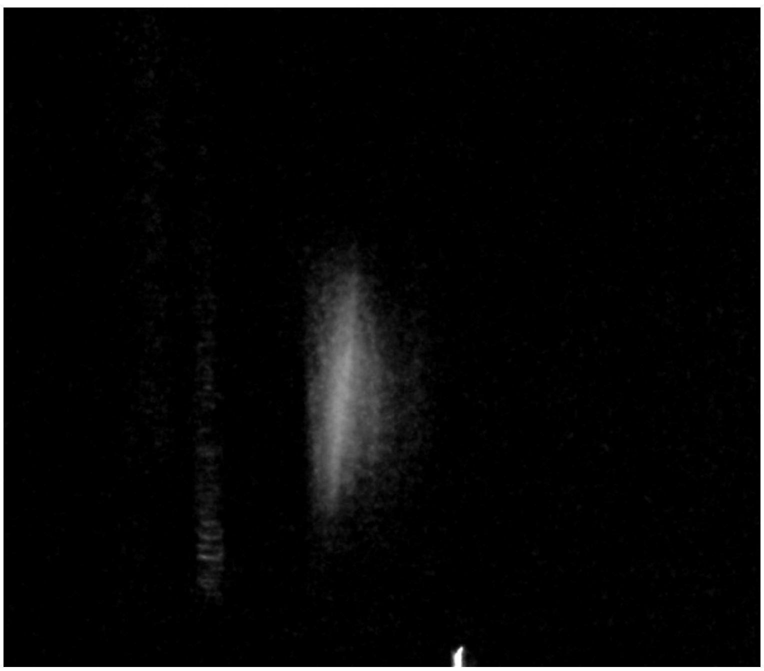

Figure 3.6 Photograph of the swirling flow when swirling intensity is too large

[(θ) is unable to determine]

Up to a Swirl number of 1.09 (Geometric Swirl number calculated from Equation (3.1) based on tangential/axial flow rate ratio), the Swirl number of a flow induced with a weak swirl can be obtained with the smoke flow visualization technique. However, when the swirling intensity is stronger and the corresponding Swirl number exceeds 1.09, the smoke flow visualization technique can no longer be used. The Swirl number of such a swirling flow will be obtained from Equation (3.1), because the axial and tangential mass flow rates used in the equation can be measured directly from the flow meters. According to the study of Tangirala et al. [4], the deviation of swirl numbers obtained by this method are much larger (may exceed 50 %) than those obtained from the visualization method at which the velocity profiles are measured by the LDA technique.

These two methods of determining the Swirl numbers will be further discussed together with the experimental results in the later chapters.

3.3 EXPERIMENTAL SETUPS TO INDUCE SWIRL

As discussed in the previous sections, the major experimental parameters to be measured in the present study are those required to study the thermal performance of a circular premixed butane/air impinging flame jet with swirl induced. These experimental parameters are: the air and fuel supplies of the burner, the local heat flux received by the impingement plate, the flame temperature, the impingement plate surface temperature, the axial and tangential components of the average velocity at the nozzle exit.

Once the flame has been ignited, the steady-state operating conditions can be reached within several minutes. It is very important for the measurements to be conducted after the steady-state conditions are achieved.

The basic configuration of the burner has been described in Section 3.1. In the present study, there were two different methods applied to generate the swirling flow. These two methods will be described clearly in the later sections, and the effects in using each of them on the thermal performance of the impinging flame jet system are also discussed. The major operating parameters will be varied in order to examine their effects on the heat transfer characteristics in both parts of the investigation. These major parameters are: the equivalence ratio (ϕ) of the butane/air mixture, the Reynolds number (Re) of the butane/air jet, the nozzle-to-plate distance (H/d), and the Swirl number (S). The ranges of these operating parameters used in the experimental work performed with each of these two experimental setups, are summarized in the following Table 3.1.

Test	**Reynolds Number (Re)**	**Nozzle-to-plate Distance (H/d)**	**Equivalence Ratio (ϕ)**	**Swirl Number (S)**
1. Separated Air and Fuel Flows	800	2	1	2.53
	1000	2	1	2.53
	1200	1.5; 2; 2.5; 3; 3.5; 4	1; 1.1; 1.2; 1.3; 1.4	1.32; 1.52; 1.78; 2.11; 2.53
	1500	2	1	2.53
	1700	2	1	2.53
2. Premixed Air and Fuel	800	2.5	1	0.144
	1000	2.5	1	0.144
	1200	2; 2.5; 3; 4; 5	1; 1.2; 1.4	0.075; 0.109; 0.144; 0.171
	1500	2.5	1	0.144
	1700	2.5	1	0.144

Table 3.1 Operating parameters applied in both experimental setups

In the first experimental setup, the axial flow contains only fuel and air is introduced via the two tangential inlets to mix with the axial fuel flow. It is found that with the use of this method, the swirl number can be adjusted to relatively high values while a stable flame is still maintained. It may be due to the large momentum associated with the rapid flow rate of air supplied through the tangential inlets, which enhances the mixing of the air and fuel to facilitate the consequent combustion process. However, there is a significant drawback in using this method: the swirl intensity is directly linked to the equivalence ratio. As the swirling intensity is regulated by changing the ratio between the tangential and axial flow rates, which are referred to the air and fuel supplies directly and hence the equivalence ratio is fixed accordingly.

In the second experimental setup, air and fuel are premixed before they are divided into two separate air/fuel streams: one will be supplied to the burner in the axial direction, whereas the other in the tangential direction. Each of these two streams can be individually regulated and measured with separate flow meter. The swirl number and equivalence ratio are no longer linked together and can be adjusted to different values, and their effects on the thermal performance of the impinging flame jet system can then be studied individually. A shortcoming of this design was that the operating range became smaller, compared with the first setup. Due to the absence of literature reporting the investigation on the heat transfer characteristics of impinging flame jet with swirl induced under low Reynolds numbers, the present study performed experiments on the thermal performance of both setups.

In the following studies, experiments will be carried out to investigate the heat transfer characteristics of the circular premixed butane/air impinging flame jet with swirl induced. Experimental results obtained from using both setups will be compared with each other, as well as the results obtained from previous work on similar impinging flame jet without the application of swirl.

CHAPTER 4

EXPERIMENTAL SYSTEMS

This chapter describes the construction of the test rig and the instrumentation used. The experimental system mainly includes the burner system, the impingement plate and the instruments for measurement. In this chapter, the operation ranges of the important parameters are described.

The flow visualization technique has been applied in the present study to determine the flow pattern of the swirling flow at the exit of the nozzle, and the study has also been reported. The last section of this chapter provides the methods applied to handle the experimental data and to estimate the possible experimental errors involved.

4.1 TEST RIG

The schematic drawing of the experimental system is shown in Figure 4.1. It mainly contains the air/fuel supply system, the burner system and the impingement plate.

4.1.1 Burner system

For the experimental setup having premixed butane/air mixture supplied through both axial and tangential inlets, butane and air are first premixed in the premixed chamber. The premixed butane/air mixture is then regulated in the equalizing chamber. The equalizing chamber is filled with stainless steel beads to well regulate the flow and to prevent the flame from flashing back. The butane/air mixture is then divided into two separate streams: one is supplied to the flame holder (conical part of the burner) through the axial inlet, whereas the other through the tangential inlets. These two separate streams will mix again in the flame holder and enter into the nozzle part of the burner, which is a 200 mm long stainless steel tube.

The burner system is firmly attached to a 3-D positioner so that it can be conveniently moved both horizontally and vertically to change the radial distance and the nozzle-to-plate distance respectively, in order to achieve a desirable position of the flame in relation to the impingement plate.

A slightly different arrangement is needed for the experimental setup having butane and air supplied separately to the flame holder. In this case, the air stream will be supplied directly to the tangential inlets of the flame holder without passing through the premixed chamber and the equalizing chamber.

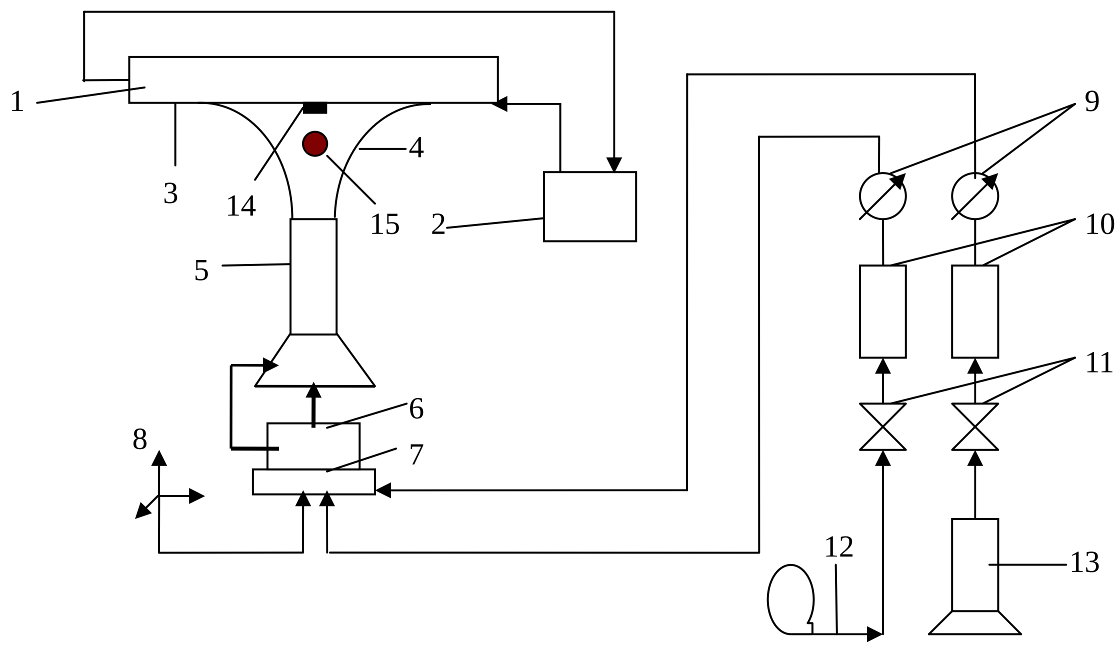

1. Cooling Water Jacket
2. Thermostat
3. Impingement Plate
4. Flame Jet
5. Flame Holder and Nozzle
6. Equalizing Chamber
7. Premixed Chamber
8. 3-D Positioner
9. Pressure Gauges
10. Flow Meters
11. Valves
12. Compressed Air Supply
13. Fuel tank
14. Heat Flux Sensor
15. B-type Thermo-probe

Figure 4.1 Schematics of the present experimental setup

4.1.2 Impingement Plate

The impingement target plate adopted in the present study is a smooth and highly polished copper plate with a total area of 400 x 400 mm^2 and a thickness of 8 mm. It is horizontally placed with a deviation of ± 0.5° to the ground. Copper is chosen as the material because of its excellent thermal conductivity.

Surface of the impingement plate is highly polished to achieve a very low surface emissivity, in order to minimize the contribution of non-luminous radiation. The impingement plate is uniformly cooled on its backside (non-flame side) by a cooling water jacket. The water's temperature is maintained at 38 ^{o}C through a thermostat to prevent the condensation of water vapor in the burned gases on the target surface, in order to minimize the condensation heat transfer [13, 14 and 58].

Detailed dimensions of the fabricated impingement plate are shown in Figure 4.2.

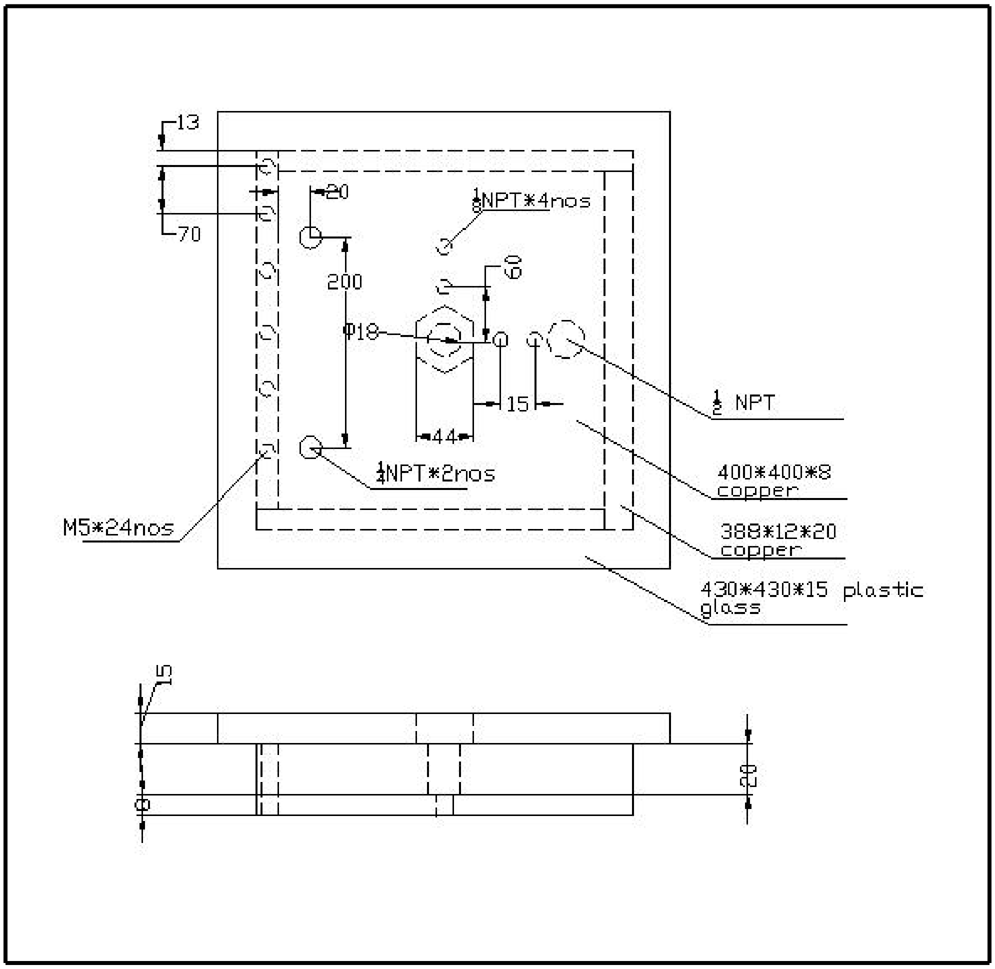

Figure 4.2 Fabrication details of the impingement plate

4.2 MEASUREMENT INSTRUMENTS

4.2.1 Flow Monitoring and Measurement

During the experimental investigations, the mass flow rates of air and butane gas supplies were closely monitored and measured with flow meters (see Figure 4.3) having an accuracy of ± 2 %. While the inlet pressures of air and butane gas were regulated by several regulators. The flow meters manufactured by the Gilmont Co. Ltd. were well calibrated before the experiment by using a piston flow calibrator corresponding to different fluid types (i.e. air, fuel or premixed flow) and different inlet pressures. The resolution of the flow meter is 0.1 lb/min within the range of 5 lb/min.

Figure 4.3 Flow meters for flow rate measurements of air and fuel

4.2.2 Heat Flux Measurement

The heat flux transferred from the flame to the impingement plate is an important parameter to quantify the heating performance of the impinging flame. In the present study, the local heat flux received by the impingement plate was measured by a heat flux sensor (Vatell Heat Flux Micro-sensor, Model: HFM-7E/H, Serial No.: 1310), which was connected to a pre-calibrated amplifier (Model: AMP-6). Two groups of data can be obtained from the readings. One is the HFS value, which corresponds to the heat flux value; while the other is the RTS value, which provides the surface temperature of the heat flux sensor. A T-type thermocouple is installed at the centre of the heat flux sensor for the temperature measurement. All the recorded readings are then converted from the voltage signal output of the sensor, by using a computer program (i.e. Personal Data acquisition view) provided by Vatell.

The heat flux sensor was mounted in a small cavity fabricated at the centre of the impingement plate, with an effective diameter of 6.35 mm, as shown in Figure 4.4. The cooling-water system installed at the backside (non-flame side) of the impingement plate prevents the sensor to be over-heated. The accuracy of the heat flux sensor as specified by the manufacturer is ± 1 %.

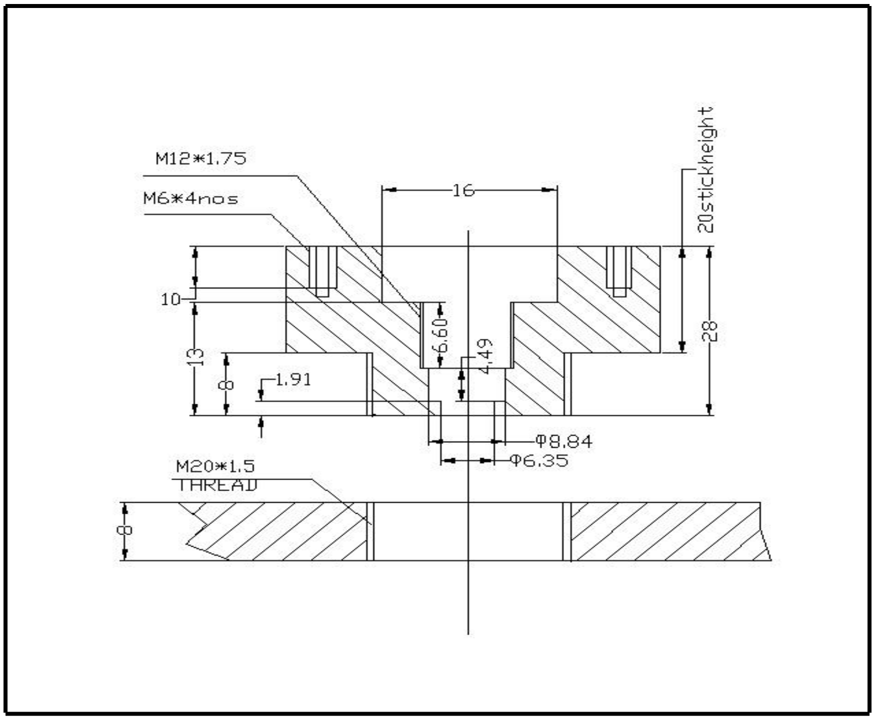

Figure 4.4 Fabrication of heat flux sensor holder

4.2.3 Gas Temperature Measurement

It is difficult to decide the appropriate reference temperature for the definition of the convective heat transfer coefficient [17]. Adiabatic flame temperature can be adopted but it is usually much higher than the actual value because of the assumptions of no heat losses and occurrence of perfect combustion. According to Dong et al. [9 – 12], the gas temperature at the location of 5 mm below the impingement plate was adopted to be the local flame temperature as reference. It was suggested to be the location very close to but was not in contact with the impingement plate surface. These local temperatures were measured by a T-type thermocouple.

The present study adopted the same method of measurement and definition. The flame temperatures (T_f) were measured by using a bare-wire B-type thermocouple with a diameter of 0.25 mm, which was located at 5 mm right below the impingement plate as shown in Figure 4.5. The temperature values were then corrected for convection and radiation effects by using the method proposed by Bradley and Matthews [44], with an accuracy estimated to be ±5 %.

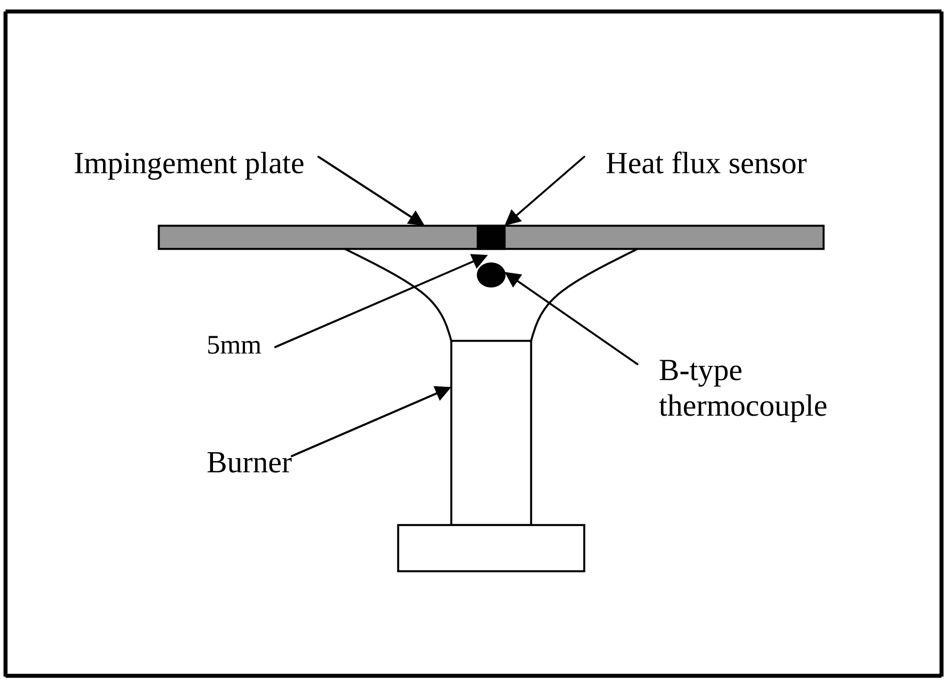

Figure 4.5 Arrangement of thermocouple for flame temperature measurement

4.2.4 Data acquisition

The heat flux and temperature data were both recorded by a computer recording program (i.e. Personal Data acquisition view), with a frequency of 2 scans per second within a duration of 120 seconds. The recorded heat fluxes and temperatures were then averaged to provide the values adopted for presentation. Due to the highly transient nature of the flame, it is necessary to average a large number of readings in order to provide reliable and consistent results in temperature and heat flux measurements.

4.3 HANDLING OF EXPERIMENTAL DATA

The equivalence ratio of the air/fuel mixture in the combustion process is pre-determined according to the readings of the flow meters. It is defined as:

$$\phi = \frac{(A/F)_{stoic}}{(A/F)} \qquad \text{......} (4.1)$$

Since the swirl applied in the present study is relatively weak, the swirling flame is still stabilized at the rim of the nozzle exit. Under the operation conditions of the present study, it should seldom demonstrate the characteristics of a turbulent flame. The present investigation was conducted essentially under the laminar flow and occasionally transitional conditions.

The flame jet exit Reynolds number is evaluated based on the unburned butane/air mixture:

$$R_e = \frac{ud\rho_{mix}}{\mu_{mix}} \qquad \ldots\ldots (4.2)$$

In Equation (4.2), " μ_{mix} " can be calculated according to Ikoku [60]:

$$\mu_{mix} = \frac{\sum(\mu_i Y_i \sqrt{M_i})}{\sum(Y_i \sqrt{M_i})} \qquad \ldots\ldots (4.3)$$

Forced convection has been identified to be the most crucial heat transfer mechanism in the premixed gas-fired impinging flame [8 – 12], with the reasons presented in the later section. Similarly, in the present study on swirling premixed butane/air impinging flame jet, radiation and TCHR can be assumed negligible when forced convection is most dominant and the local Nusselt number (i.e. non-dimensional heat transfer coefficient) is therefore defined as:

$$N_u = \frac{hd}{\tilde{k}(T)} \qquad \ldots\ldots (4.4)$$

The convective heat transfer coefficient "*h*" can be obtained from the Newton's law of cooling:

$$h = \frac{\dot{q}}{T_f - T_p} \quad \text{...... (4.5)}$$

While the thermal conductivity of the combustion gas "*k*" is a weighted average value related to the gas temperature as shown:

$$\tilde{k} = \frac{1}{T_f - T_p} \int_{T_p}^{T_f} k(T)\, dT \quad \text{...... (4.6)}$$

Equations (4.4) and (4.5) are combined to give the definition of the local Nusselt number in the present study:

$$N_u = \frac{\dot{q}\, d}{(T_f - T_p)\tilde{k}(T)} \quad \text{...... (4.7)}$$

As indicated in the study of Beer and Chigier [56], for a gas-fired flame jet impinging directly to a target surface, around 90% of the heat should be transferred by convection. In many studies of the impinging flame jet heat transfer, the non-luminous radiation is usually assumed negligible. Moreover, the heat transfer mechanism of TCHR (Thermo-Chemical-Heat-Release) is assumed to be less important in the premixed gas-fired flame jet heat transfer since the flame temperature is rather low [14]. So the area-averaged heat flux can be derived from the total amount of heat transfer to the impingement plate ($\dot{Q}$), which is obtained through integration of the local heat flux ($\dot{q}$) over the impingement area on the plate under consideration as shown in Equation (4.8):

$$\dot{Q} = \int_0^R 2\pi r \dot{q} dr \qquad \text{...... (4.8)}$$

Thus, the average heat flux $\bar{\dot{q}}$ can be expressed by:

$$\bar{\dot{q}} = \frac{\dot{Q}}{\pi R^2} = \frac{\int_0^R 2\pi r \dot{q} dr}{\pi R^2} \qquad \text{...... (4.9)}$$

In Equation (4.9), "*R*" is the largest radial distance away from the stagnation point in the present investigation, which indicates the magnitude of the impingement area. Substitute Equation (4.9) into Equation (4.7), the area-averaged Nusselt number can be shown to be:

$$\overline{Nu} = \frac{\int_0^R \frac{2\pi r \dot{q} dr}{T_f - T_p}}{\pi R^2} \cdot \frac{d}{\tilde{k}(T)} \qquad \text{...... (4.10)}$$

In the study of the impinging flame jet with induced swirl, the swirl number is an important parameter. Claypole and Syred [59] defined the swirl number as:

$$S = \frac{\pi \ r_0 R}{A_t} \left(\frac{\dot{m}_t}{\dot{m}_\theta + \dot{m}_t}\right)^2 \qquad \text{...... (4.11)}$$

In the present study, the swirl number would also be calculated by Equation (4.12) according to the work of Chan et al. [49]:

$$S = \frac{\int UWr^2 dr}{R\int \left(U^2 - \frac{W^2}{2}\right) rdr} \qquad \text{. . . . . . (4.12)}$$

4.4 ERROR ANALYSIS

Heat fluxes and temperatures recorded by the heat flux sensor and thermocouple were collected via the data acquisition system as described in Section 4.2.4. They were both recorded via a computer recording program (i.e. Personal Data acquisition view), with a frequency of 2 scans per second within a duration of 120 seconds. The recorded heat fluxes and temperatures were then averaged to provide the final values.

Three experiments were conducted under the same operating conditions to ensure the reliability and repeatability of the results. Every presented value is the average of the recorded data in the three experiments.

The uncertainly analysis had been carried out based on the method suggested by Kline and McClintock [61], with a confidence level of 95 %. The instrumentation errors of the present experimental investigation were analyzed. The minimum and maximum uncertainties in the surface temperature measurements are respectively 3.1 % and 6.7 %. The measured flame temperature uncertainties vary from 2.4 % to 10.6 %. The minimum and maximum deviations from the mean value of the local heat flux measurements are

4.2 % and 13.3 % respectively. The uncertainty of the visualization method mainly lies in the determination of the swirling angle. As indicated in Figure 4.6, the inclined angle determined by the smoke flow technique varies within the range of ± 1.5º. By summarizing all the errors involved, the maximum uncertainty of the present experimental study is estimated to be ± 16 %.

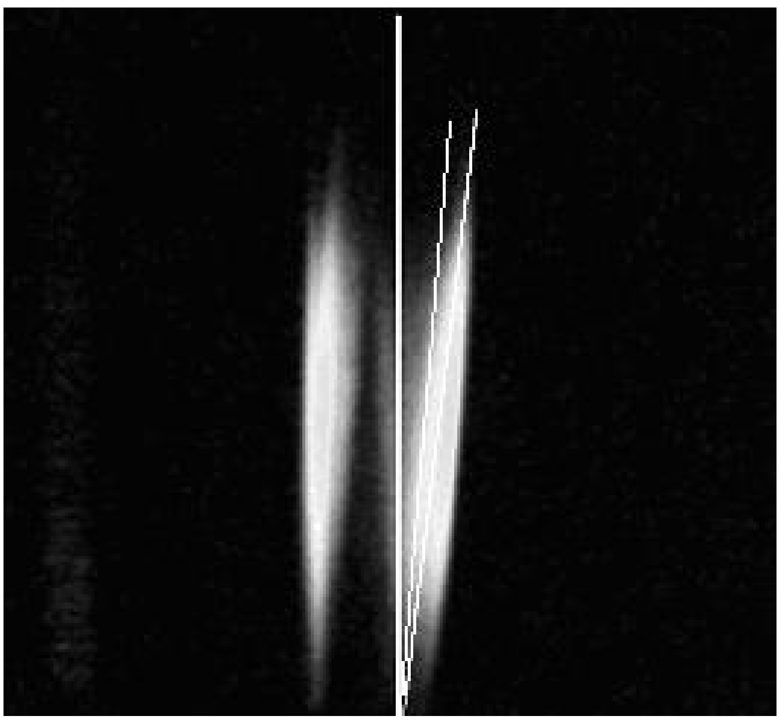

Figure 4.6 Uncertainty in the inclined angle determination

CHAPTER 5

EXPERIMENTAL STUDY WITH SETUP – I

As mentioned in Chapter 3, there were two experimental setups used to generate the swirling flow. In the first experimental setup, air is introduced via the two tangential inlets to mix with the axial fuel flow. In the second experimental setup, air and fuel are previously premixed before they are divided into two separate air/fuel streams: one will be supplied to the burner in the axial direction, whereas the other in the tangential direction.

This chapter reports the experimental results obtained by using the first experimental setup: the axial flow contains only fuel whereas air is tangentially admitted through the tangential inlets. The air and fuel are then mixed in the conical chamber before they are burned at the nozzle exit. In this chapter, the local heat flux distributions under different operating conditions are shown, so that the average heat fluxes can be obtained which provide a better criterion for comparison. The effects of different parameters: Reynolds number (*Re*), equivalence ratio (Φ) and the nozzle-to-plate distance (*H/d*), on the thermal performance of a premixed butane/air circular impinging flame jet with induced swirl, are discussed. Then, the results are compared with those of the similar non-swirling impinging flame jet operating under the same experimental conditions.

5.1 FLAME SHAPE

Figure 5.1 shows the flame shapes of a swirling flame, which are indicated from the photographs taken by a digital camera. It is observed that a stable flame can be produced by inducing swirl.

Comparing Figures 5.1 (a) and (b), the flame length is found to increase when burning a fuel-rich mixture. When the equivalence ratio is increased, the flame becomes longer. The heating around the stagnation point is reduced due to the incomplete combustion of fuel there as the nozzle-to-plate distance is maintained unchanged. However, there is more unburned fuel consumed at locations away from the stagnation point on the plate, which leads to a wider spread of the luminous flame.

Moreover, impingement causes more species including oxygen and unburned fuel to flow outwards along the radial direction away from the stagnation point, such phenomenon becomes more obvious as the flame length is increased. In this case, more fuel will be consumed towards the wall-jet region, which results in a more uniform distribution of heat flux on the impingement plate.

Comparing Figures 5.1 (a) and (c), as Reynolds number is increased, the flame is observed to become brighter which implies the occurrence of a higher flame temperature and hence a higher heat transfer. It agrees with the fact that heat transfer is enhanced with the increasing Reynolds number.

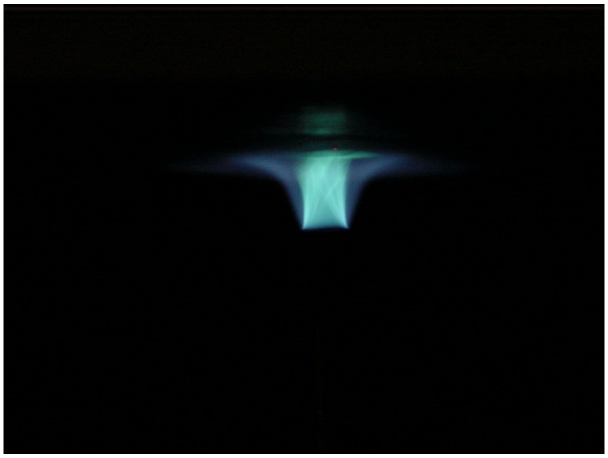

Figure 5.1 (a)   Flame shape

(Re = 1200, ϕ = 1.0, S = 2.53)

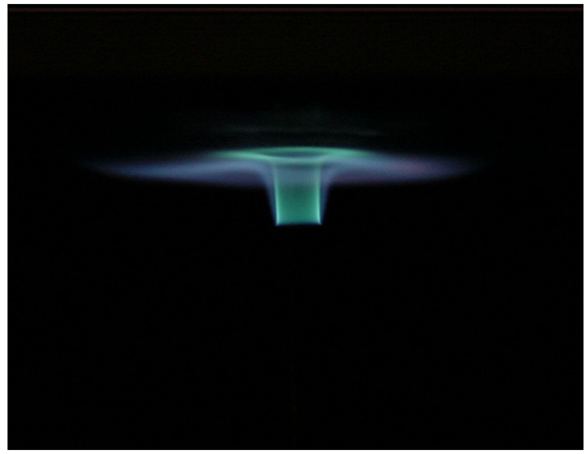

Figure 5.1 (b)   Flame shape

(Re = 1200, ϕ = 1.3, S = 1.52)

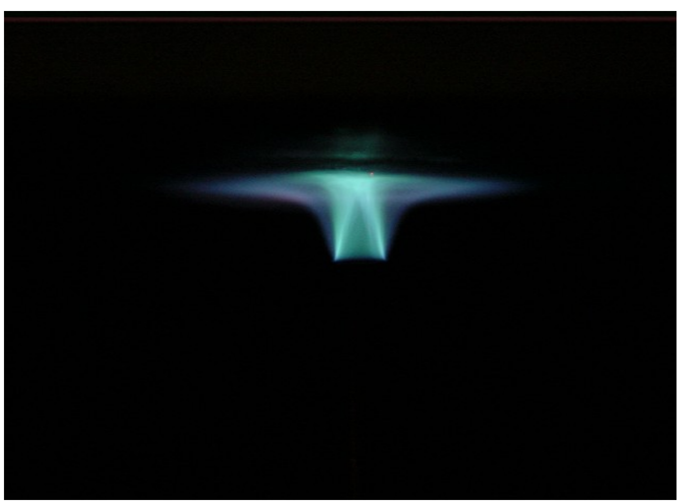

Figure 5.1 (c)   Flame shape (Re = 1500, ϕ = 1.0, S = 2.53)

5.2 LOCAL HEAT FLUX DISTRIBUTION

Previous research works on the application of induced swirl to combustion are essentially concerned with open diffusion flames operating at large-scale, high-pressure and highly turbulent-flow conditions. Investigations on swirling impinging flame jets have rarely been reported, especially those operating with low Reynolds numbers. The present experimental study was conducted to investigate the heat transfer characteristics of a small-scale circular premixed butane/air impinging flame jet with swirl induced.

A parametric study had been performed to identify the ranges of experimental parameters to be adopted in the present study. It was found that a swirling impinging flame can be operated with good stability over rather wide ranges of Reynolds numbers and equivalence ratios. It was also identified that the swirling impinging flame is able to produce a very symmetrical heat flux distribution around the stagnation point of the impingement plate. So the heat flux results are presented as radial distribution away from the stagnation point (i.e. centre point) on the impingement plate.

In the present experimental study, effect of Reynolds number (Re) on the heat flux distribution on the impingement plate impinging upon by a swirling flame jet was firstly examined, with Re ranging from 800 to 1700 at a nozzle-to-plate distance of 2d under the stoichiometric condition (Φ= 1). Then, effect of the nozzle-to-plate distance (H/d) on the heat flux distribution was investigated by varying from H/d = 1.5 to H/d = 4, when Re equals to 1200 and Φ is fixed at unity.

Following this, effect of the equivalence ratio (Φ) on the heat flux distribution was studied by varying the equivalence ratio from Φ = 1 to Φ = 1.4, to cover stoichiometric to fuel-rich combustion, at Re = 1200 and H/d = 2. In this experimental setup, the ratio between tangential air flow and axial fuel flow determines not only the equivalence ratio but also the swirl number, according to Claypole and Syred [59]. So the effect of swirling intensity of the impinging flame jet with swirl induced on the heat flux distribution can also be explored through this study.

5.2.1 Effect of Reynolds number

Figure 5.2 demonstrates the local heat flux distribution along the radial direction on the impingement plate under different Reynolds numbers at an equivalence ratio of $\Phi = 1$, a nozzle-to-plate distance of H/d = 2 and a Swirl number of S = 2.53. The flame is believed to extend from the laminar-flow to transitional conditions.

It is indicated from the distribution that the impinging flame jet with swirl induced is able to produce a symmetrical and uniform heat flux distribution around the stagnation point of the impingement plate. The peak heat flux occurs at a location at or close to the stagnation point. When Reynolds number is increased, the heat flux value on the entire impingement area including the stagnation and wall-jet regions increases as the turbulence in the reacting flow becomes greater. Firstly, mixing of the air and fuel is enhanced by the increasing turbulence which results in a more complete combustion.

Secondly, the larger supply of air/fuel mixture provides more reactive gas species around the stagnation point, so that more heat is generated during the combustion process.

Moreover, use of the swirling flame provides a larger space for the combustion to become more complete within the same distance between the nozzle exit and the impingement plate surface. However, when the Reynolds number increases continuously to the transitional condition at Re = 1700, as suggested by Dong et al. [12], heat flux value around the stagnation point is found to decrease instead of increase continuously. The flame length increases with the increasing Reynolds number, and the same nozzle-to-plate distance becomes too small for the complete combustion to take place. Thus, there is some relatively low temperature unburned air/fuel mixture impinging upon the stagnation point of the impingement plate surface, which leads to the occurrence of a lower local heat flux at this point by comparing the heat flux distributions at Re = 1500 and Re = 1700.

The unburned air/fuel mixture will later be consumed at the wall-jet region, leading to a higher local heat flux there at Re = 1700. Such phenomenon is also shown in Figure 5.2.

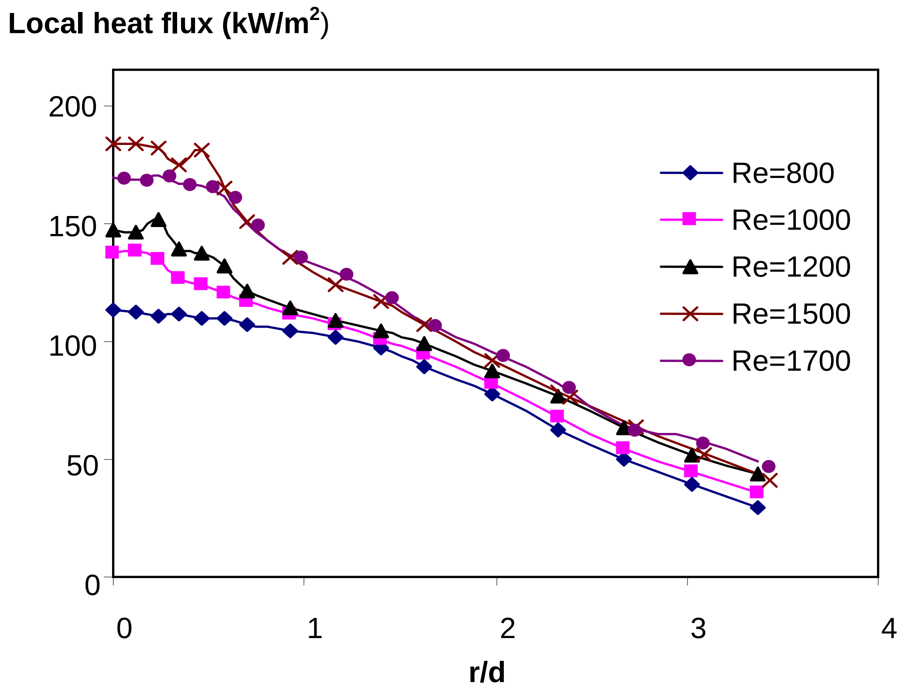

Figure 5.2 Radial heat flux distribution under different Reynolds numbers

(Φ = 1, H/d = 2, S = 2.53)

Figure 5.3 shows a comparison of the area-averaged heat flux on the impingement plate under different Reynolds numbers at $\phi = 1$, H/d = 2 and S = 2.53. It is found that the heat flux received by the plate increases with Re. As mentioned previously, at high Re the flow turbulence enhances the mixing of air and fuel and hence enhances the convection heat transfer. Moreover, more fuel is burned as Re is increased. It is noted that the increase in average heat flux is stopped at Re = 1700, and the reason has been explained in the previous section.

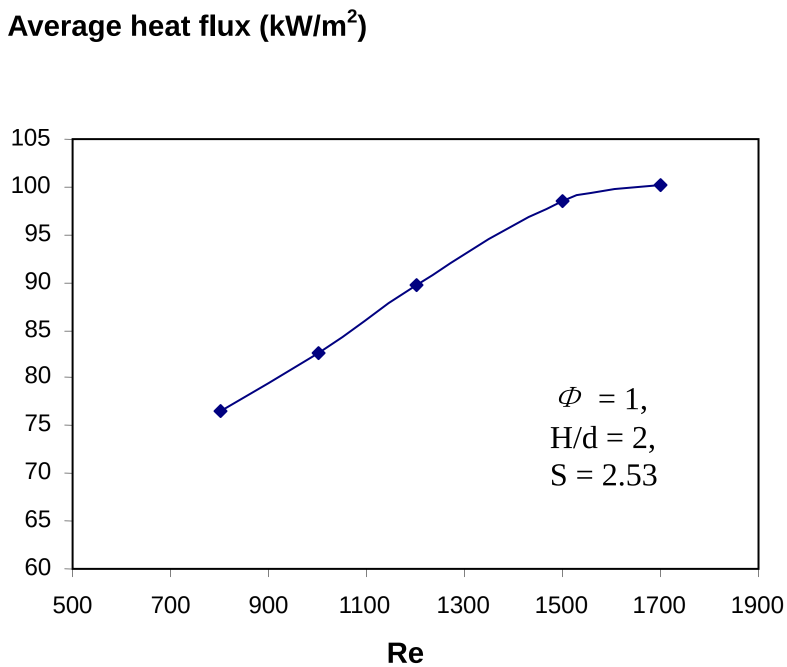

Figure 5.3 Area-averaged heat flux on the impingement plate under different Reynolds numbers (Φ = 1, H/d = 2, S = 2.53)

5.2.2 Effect of nozzle-to-plate distance

The effect of nozzle-to-plate distance is investigated by comparing the local heat flux distribution and the area-averaged heat flux on the impingement plate at Φ = 1, Re = 1200 and S = 2.53. The results are shown in Figure 5.4 and Figure 5.5, respectively. The heat flux distribution around the stagnation point becomes more uniform when the burner is moved away from the impingement plate, i.e. the H/d ratio is increased. But the local heat flux there is lower. For the H/d ratio around 2.0, the high-temperature combustion gases impinge directly onto the plate surface to give the highest local heat flux at the stagnation point, as shown from Figure 5.4. However, as the H/d ratio is either decreased to 1.5 or increased to 2.5, a lower heating value is obtained around the stagnation point.

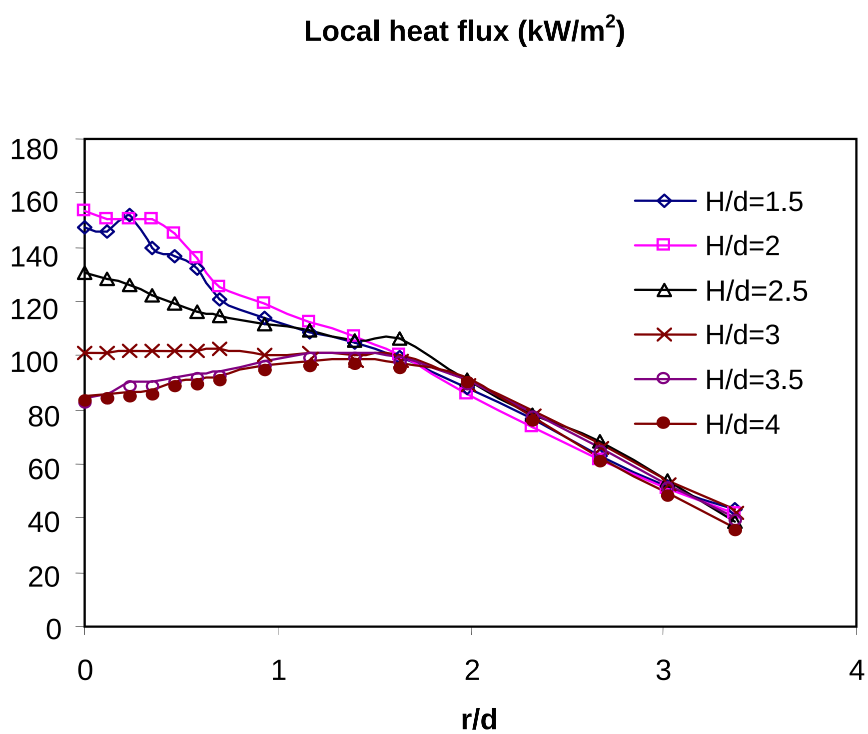

Figure 5.4 Radial heat flux distribution under different nozzle-to-plate distances (ϕ = 1, Re = 1200 and S = 2.53)

It can be concluded that the nozzle-to-plate distance should not be too small, in order to provide sufficient space for the flame to become fully-developed. However, the heat flux received by the impingement plate surface decreases when the distance between the potential core of the flame and the plate surface is excessively large. When the H/d ratio is varied from 1.5 to 4, there is almost no difference in local heat flux received by the impingement plate at its wall-jet region (i.e. r/d > 1.7), except that obtained at H/d = 2.5 is slightly higher, which is a normal phenomenon of premixed impinging flame jet as suggested by Dong et al. [12].

The area-averaged heat flux values obtained on the impingement plate surface are shown in Figure 5.5. It indicates that the swirling impinging flame jet is able to produce higher average heat flux at the small H/d ratios (i.e. from 1.5 to 2.5), while the maximum average heat flux is obtained at H/d = 2.5. As explained in the previous section, use of the swirling flame provides a larger space for the combustion to become more complete within the same nozzle-to-plate distance, hence higher heat flux is obtained at the small H/d ratios.

Besides, the introduction of swirl causes the flame tip to diverge so that the flame surface area at that point is enlarged as shown in Figure 5.1. When the nozzle-to-plate distance is large enough for the fully-development of the flame, not only the heat flux is increased and its distribution also becoming more uniform. However, further increasing the nozzle-to-plate distance will move the high-temperature outer layer of the flame away from the plate surface, which leads to a decline of the heating performance.

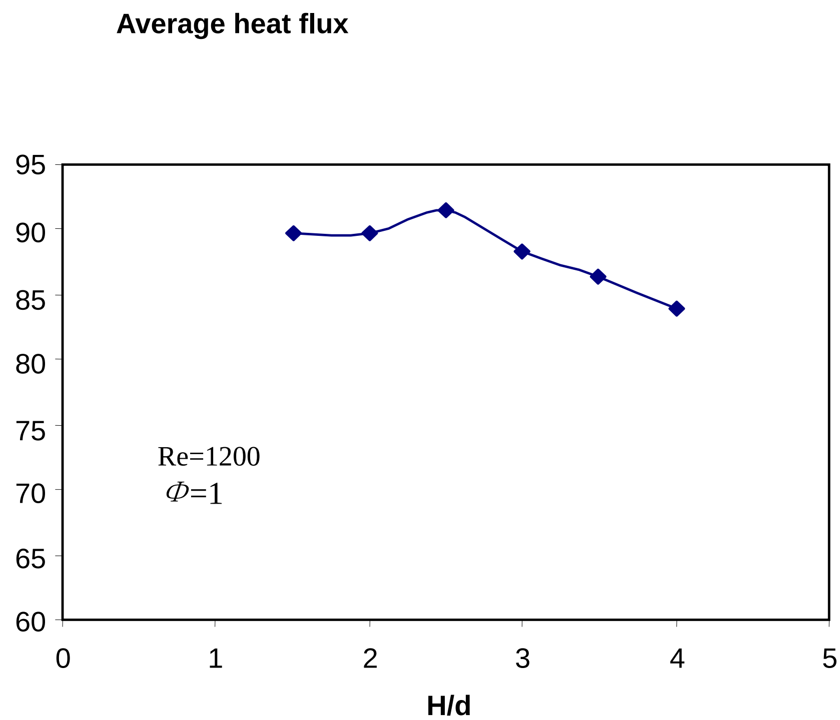

Figure 5.5 Area-averaged heat flux on the impingement plate under different nozzle-to-plate distances (ϕ = 1, Re = 1200 and S = 2.35)

5.2.3 Effect of equivalence ratio/Swirl number

It was concluded by previous researchers [13, 14 and 35] that the maximum heat transfer occurs at a slightly fuel-rich laminar condition for the circular non-swirling flame jet. In the present study on the impinging flame jet with swirl induced, the equivalence ratio is varied to observe its effect on the heating performance of the flame jet system.

Since the tangential air flow and axial fuel flow arrangement is used in this part of study, the air/fuel ratio and hence equivalence ratio is therefore linked directly to the Swirl number according to Equation (3.1):

$$S = \frac{\pi\ r_0 R}{A_t} \left(\frac{\dot{m}_t}{\dot{m}_\theta + \dot{m}_t}\right)^2$$

When more fuel is added to the axial flow, equivalence ratio of the air/fuel mixture increases but due to the decrease in the ratio of the tangential flow / axial flow, the Swirl number is reduced. At the stoichiometric condition (i.e. $\Phi = 1$), the corresponding Swirl number calculated via Equation (3.1) is as high as 2.53, so that the smoke-flow visualization technique can not be applied for the calculation of Swirl number.

The local heat flux distribution under different equivalence ratio and hence Swirl number, at H/d = 2 and Re = 1200 is shown in Figure 5.6. Relationships between equivalence ratio and Swirl number are provided in the following Table 5.1:

Table 5.1 **Direct Relationship Between "Φ" and "S" for Experimental Setup 1**

Equivalence Ratio	**Corresponding Swirl Number**
1.0	2.53
1.1	2.11
1.2	1.78
1.3	1.52
1.4	1.32

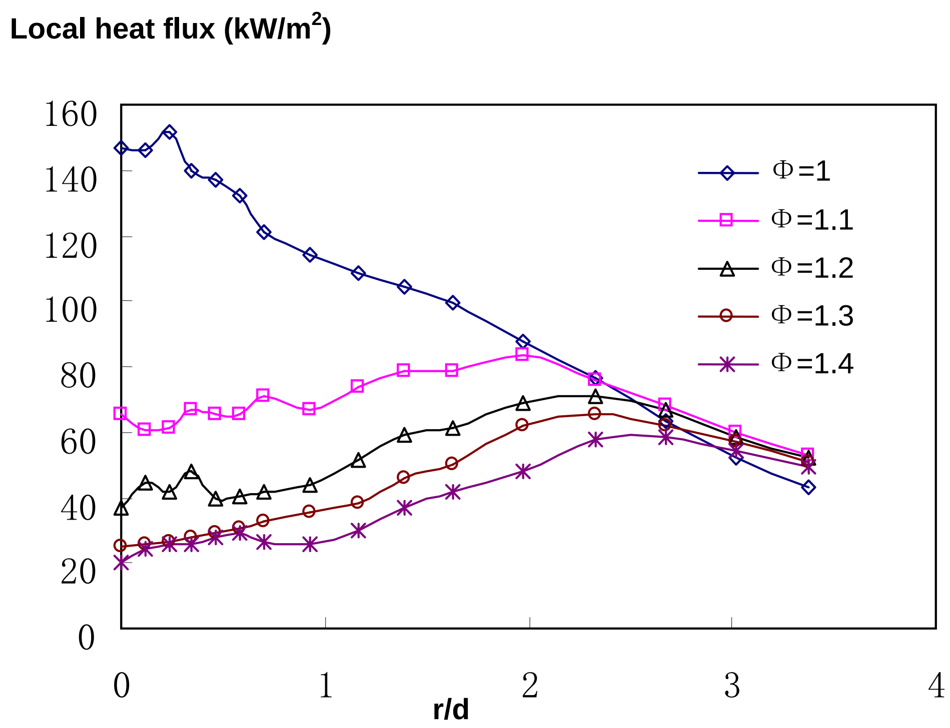

Figure 5.6 Radial heat flux distribution under different equivalence ratios and Swirl numbers (Re = 1200, H/d = 2)

Heat flux around the stagnation point decreases severely when the equivalence ratio increases from unity. The location of the peak heat flux also shifts outwards from the stagnation point of the impingement plate. Although the heat flux continues to decrease as the equivalence ratio is increased, their distributions are similar under the fuel-rich conditions.

When the air/fuel mixture varies from the stoichiometric to fuel-rich conditions, the increasing fuel supply will eventually becomes excessive leading to the occurrence of significant amount of relatively low temperature unburned air/fuel mixture at the stagnation point of the impingement plate. Moreover, a higher equivalence ratio implies a lower Swirl number, which leads to a poorer mixing of the air and fuel and hence the convection heat transfer is suppressed.

According to the study of Dong et al. [9 – 12], flame length of a premixed impinging flame jet is slightly increased when its equivalence ratio increases. As the flame length increases while the nozzle-to-plate distance is maintained constant, less space is therefore available for the combustion to become complete. The situation becomes worse as the induced swirl is reduced. There are more unburned air/fuel mixtures occurring at the stagnation point region, and they will be consumed in the later wall-jet region. Because of that, the location of peak heat flux is shifting outwards away from the stagnation point. It is worth to note that the heat flux distribution along the impingement plate has the similar trend with that of a non-swirling slot premixed impinging flame jet operating under fuel-rich conditions [13].

The area-averaged heat fluxes obtained on the impingement plate surface under various equivalence ratios and also Swirl numbers are compared and presented in Figure 5.7. The maximum heat transfer is found to occur under the stoichiometric condition and hence the highest Swirl number for the present experimental setup.

However, due to the direct linking between the equivalence ratio and the Swirl number of the air/fuel jet for the present experimental setup, their effects on the heat flux received by the impingement plate can not be separately identified. It is therefore a drawback of this arrangement.

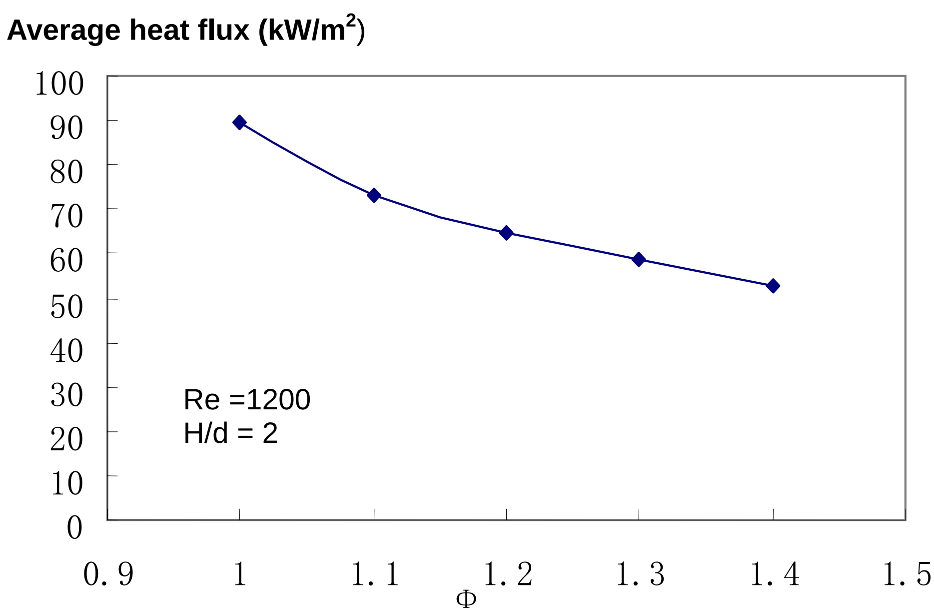

Figure 5.7 Area-averaged heat flux on the impingement plate under different equivalence ratios and Swirl numbers (Re = 1200, H/d = 2)

5.3 SUMMARY

Experiments were carried out to study the heat transfer characteristics of a circular premixed butane/air impinging flame jet with swirl induced via the first experimental setup. In this particular experimental setup, fuel is admitted into the burner via the axial inlet while air is supplied into the burner as separate streams through the two tangential inlets.

Effects of the Reynolds number of the air/fuel jet, the equivalence ratio of the air/fuel mixture, the Swirl number of the air/fuel jet and the nozzle-to-plate distance between the nozzle rim and the impingement plate surface, have been examined. For the present experimental setup, the swirl number is determined by the ratio between the tangential flow and the axial flow and is therefore directly linked to the equivalence ratio. Due to this direct linking, the effects of equivalence ratio and Swirl number on the heat flux received by the impingement plate can not be separately identified. It is a drawback of this arrangement.

Based on this part of experimental study, the following conclusions can be drawn:

1) The swirling flame is able to produce a more uniform heat flux distribution on the impingement plate around the stagnation point. Introduction of swirl causes the flame tip to diverge so that the flame surface area at that point is enlarged such that the heat flux distribution becomes more uniform.

2) When the Reynolds number is increased, the heat flux is enhanced. Firstly, it is due to the increasing supply of air and fuel. In addition, the mixing between air and fuel is enhanced because of the increasing turbulence.

3) The optimum nozzle-to-plate distance corresponding to the occurrence of the peak heat flux is H/d = 2.5. While in the previous studies on single circular premixed butane/air impinging flame jet without swirl induced [8 – 12], the best thermal performance is obtained when H/d = 6, which is much larger. Use of the swirling flame is able to provide a larger space for the combustion to become more complete within the same nozzle-to-plate distance, hence higher heat flux is obtained at the small H/d ratios.

4) When the equivalence ratio is increased, the air supply starts to become insufficient for the complete combustion to proceed. Occurrence of the relatively cool region consisting of significant unburned air/fuel mixture becomes obvious when the fuel supply is excessive for very fuel-rich air/fuel mixture. It reduces the heat flux received by the impingement plate. Besides, the Swirl number is also decreased as the equivalence ratio increases for the present experimental setup, which also provides a negative effect on the heat transfer to the plate from the impinging flame jet.

CHAPTER 6

EXPERIMENTAL STUDY WITH SETUP – II

This part of experimental study was conducted with the experimental setup II, in which air and fuel are previously mixed. The premixed butane/air mixture is then divided into two separate streams: one is admitted into the burner via the axial inlet, whereas the other is supplied into the burner through the two tangential inlets. Each of these two streams is monitored and controlled by a rotameter. A better mixing of air and fuel is expected to achieve before they reach the nozzle exit. Moreover, the swirl number determined by the ratio between the tangential flow and the axial flow is totally independent from the equivalence ratio so that the effects of these two parameters on the heat flux received by the impingement plate can be studied separately.

In this chapter, the local heat flux distributions on the impingement plate obtained under different operating conditions are reported, and the area-averaged heat flux received by the plate can then be calculated to facilitate comparison. The effects of different major parameters including Reynolds number (*Re*), equivalence ratio (Φ), nozzle-to-plate distance (*H/d*) and Swirl number (*S*) are investigated. The results obtained are compared with those obtained from the experimental setup I and the previous studies on similar circular premixed gas-fired impinging flame jets without swirl.

6.1. FLOW VISUALIZATION

As described in Chapter 3, a smoke-flow technique has been used to visualize the flow field of an open premixed butane/air flame jet with different swirl intensities. One of the tangential sub-streams is used to mix with smoke generated from a smoke generator. Laser is applied to illuminate the flow field to facilitate a clear visualization and quantitative analysis of the flow field.

The photographs are taken at different tangential/axial flow ratios. The Swirl number of the flow is then calculated with the aid of Equation (3.2). In the present study, the Swirl numbers are determined to be 0.075, 0.109, 0.144, and 0.171.

The swirl number under each operating condition is calculated according to Equation (3.2). It can also be obtained by the equation, i.e. Equation (3.1), provided by Claypole and Syred [59], in this case, they are 0.067, 0.112, 0.24, and 0.37, respectively. They are found to agree well with the values obtained from the flow visualization method when the swirl intensity is weak (i.e. comparing $S = 0.075$ with 0.067, and $S = 0.109$ with 0.112, giving a difference of only 10.7 % and 2.8 %). However, the Swirl numbers obtained from both methods have rather significant deviation from each other when the swirl intensity becomes larger (i.e. comparing $S = 0.144$ with 0.24, and $S = 0.171$ with 0.37, giving a difference of 66.7 % and 116.4 %).

When turbulence is enhanced due to the increasing swirl, the velocity profile becomes complicated as observed in the photographs and a clear observation is relatively difficult to obtain. In this case, the inclined angle obtained from the photograph may contain error. In addition, when the turbulence is enhanced, the flow decay increases so that the difference between the swirl number at the nozzle exit and that at the throat of the tangential inlets becomes very significant.

It is observed that very stable flame can also be produced by inducing weak swirl. There is no undesirable phenomenon observed including uplift, flash back and smoke production.

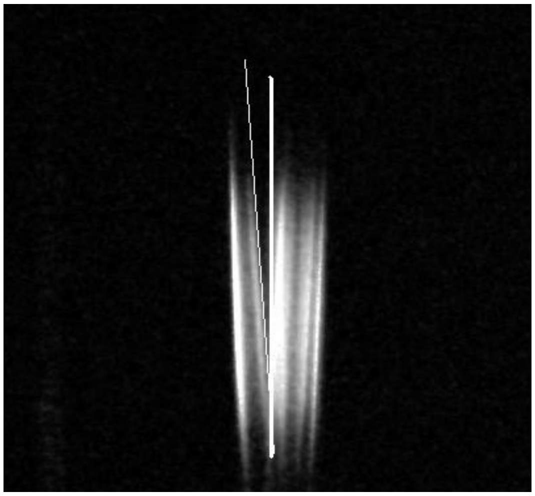

(a)

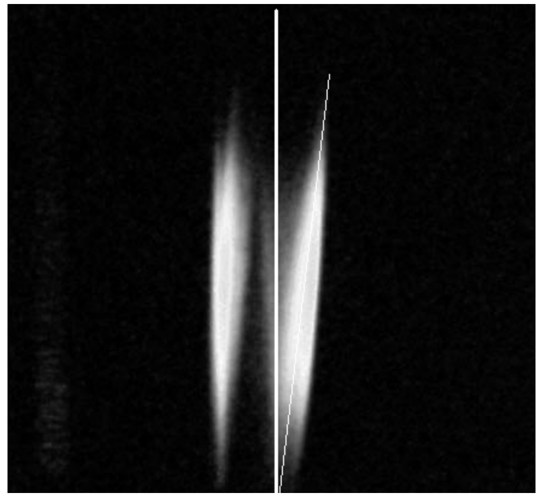

(b)

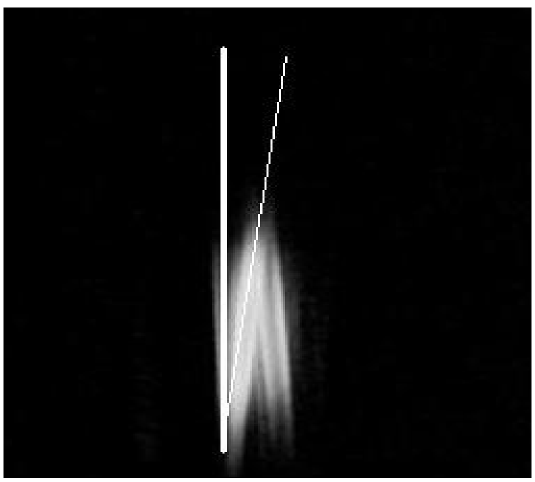

(c)

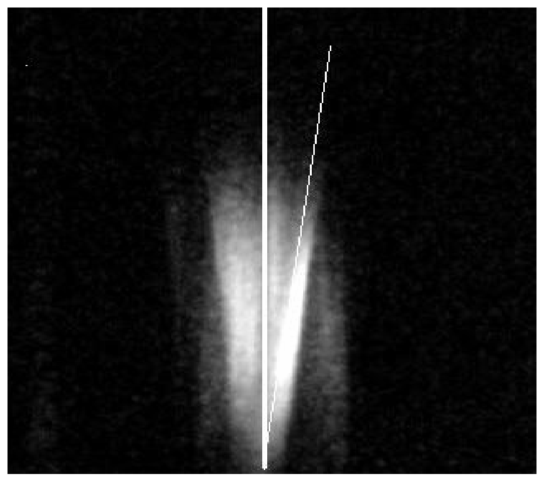

(d)

Figure 6.1 (a) to (d) Smoke-flow visualization of the open gaseous flows at the nozzle exit under different swirling intensities (Re = 1200):

(a) $\theta = 4.5^\circ$, u = 1.67 m/s, S = 0.075;

(b) $\theta = 6.5^\circ$, u = 1.54 m/s, S = 0.109;

(c) $\theta = 8.5^\circ$, u = 1.33 m/s, S = 0.144;

(d) $\theta = 10^\circ$, u = 1.21 m/s, S = 0.171.

6.2 LOCAL HEAT FLUX DISTRIBUTION

Air and fuel are first premixed in the equalizing chamber to provide more sufficient mixing. Local heat flux distributions on the impingement plate obtained under different operating conditions are compared, in order to examine the effects of different parameters on the heating performance of the impinging flame jet system with swirl induced.

Firstly, Reynolds number (Re) is varied from 800 to 1700 under the stochiometric combustion condition ($\Phi = 1$) at a fixed nozzle-to-plate distance ratio (H/d) of 2.5, as well as a fixed Swirl number (S) of 0.144. Then the nozzle-to-plate distance is varied from 2d to 5d at a Reynolds number of 1200 and an equivalence ratio of unity, whereas all four Swirl numbers have been used in this part of study.

Different swirling intensities have been adopted such that effects of the nozzle-to-plate distance and Swirl number are investigated, besides, their interactions can also be studied. Finally, the equivalence ratio is varied from 1.0 to 1.2 and 1.4 at Re = 1200 and H/d = 2.5, whereas the four Swirl numbers are again applied. Therefore the effect of equivalence ratio on the heat flux received by the impingement plate can be observed, as well as the interaction between equivalence ratio and Swirl number studied.

6.2.1 Effect of Reynolds number

Figure 6.2 presents the local heat flux distribution along the radial direction on the impingement plate obtained under different Reynolds numbers when the equivalence ratio $\Phi = 1$, the nozzle-to-plate distance ratio H/d = 2.5, and the Swirl number S = 0.144.

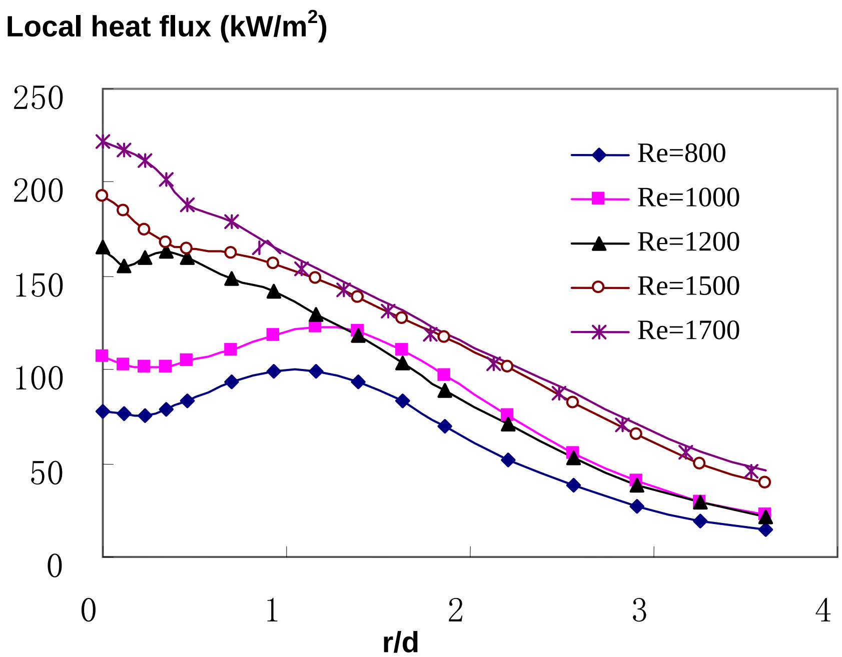

Figure 6.2 Radial heat flux distribution under different Reynolds numbers

($\Phi = 1$, H/d = 2.5 and S = 0.144)

It is obvious that as Reynolds number increases, the heat flux along the whole impingement area is increased. There are more high-temperature combustion gases impinging onto the impingement plate to enhance the heat transfer. The increasing turbulence leads to more rigorous mixing to facilitate a more complete combustion process. When the Reynolds number is low, for example Re = 800, the heat flux distribution around the stagnation point is rather uniform and shows some characteristics of a non-swirling laminar impinging flame jet. It is found that under a low Reynolds number and a low Swirl number, effect of inducing swirl on the thermal characteristics of a premixed butane/air impinging flame jet is less significant.

The area-averaged heat fluxes on the impingement plate obtained under different Reynolds numbers are compared and presented in Figure 6.3. It can be seen that the heat flux is increased with Reynolds number, at which a higher flow rate of air/fuel mixture implies that more reacting gases are brought to the combustion zone within the same time period. Also, it is noted that when Reynolds number is increased from 1200 to 1500, the heat flux value experiences a rather rapid augmentation. The swirling flow added to the turbulence of the flame may lead to the development of laminar flow into transitional flow at a lower Reynolds number compared with the non-swirling impinging flame jets.

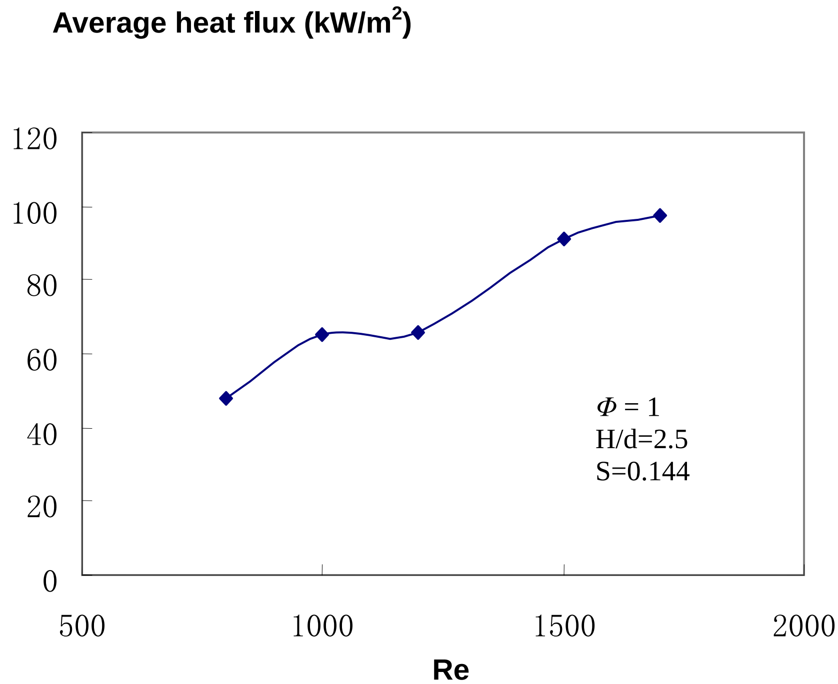

Figure 6.3 Area-averaged heat fluxes on the impingement plate under different Reynolds numbers (Φ = 1, H/d = 2.5 and S = 0.144)

6.2.2 Effect of nozzle-to-plate distance

Figures 6.4 (a) to (d) show the comparison of local heat flux distributions on the impingement plate obtained at various nozzle-to-plate distances under different swirling intensities at Re = 1200 and Φ = 1. Use of the induced swirl enhances the space between the nozzle exit and the impingement plate surface, such that more complete combustion can be achieved at the same nozzle-to-plate distance so that the heat transfer rate around the stagnation point is rather high even though at the rather small nozzle-to-plate distance of H/d = 2.

When the flame jet is operating under a laminar flow condition and a low swirling intensity the centrifugal force generated by the swirling flow results in a divergence of the flame. As a result, the flame surface area at the flame tip is enlarged. Hence the heat flux distribution is rather uniform around the stagnation point.

However, when the swirl intensity is rather low (i.e. $\theta = 4.5^{o}$ and S = 0.075), the central cool core of significant amount of unburned air/fuel mixture which is the characteristics of a non-swirling laminar impinging flame jet appears when H/d = 2. The swirl is too weak to effectively enhance the mixing so that when the nozzle exit is too close to the impingement plate, this unburned air/fuel mixture impinges directly onto the plate.

When the burner is moved away from the impingement plate, the longer distance between the nozzle exit and the impingement plate allows the flame to become fully-developed so that the cold core disappears and the local heat flux around the stagnation point becomes more uniform.

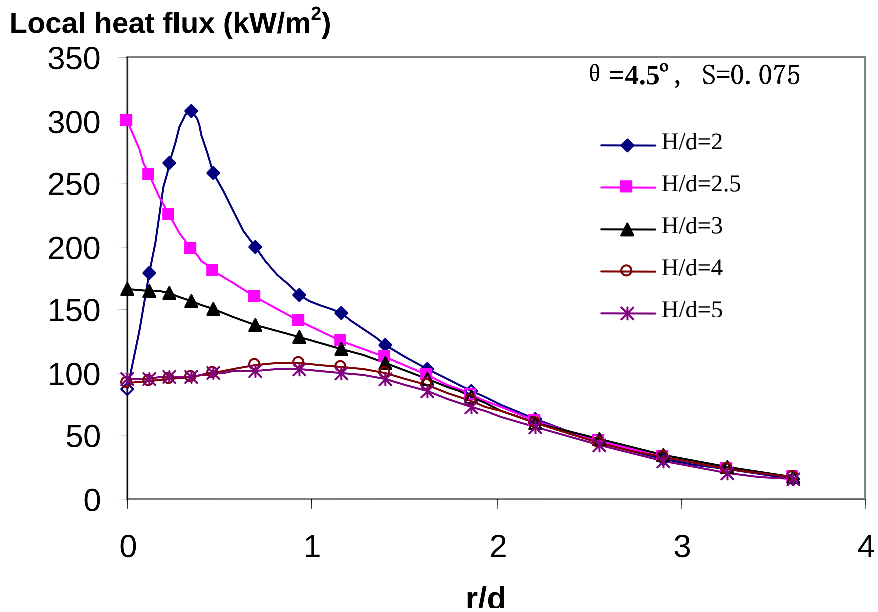

Figure 6.4 (a) Radial heat flux distribution at different nozzle-to-plate distances

($\Phi = 1$, Re = 1200 and S = 0.075)

In addition, influence of the nozzle-to-plate distance on the heat flux distribution at the stagnation region is rather similar when the Swirl number is increased from 0.075 to 0.171. One more thing to be noted is that the difference in local heat flux on the impingement plate caused by changing the nozzle-to-plate distance is rather small when the radial distance exceeds 1.7d away from the stagnation point (i.e. the wall-jet region).

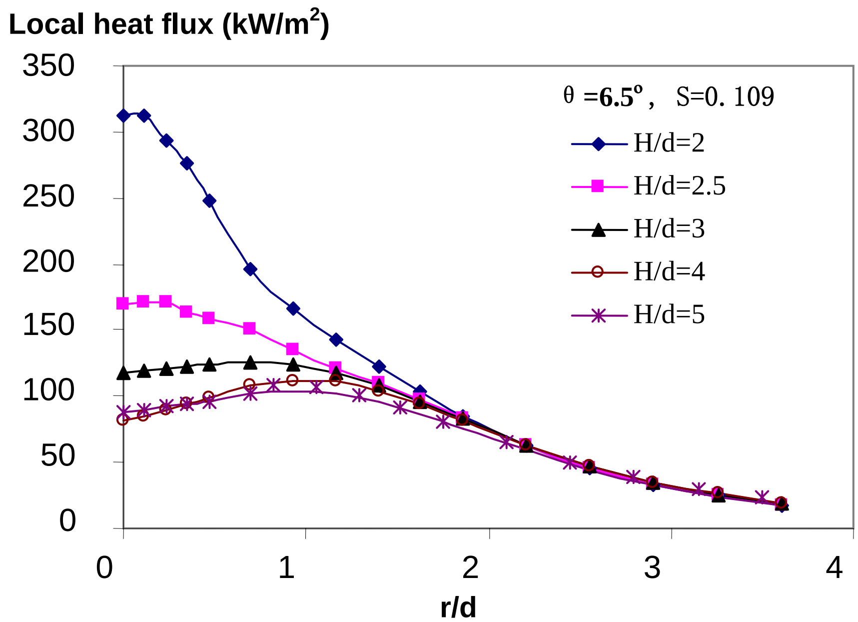

Figure 6.4 (b) Radial heat flux distribution at different nozzle-to-plate distances

(Φ = 1, Re = 1200 and S = 0.109)

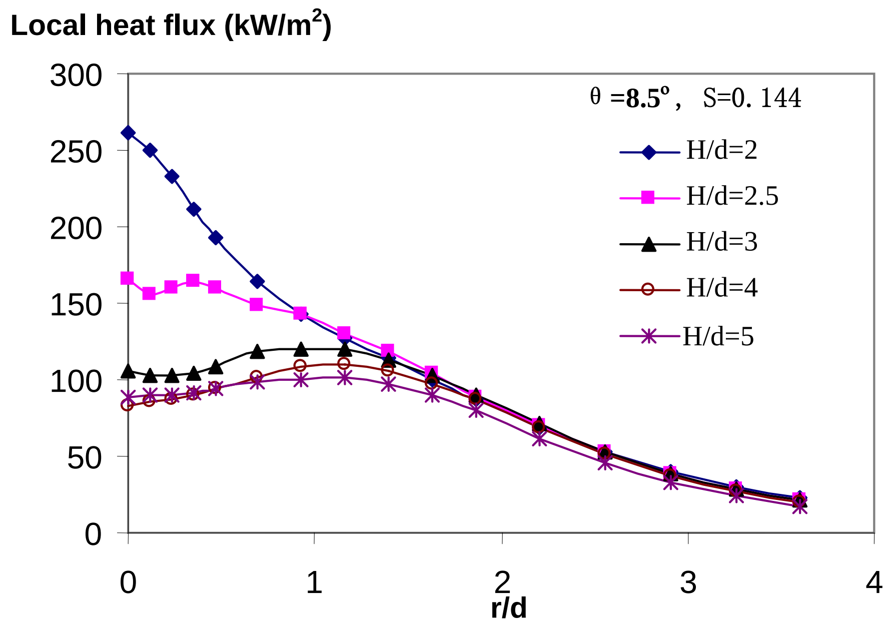

Figure 6.4 (c) Radial heat flux distribution at different nozzle-to-plate distances

(Φ = 1, Re = 1200 and S = 0.144)

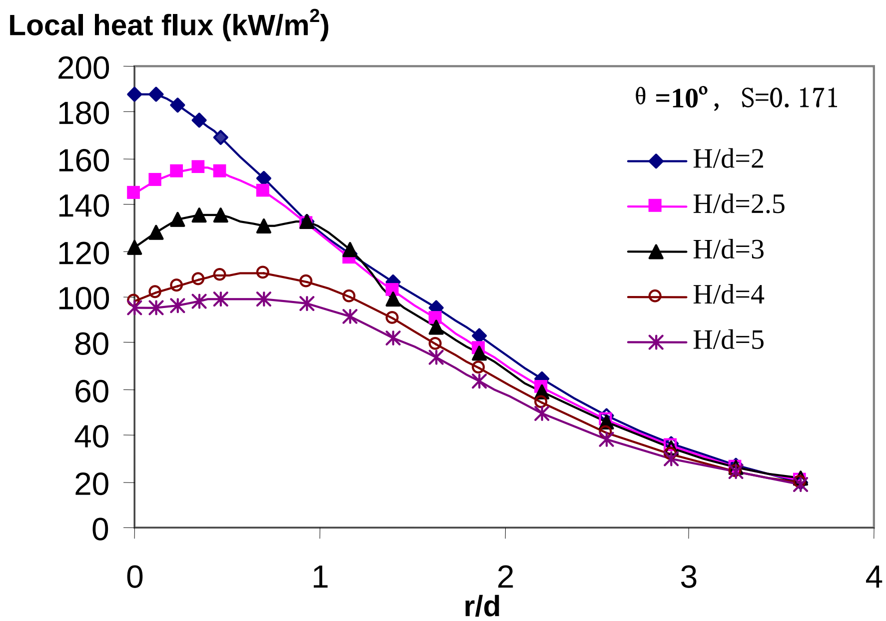

Figure 6.4 (d) Radial heat flux distribution at different nozzle-to-plate distances

(Φ = 1, Re = 1200 and S = 0.171)

The area-averaged heat transfer rate that varied with the nozzle-to-plate distance is shown in Figure 6.5. The area-averaged heat flux on the impingement plate decreases as the nozzle-to-plate distance is increased from 2d to 5d. The induced swirl reduced the flame length in the axial direction leading to the occurrence of a very short optimum nozzle-to-plate distance of 2d, which is corresponding to a maximum impinging heat transfer.

According to Dong et al. [11 and 12] that a peak area-averaged heat flux is occurred at H/d = 5 for a premixed butane/air non-swirling impinging flame jet of the same geometrical configuration. The reduction in flame length of a premixed flame jet with induced swirl has been confirmed by Zhao et al. [15] in their numerical study of a swirl-stabilized premixed open flame. Therefore there is no contradiction between the present findings with that suggested by Dong et al. [11 and 12]. The swirl induced promotes a more rigorous mixing of the air and fuel within a smaller distance between the nozzle exit and the impingement plate surface, which leads to a more complete combustion to occur within a smaller nozzle-to-plate distance.

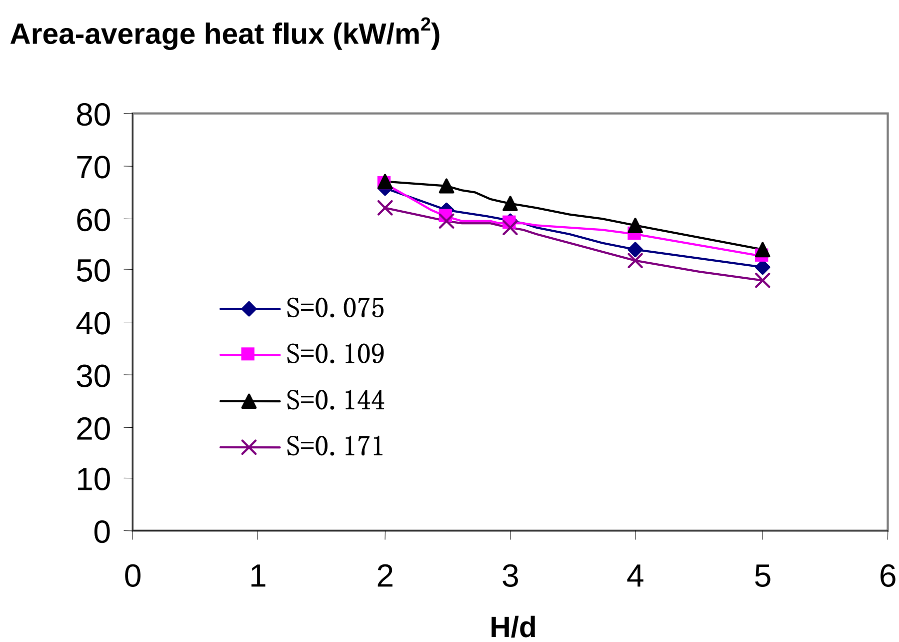

Figure 6.5 Area-averaged heat flux on the impingement plate at different nozzle-to-plate distances and Swirl numbers (Φ = 1 and Re = 1200)

6.2.3 Effect of Swirl number

The heat flux distributions on the impingement plate obtained under different swirl intensities are compared and presented in Figure 6.6. The centrifugal force generated by the swirling flow produces an outflow of high temperature gas species so that when the swirl intensity and hence the Swirl number is increased from 0.075 to 0.144, location of the peak heat flux shifts outwards from the stagnation point. Besides, the local heat flux at the stagnation point is slightly reduced.

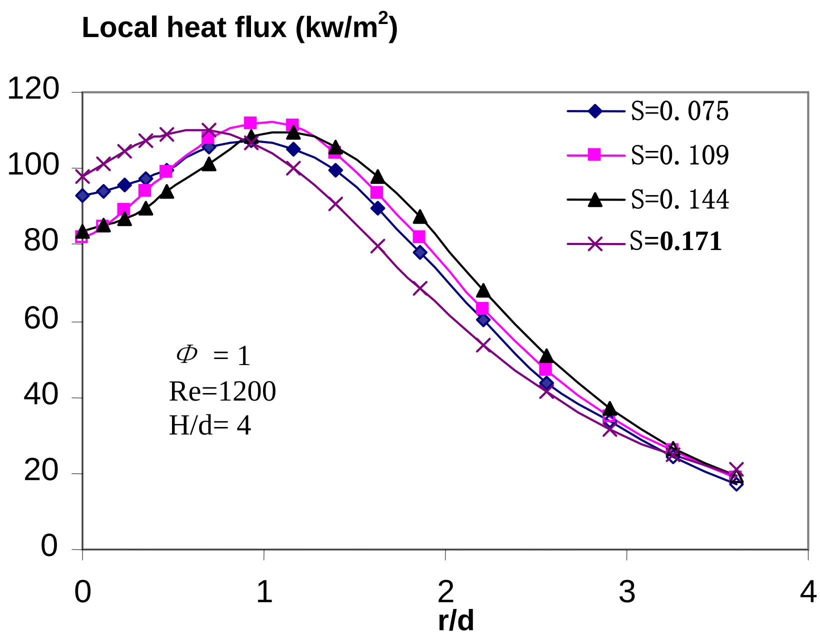

Figure 6.6 Radial heat flux distribution under different swirl intensities

(Φ = 1, Re = 1200 and H/d = 4)

However, it is interesting to note that when the Swirl number is further increased to 0.171, the turbulence in the flame can be easily observed. The swirling flow may produce a recirculation zone around the stagnation point as suggested by the flow model developed by Huang and El-genk [7]. Thus, a higher heat transfer from the impinging flame to the stagnation point of the impingement plate is obtained. In addition, the outward shift of the peak heat flux is slightly reduced and the heat flux is much lower at the wall jet region, which indicates the outflow of the high temperature gas species becomes less serious.

Figure 6.7 indicates the area-averaged heat flux on the impingement plate under different Swirl numbers. It is observed that the area-averaged heat transfer to the impingement plate is not much varied with the swirl intensity, disregarding the change in nozzle-to-plate distance. The heat transfer rate first slightly increases with the increasing Swirl number, but declines suddenly when the swirl intensity becomes stronger at S = 0.171.

As shown in Figure 5.1, when a tangential stream is applied, the flow of butane/air mixture at the nozzle exit diverges from the axial direction due to the centrifugal force generated so that the flame surface area becomes larger. Besides, increase of the tangential flow rate results in an enhanced mixing of the air and fuel which leads to a more complete burning of the fuel. It is the reason for the area-averaged heat flux to increase when the tangential stream continues to increase.

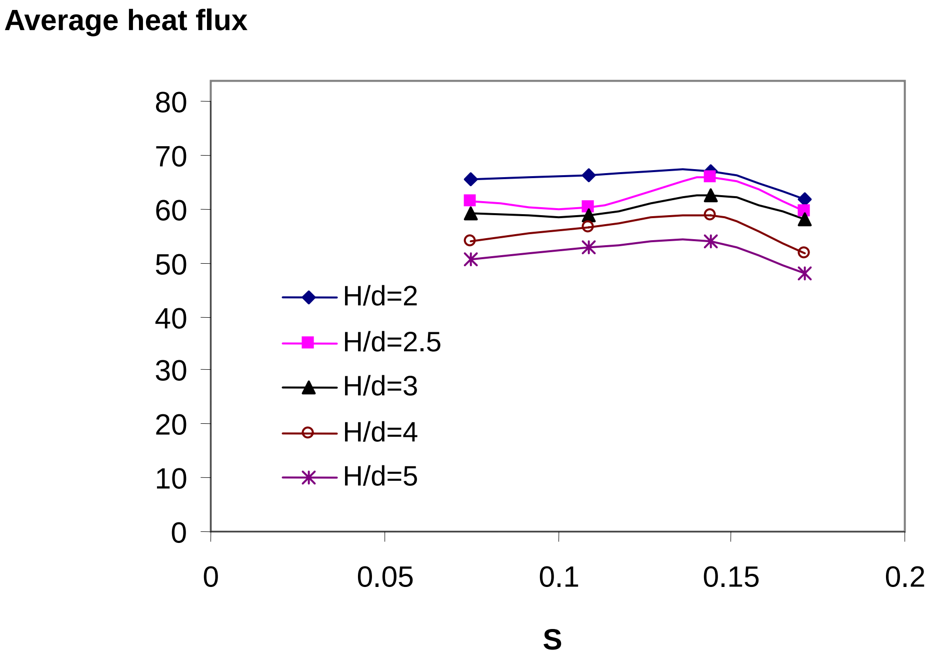

Figure 6.7 Area-averaged heat flux on the impingement plate under different swirl intensities and nozzle-to-plate distances (Φ = 1 and Re = 1200)

In addition, the flow starts to change from laminar to turbulent conditions, which can be observed in Figure 6.1 (d). The same phenomenon is observed in the work of Huang and El-genk [7], in which the heat transfer of swirling impinging jets has been studied and the influence of Swirl number on the heat transfer performance is examined. It is suggested that heat transfer to a heating object is first augmented with larger swirl intensities and then decreases when the swirl intensity is further increased.

In the present study, when the flow of butane/air mixture at the nozzle exit is developed from laminar to transitional conditions, the flame front becomes vague because of the increasing turbulence which is enhanced by the increasing swirl intensity. It is possible for the flame to approach the flammable limit and the heating performance begins to decrease at the same nozzle-to-plate distance. The findings agreed closely with those suggested by Zhang and Hill [62]: further increase of the swirling intensity may cause the flame to become unstable and even blow off.

6.2.4 Effect of equivalence ratio

The premixed air/fuel ratio is varied to examine the effect of the equivalence ratio on the heat transfer characteristics of the circular swirling impinging flame jet, as shown in Figures 6.8 (a) to (d). The influence of the equivalence ratio on the heat transfer between the swirling flame and the impingement plate is different from that of the non-swirling flame. When the swirl intensity is rather low ($\theta = 4.5^{\circ}$, $S = 0.075$), the heat flux value around the stagnation point is highest under the stoichiometric condition, which is the same as the non-swirling flame jet. However, the induced swirl not only effectively enhances the mixing of air and fuel but also entrains more ambient air into the burning zone around the nozzle exit, so that the heating performance of the swirling impinging flame jet under fuel-rich conditions becomes better than that of the non-swirling flame jet.

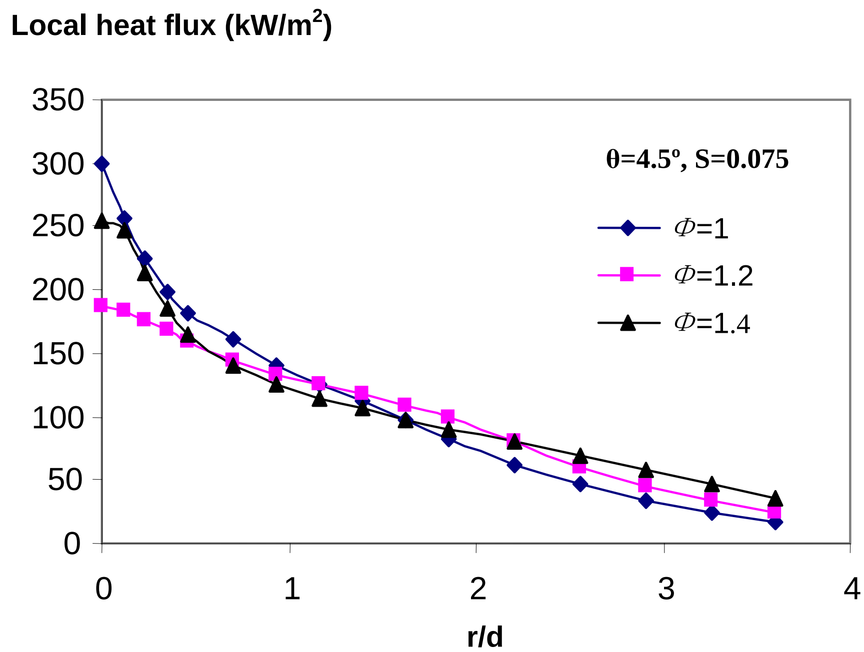

Figure 6.8 (a) Radial heat flux distribution under different equivalence ratios (Re = 1200, H/d = 2.5 and S = 0.075)

When the equivalence ratio increases to 1.2, the flame length increases which results in the outflow of high-temperature combustion gases after impingement, thus the heat flux value in the stagnation region decreases and the heat flux distribution becomes more uniform. As the equivalence ratio continues to increase, more fuel is added to the combustion process but the induced swirl is able to entrain more air into the combustion zone and the heating performance can be further enhanced.

The flame length is increased as a result of the increasing equivalence ratio. It enlarges the area impinged by the flame on the impingement plate, which also provides a positive effect on the heat flux received by the plate.

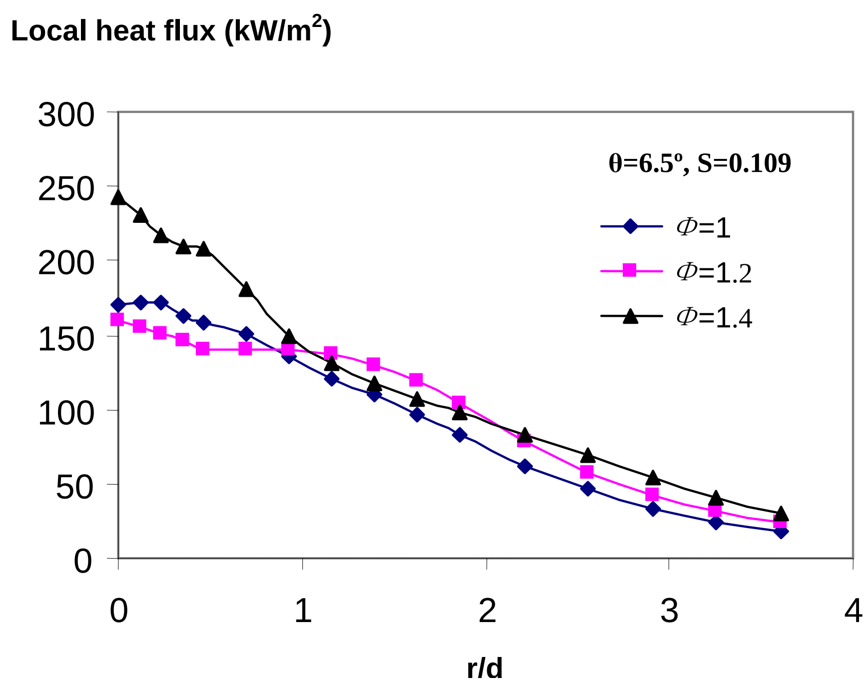

Figure 6.8 (b) Radial heat flux distribution under different equivalence ratios

(Re = 1200, H/d = 2.5 and S = 0.109)

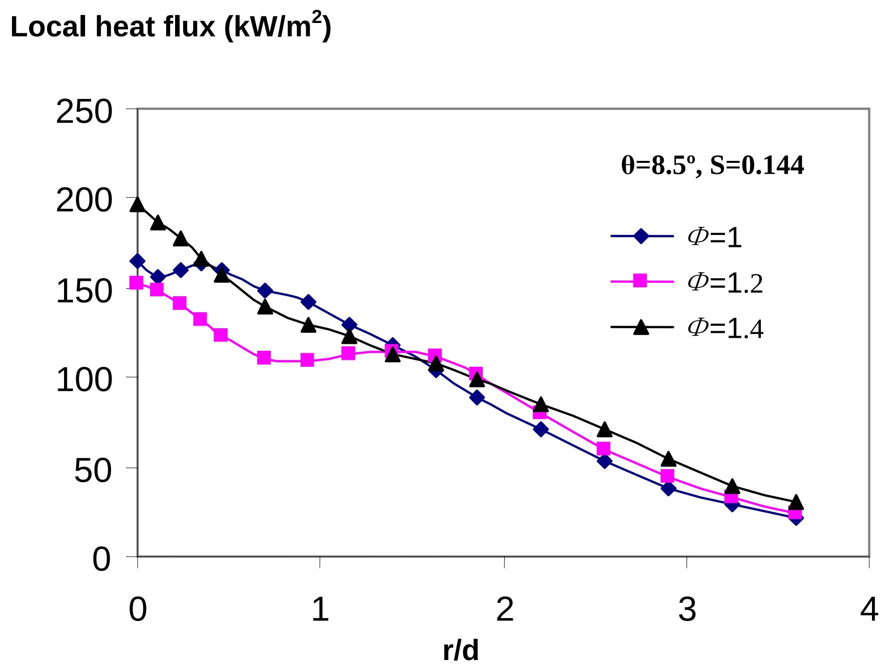

Figure 6.8 (c) Radial heat flux distribution under different equivalence ratios (Re = 1200, H/d = 2.5 and S = 0.144)

It is observed from Figures 6.8 (a) to (d) that heat fluxes received by the impingement plate at different equivalent ratios are slightly different at the wall-jet region. It may be due to the rather excessive amount of unburned air/fuel mixture obtained at the wall-jet region when the equivalence ratio is high (i.e. $\Phi = 1.4$). Consumption of this unburned air/fuel mixture increases the heat flux received by the impingement plate at its wall-jet region.

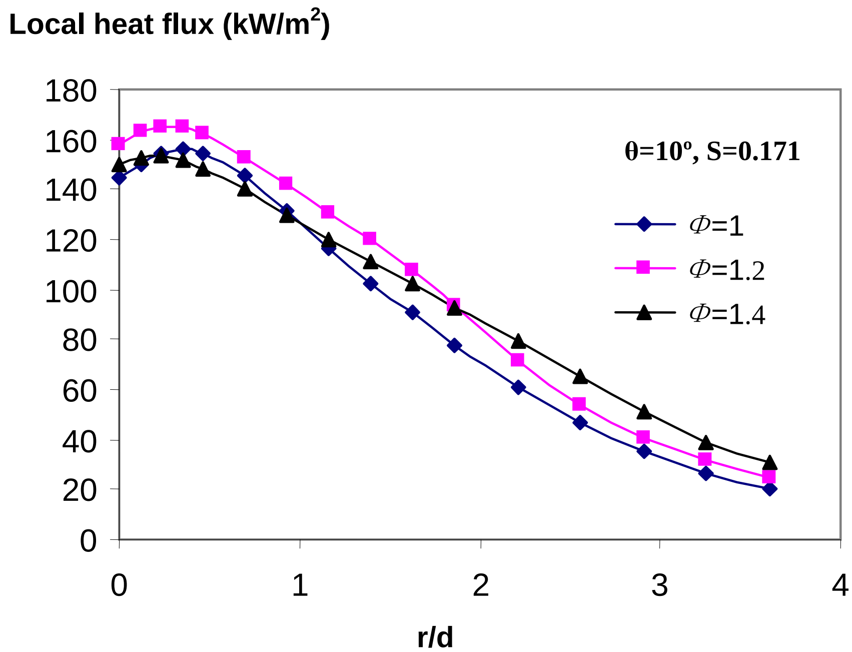

Figure 6.8 (d) Radial heat flux distribution under different equivalence ratios

(Re = 1200, H/d = 2.5 and S = 0.171)

The area-averaged heat flux on the impingement plate increases rather slightly when more fuel is provided, which is shown in Figure 6.9. It is worth to note that when the swirl is strong enough to produce a transitional flame (θ = 10º and S = 0.171), the turbulence causes a change in the effect of equivalence ratio on the heat flux distribution at the stagnation point region. The heat transfer rate shows small difference between different air/fuel mixture ratios.

As the fuel supply is increased, the peak heat flux occurs at a location closer to the stagnation point. Besides, a fuel-rich mixture of $\Phi = 1.2$ provides the highest maximum heat transfer rate. It is assumed that the turbulence can promote a more complete combustion within a shorter nozzle-to-plate distance at the equivalence ratio of 1.2. But when the fuel supply becomes too rich, more high-temperature gases flow out from the stagnation point region causing a drop of local heat flux at the stagnation point due to the occurrence of a larger cool region of significant amount of unburned air/fuel mixture.

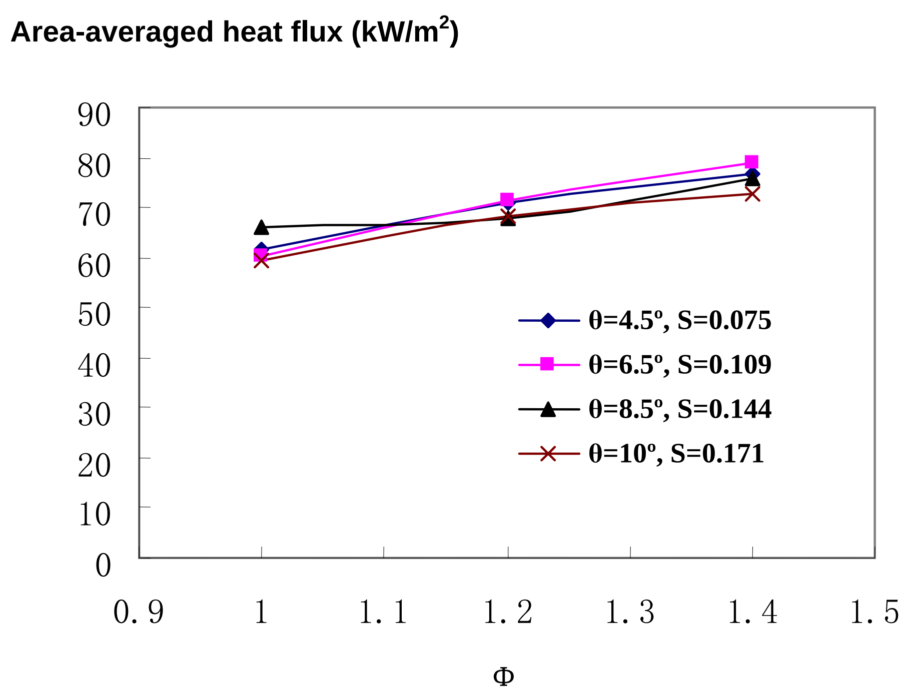

Figure 6.9 Area-averaged heat flux on the impingement plate under different equivalence ratios and Swirl numbers (Re = 1200 and H/d = 2.5)

6.3 SUMMARY

Experimental studies have been conducted to investigate the heat transfer characteristics of a butane/air premixed impinging round flame jet with swirl induced via the second experimental setup. In this particular setup, air and fuel are premixed before they are divided into two separate streams: one is supplied to the burner through the axial entrance, whereas the other is admitted into the burner via the tangential inlets. The effects of important parameters, including Reynolds number of the air/fuel jet, nozzle-to-plate distance, Swirl number of the air/fuel jet and equivalence ratio of the air/fuel mixture, on the local heat flux distribution along the radial direction of the impingement plate and the area-averaged heat flux arriving at the plate are examined.

Based on the experimental results, the following conclusions can be made:

1) When the experimental setup II is applied, effects of the equivalence ratio and Swirl number on the heat flux received by the impingement plate are no longer depended on each other, and can be individually assessed. It is definitely an advantage in using this particular setup. However, only very weak swirl can be introduced via this approach, which is a significant drawback of the method. On the one hand, the smoke-flow visualization method is unable to accurately identify the swirl number when the swirl intensity becomes too large. On the other hand, because of the rather narrow flammable limits such swirling flame could be operated within a small operation range only.

2) The heat transfer rate on the whole impingement plate increases with the increasing Reynolds number, which agrees with the study on non-swirling impinging flame jet with similar configuration and operating conditions. It is noted that the average heat flux experienced a more rapid increase when Re is increased from 1200 to 1500, but the increase becomes less significant when Re is further increased to 1700, at which point the transitional flow is assumed to start to occur.

3) Use of a swirling flow can promote the local turbulence and enhance the mixing of air and fuel, which enables a complete combustion to occur within a smaller nozzle-to-plate distance. Thus, a smaller optimum nozzle-to-plate distance (i.e. around H/d = 2 to 2.5), corresponding to a maximum heat transfer received by the impingement plate, is obtained. Such phenomenon is also found in the experimental work conducted with the experimental setup I. Thus, it is suggested that a smaller nozzle-to-plate distance can be used to enhance the thermal performance of a swirling impinging flame jet.

4) As mentioned in the previous section, a smaller nozzle-to-plate distance can be adopted when a swirling impinging flame jet is used even though a complete combustion is aimed to achieve. In fact, the axial component of the flame length is reduced by applying swirl. Occurrence of the cool central core consisting of a significant amount of unburned air/fuel mixture of a premixed flame, which is the characteristics of a laminar impinging flame jet without swirl induced, can be

avoided. It is achieved by applying a swirling flow with sufficiently large swirl intensity.

5) The local heat flux distribution is far more uniform around the stagnation point of the impingement plate when a swirling impinging flame with large intensity is applied. The divergence of the flame tip enlarges the flame’s surface area there so that the heat transfer rate in the stagnation zone is higher. In addition, location of the maximum local heat flux is shifted outwards away from the stagnation point as intensity of the induced swirl is increased because of the increasing centrifugal force. Such that a significant amount of active gaseous species is brought to the wall-jet region from the stagnation region.

6) The total heat flux received by the impingement plate is first increased with the swirl intensity because of a better mixing between the air and fuel. However, it decreases as the Swirl number becomes too large. When the flow of butane/air mixture at the nozzle exit is developed from laminar to transitional flow conditions, the flame front becomes vague because of the increasing turbulence which is enhanced by the increasing swirl intensity. It is possible for the flame to approach the flammable limit, beyond this the flame starts to flicker and becomes unstable and the heating performance begins to decrease at the same nozzle-to-plate distance.

7) The influence of equivalence ratio on the heat transfer characteristics of the swirling impinging flame jet system is different from that concluded in the experimental work conducted with the experimental setup I, as well as those reported by previous studies on the impinging flame jet without swirl induced. The induced swirl enables more ambient air to be entrained so that even though the premixed butane/air mixture is fuel-rich, the combustion can still be more complete when compared to that of the non-swirling flame jet of similar configuration. The heating performance is only slightly enhanced when more fuel is provided. The flame length is slightly lengthened as the equivalence ratio increases, which enlarges the surface area on the impingement plate to be impinged by the swirling flame jet. It leads to an increase of the heat flux values along the whole plate. When the swirl intensity is further enhanced, more high-temperature gases flow out from the stagnation point region causing a drop of local heat flux at the stagnation point due to the occurrence of a larger cool region of significant amount of unburned air/fuel mixture.

CHAPTER 7

COMPARISON WITH NON-SWIRLING FLAME JET

In this chapter, the heat transfer characteristics of the premixed impinging flame jet with swirl induced obtained from both setups of the present experimental study are compared with those obtained from previous studies on the non-swirling single impinging circular and slot flame jets.

7.1 COMPARISON BETWEEN SWIRLING AND NON-SWIRLING FLAME JETS

7.1.1 Comparison between swirling flame jet of experimental setup I and non-swirling flame jet

Heat flux distributions on the impingement plate obtained from the present study conducting with the experimental setup I are compared with the results obtained from previous studies on non-swirling premixed impinging flame jets of similar configuration [9 – 14] operating under the same operating conditions, and presented in Figure 7.1.

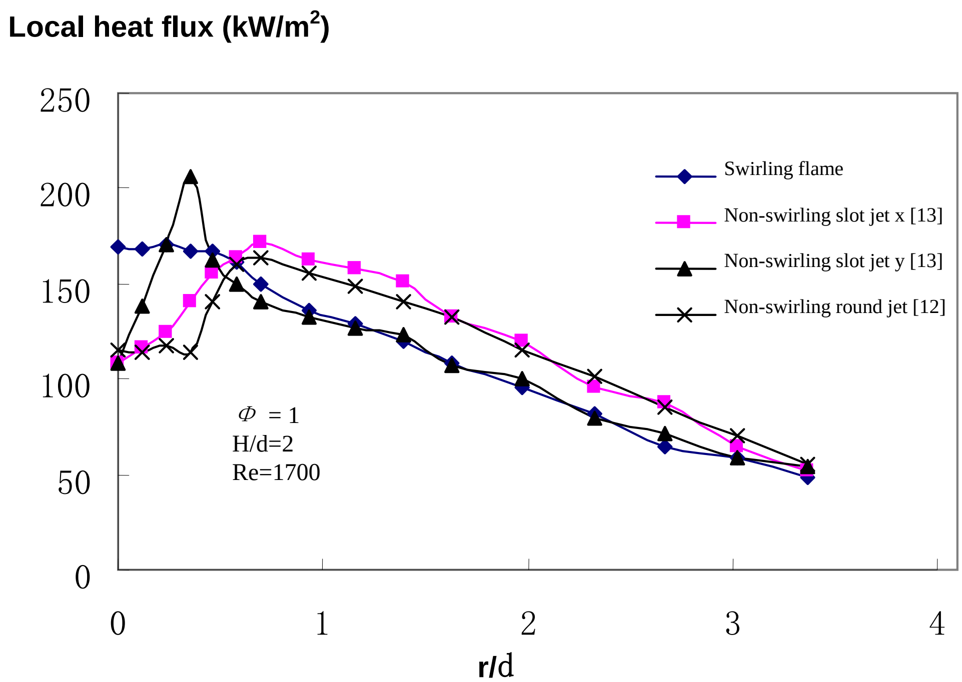

Figure 7.1 Comparison of heat flux distributions between swirling and non-swirling premixed impinging flame jets (Φ = 1, H/d = 2 and Re = 1700)

It is concluded by Dong et al. [12] that the cool central core consisting of a significant amount of unburned fuel as shown in Figure 7.1, which is a special feature of the laminar impinging flame jet, usually occurs at the stagnation region of impingement plate for both circular and slot flame jets. Besides, it is more pronounced in the circular instead of slot flame jets due to the influence of nozzle shape. As described previously, the inner reaction zone of an impinging flame jet acts as a barrier to a certain extent to prevent the entraining of ambient air. This results in the occurrence of the central cool core and the direct impingement of unburned air/fuel mixture onto the plate. However, use of the circular impinging flame jet with swirl induced helps minimizing the occurrence of such central cool core. The heat flux distribution on an impingement plate operating with a swirling flame is more uniform around its stagnation point, and the peak heat flux is also occurred in this region.

The introduction of swirl is able to shorten the axial component of the flame length so that the flame can be developed better within the same nozzle-to-place distance before it is impinging upon impingement plate. Moreover, the divergence of the flame tip enhances the flame’s surface area and therefore increases the contacting area between the flame and the plate. In addition, the induced swirl also promotes local turbulence in the reacting flow, which enhances the mixing of air and fuel to facilitate a more complete combustion at the stagnation point region.

It is impossible to consider accurately the difference in surface properties including material’s thermal conductivity, surface emissivity and surface roughness, and heat loss from the flame jet system to its surroundings, between the present experimental systems with those applied in the previous studies. However, thermal performance of the swirling impinging flame jet can be estimated to be comparable with that of the non-swirling flame jet, as shown on Figure 7.1.

7.1.2 Comparison between swirling flame jet produced by experimental setup II and non-swirling flame jet

Figure 7.2 indicates the comparison between the heat flux distributions on the impingement plate obtained with a swirling impinging flame jet operating with different swirl intensities and those obtained with a single non-swirling circular or slot impinging flame jet with similar configuration [12 and 13], and operating under the same operation conditions. It is concluded that the optimum nozzle-to-plate distance corresponding to the maximum area-averaged heat flux on the impingement plate is obtained at H/d = 5 under the stoichiometric combustion condition for non-swirling flames. The cool core appears in both non-swirling circular and slot flame jets. However, the optimum nozzle-to-plate distance for the swirling impinging flame jet is obtained at H/d = 2, according to the present study.

There are two important findings observed through the comparison. Firstly, the cool core of the flame at the stagnation point region occurring in both circular and slot flame jets can be avoided by inducing swirl even with rather low swirl numbers. Thus, inducing swirl help producing a more uniform heat flux distribution on the impingement plate, especially around the stagnation point. Secondly, it is able to develop a stable premixed impinging flame with induced swirl at low Reynolds numbers and swirl numbers. However, further investigations are desirable to identify the most suitable operation conditions to utilize its better thermal performance.

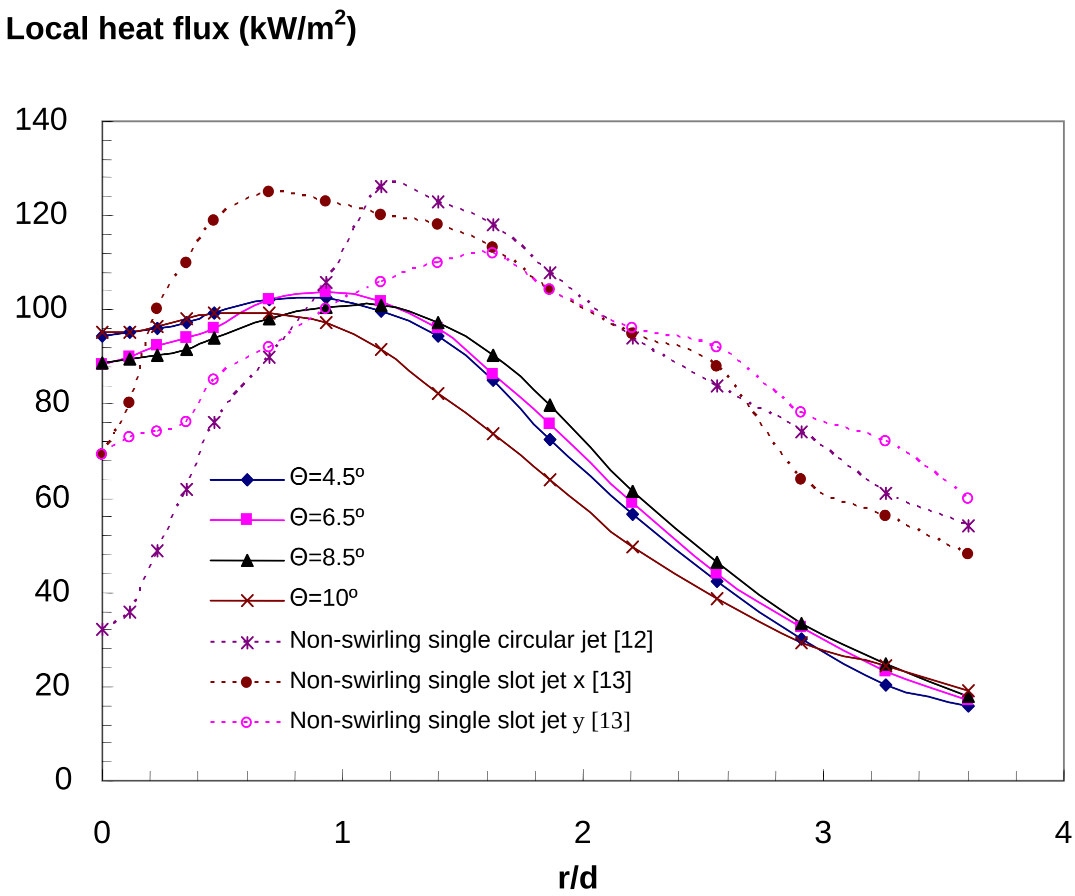

Figure 7.2 Heat flux distribution comparison of flame jets with and without swirl on the impingement plate (ϕ = 1, Re = 1200 and H/d=5)

Again, it is impossible to consider accurately the difference in surface properties and the heat loss from the flame jet system to its surroundings, between the present experimental systems with those applied in the previous studies. Besides, the swirling impinging flame jet appears to have better thermal performance around the stagnation region, but a lower heat flux distribution is obtained at the wall-jet region. The swirling flames are able to produce a more uniform heat flux on the impingement plate when compared to their counterparts, as shown on Figure 7.2.

It seems possible to achieve comparable thermal performance by the non-swirling flames when they are working under the optimized operation conditions. However, further investigations will be required to utilize their applications.

7.2 COMPARISON BETWEEN SWIRLING FLAME JETS PRODUCED BY EXPERIMENTAL SETUPS I AND II

Figure 7.3 illustrates the heat flux distributions on the impingement plate obtained from the premixed swirling impinging flame jets produced from both experimental setups I and II.

The heat transfer rate around the stagnation point is evidently enhanced in the setup II. The mixing of air and fuel is more rigorous as they have been premixed in the premixed chamber. Even though the swirl number of the swirling flow produced by the experimental setup I, as calculated from Equation (3.1), is much larger than that obtained from the experimental setup II, its heating performance around the stagnation point is actually lower.

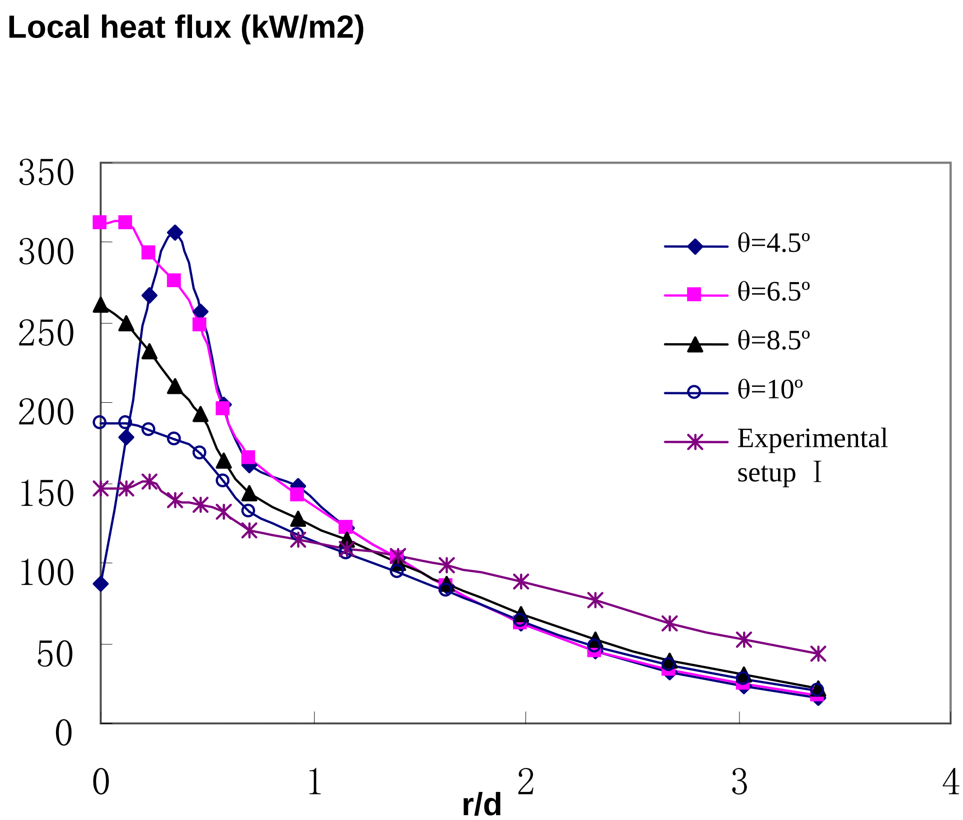

Figure 7.3 Heat flux distributions on the impingement plate in Experimental setups I and II (ϕ = 1, Re = 1200 and H/d = 2)

For example, at $\phi = 1$ and Re = 1200, the swirl number is determined from Equation (3.1) to be 2.53, which is very large. However, as shown from the experimental results, the area-averaged heat fluxes on the impingement plate obtained from the experimental setup I are still lower than those obtained from the experimental setup II, when both systems are operating under the same operation conditions. Such discrepancy may also be attributed to the over-estimate of the actual Swirl number by using Equation (3.1), which is a drawback of the experimental setup I.

For the experimental setup I, the swirl number is determined by the ratio between the tangential flow and the axial flow and is therefore directly linked to the equivalence ratio. Effects of equivalence ratio and Swirl number on the heat flux received by the impingement plate are unable to be separately identified. It becomes another drawback of this arrangement.

Considering the experimental setup II, effects of the equivalence ratio and Swirl number on the heat flux received by the impingement plate can be individually assessed, which is definitely an advantage in using this particular setup. It is found that only very weak swirl can be introduced via this approach, which is a drawback of the method. However, such drawback may be compensated to a certain extent because the air and fuel are premixed thoroughly before they are delivered to the burner in this arrangement.

CHAPTER 8

ANALYSIS OF IMPINGEMENT HEAT TRANSFER

In this chapter, non-dimensional heat transfer coefficient, the Nusselt number, is analytically correlated with the major non-dimensional experimental parameters, including Prandtl number (Pr), Reynolds number (Re), equivalence ratio (Φ), nozzle-to-plate distance (H/d) and Swirl number (S), by using the multiple regression method in Matlab 7. Comparison of heat transfer characteristics can then be made between the present study and previous studies on premixed circular impinging flame jets without swirl.

8.1 MAXIMUM LOCAL NUSSELT NUMBER

For the swirling impinging flame jet system under consideration, the non-dimensional correlation of maximum local Nusselt number (hence maximum local convective heat transfer coefficient) with the other major operating parameters for the premixed gas-fired circular impinging flame jets with swirl induced can be developed with the following general form:

$$Nu_{\max}\ \Pr^{a} = C\ \mathrm{Re}^{b}\ \phi^{c} \left(\frac{H}{d}\right)^{d}\ S^{e} \qquad \ldots\ldots (8.1)$$

With the aid of the experimental results obtained from the experimental setup II of the present study, the unknowns in Equation (8.1) (i.e. C, a, b, c, d and e) can be determined and the resultant non-dimensional semi-empirical equation takes the following form:

$$Nu_{\max} \cdot \Pr^{-0.4} = 3.1267\,\mathrm{Re}^{0.2334}\ \phi^{0.9738} \left(\frac{H}{d}\right)^{-0.7544} S^{e}, \left\{\begin{array}{l} 800 \le \mathrm{Re} \le 1500,\ e = 0.3108 \\ 1500 \le \mathrm{Re} \le 1700,\ e = -0.1097 \\ 1 \le \phi \le 1.4 \\ 2 \le \dfrac{H}{d} \le 5 \\ 0 \le \dfrac{r}{d} \le 3.5 \\ 0.075 \le S \le 0.171 \end{array}\right\}$$

…………..(8.2)

The correlation line and the experimental data are shown in Figure 8.1, with a maximum deviation of 7.5 %. It is suggested by Dong et al. [12] that the correlation of maximum local Nusselt number for the similar impinging flame jet without swirl induced as:

$$Nu_{\max} \cdot \Pr^{-0.4} = 3.988\,\mathrm{Re}^{0.2127}\ \phi^{-0.6458} \left(\frac{H}{d}\right)^{0.0722}, \quad \left\{\begin{array}{l} 600 \le \mathrm{Re} \le 1500 \\ 0.7 \le \phi \le 1.2 \\ 1.0 \le \dfrac{H}{d} \le 8.0 \\ 0 \le \dfrac{r}{d} \le 6.5 \end{array}\right\} \qquad \ldots\ldots (8.3)$$

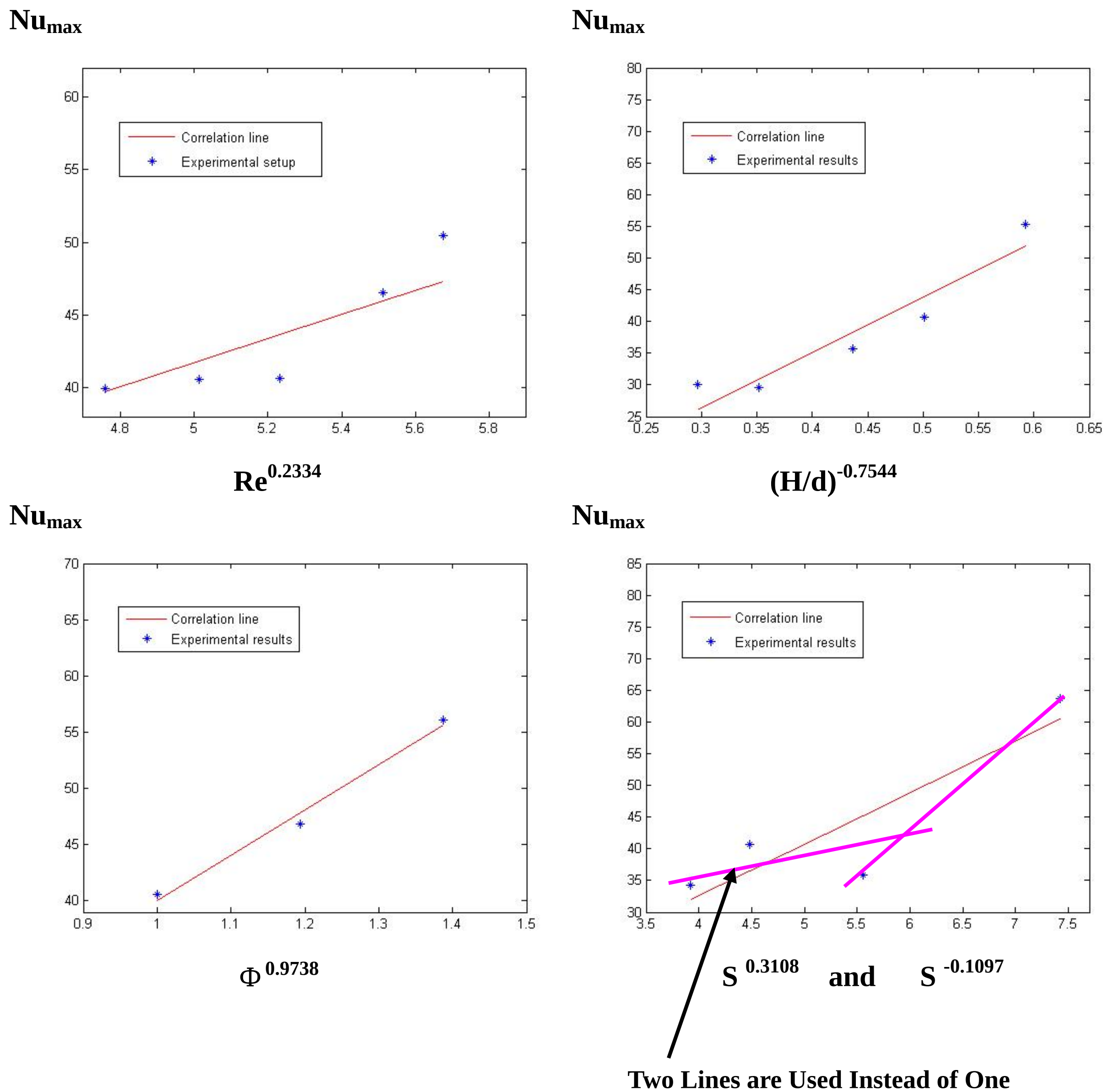

Figure 8.1 Maximum local Nusselt number correlation for swirling impinging flame jet

8.2 AREA-AVERAGED NUSSELT NUMBER

The correlation of area-averaged Nusselt number $\left(\overline{Nu}\right)$ (hence the area-averaged convective heat transfer coefficient) and the major non-dimensional experimental parameters, including Prandtl number (Pr), Reynolds number (Re), equivalence ratio (Φ), nozzle-to-plate distance (H/d) and Swirl number (S), for the premixed gas-fired circular impinging jets with swirl induced is obtained with the following general form:

$$\overline{Nu}\,\mathrm{Pr}^{a1} = C1\,\mathrm{Re}^{b1}\,\phi^{c1}\left(\frac{H}{d}\right)^{d1} S^{e1} \qquad \ldots\ldots (8.4)$$

$\overline{Nu}$ is calculated according to Equation (4.10). With the aid of the experimental results obtained from the experimental setup II of the present study, the unknowns in Equation (8.4) (i.e. C1, a1, b1, c1, d1 and e1) can be determined to give an equation for solving $\overline{Nu}$. The integration area under consideration contains the stagnation zone and the early wall-jet region (i.e. $0 \leqq r/d \leqq 3.5$). Equation (8.5) indicates the non-dimensional correlation for the determination of the area-averaged Nusselt number. As shown in Figure 8.2, the maximum deviation of the experimental results from the correlation line is 8.9 %.

$$\overline{Nu}\cdot \mathrm{Pr}^{-0.4} = 18.647\,\mathrm{Re}^{0.1035}\,\phi^{\,1.164}\left(\frac{H}{d}\right)^{-0.3247} S^{e1},\begin{Bmatrix} 800 \le \mathrm{Re} \le 1500,\ e1 = 0.2307 \\ 1500 \le \mathrm{Re} \le 1700,\ e1 = -0.3078 \\ 1 \le \phi \le 1.4 \\ 2 \le \dfrac{H}{d} \le 5 \\ 0 \le \dfrac{r}{d} \le 3.5 \\ 0.075 \le S \le 0.171 \end{Bmatrix}$$

. . . . . . (8.5)

Similarly, the correlation for the similar impinging flame jet without swirl induced which is proposed by Dong et al. [12] is shown in Equation (8.6):

$$\overline{Nu}\cdot \mathrm{Pr}^{-0.4} = 0.159\,\mathrm{Re}^{0.4745}\,\phi^{-0.382}\left(\frac{H}{d}\right)^{0.2908},\begin{Bmatrix} 600 \le \mathrm{Re} \le 1500 \\ 0.7 \le \phi \le 1.2 \\ 1.0 \le \dfrac{H}{d} \le 8.0 \\ 0 \le \dfrac{r}{d} \le 6.5 \end{Bmatrix} \quad \text{. . . . . . (8.6)}$$

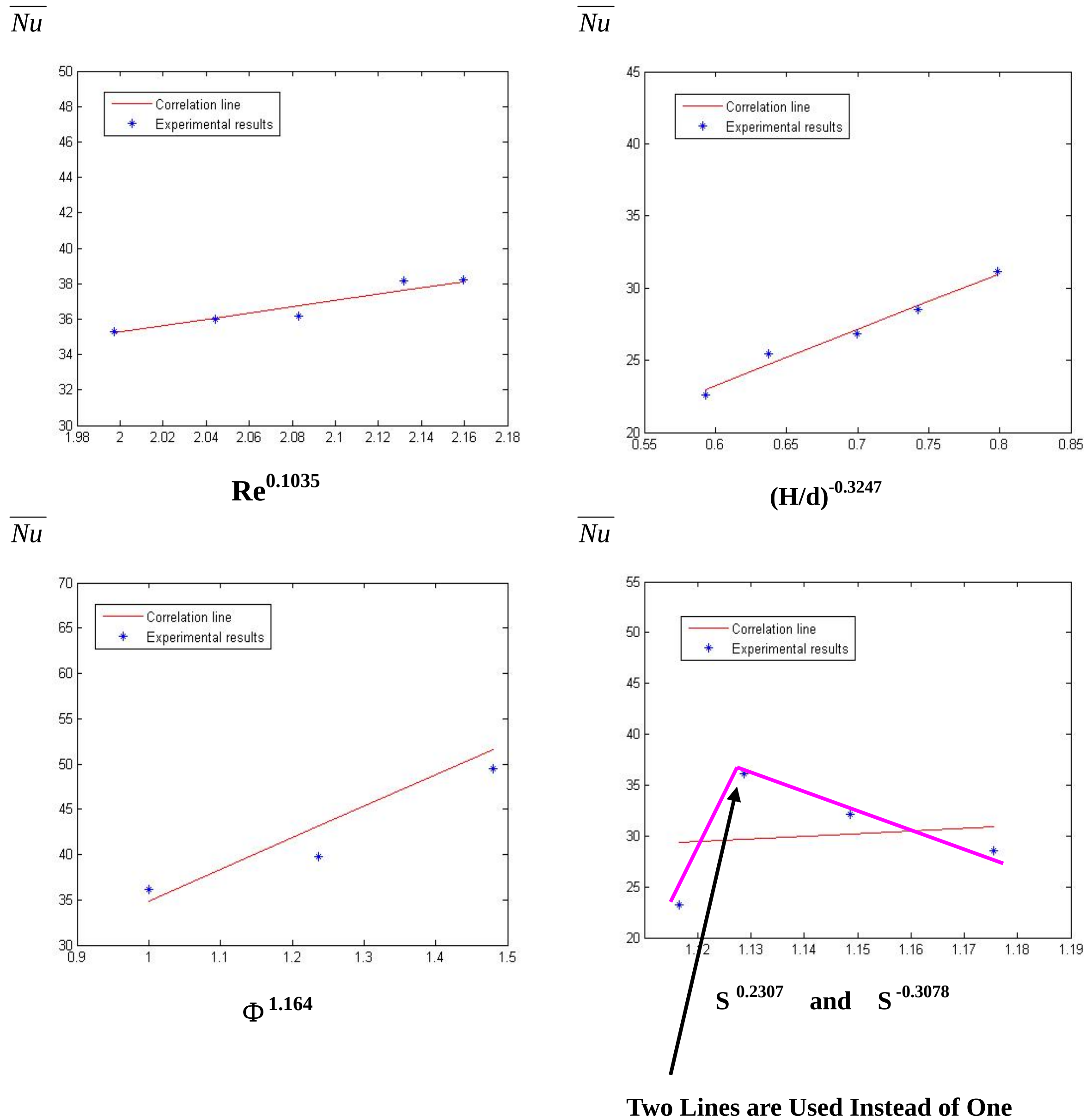

Figure 8.2 Area-averaged Nusselt number correlation for swirling impinging flame jet

8.3 COMPARISON BETWEEN SWIRLING AND NON-SWIRLING CIRCULAR PREMIXED IMPINGING FLAME JETS

The effect of Reynolds number on the variation of maximum local Nusselt number is similar for both swirling and non-swirling flame jets, as shown by comparing Equations (8.2) and (8.3). However, when the equivalence ratio is increased to achieve the fuel-rich combustion, swirling flame jet shows advantage over its counterpart in term of maximum local heat transfer rate on the impingement plate. The difference is also caused by the influence of nozzle-to-plate distance. The peak value of local Nusselt number starts to decrease when the swirling flame jet is moved away from the plate (i.e. H/d ratio is increased) while an opposite trend is obtained for the non-swirling impinging flame. In addition, effect of the Swirl number can be concluded from the correlation. When the swirl intensity becomes too strong, the maximum heat transfer rate on the impingement plate is decreased instead of increased.

As can be seen in the Equations (8.5) and (8.6), the area-averaged heat transfer rate on the impingement plate is enhanced when the Reynolds number increases for both the non-swirling and swirling flame jets, but the increasing rate is much rapid for the non-swirling flame jet. The induced swirl enhances the local turbulence of the air/fuel mixture so that the influence of increasing Reynolds number becomes less obvious. In the swirling impinging flame jet, Swirl number becomes an important factor to affect the flow, combustion and heat transfer characteristics.

It is suggested by Dong et al. [12] that not only the maximum local heat transfer rate but also the area-averaged heat transfer increase when the nozzle-to-plate distance is increased from very small value, with an optimum nozzle-to-plate distance corresponding to a maximum heat transfer obtained at H/d = 5. In the present study of impinging flame jet with swirl induced, it is found that the axial component of the flame length is shortened and the mixing of air and fuel becomes more rigorous, so that the best heating performance is obtained at a smaller H/d ratio between 2 and 2.5. The heat flux decreases when the burner is moved away from the plate, i.e. H/d > 2.5. Thus, it is suggested that a smaller optimum nozzle-to-plate distance occurs for the swirling flame jets.

Another finding which is worth to note is both the maximum and area-averaged heat transfer rates increase when the equivalence ratio is raised to the fuel-rich condition. The swirl entrains more ambient air into the combustion zone during the combustion process so that the extra fuel can be burned, which contributed to the amount of heat produced. This is favorable in practical applications because the gas-fired domestic heating appliances commonly adopted are mainly operated under fuel-rich conditions.

The heat transfer rates produced by a premixed impinging flame jet with induced swirl as measured in the present study are compared with those obtained from previous works on similar non-swirling flame jets as shown in Figures 7.1 and 7.2. It is noted from the heat transfer rates obtained at the stagnation point that, use of a premixed flame jet with induced swirl is able to reduce the production of a central cool core, which is usually found in the non-swirling laminar flame jet. Therefore the local heat flux received at the stagnation point of the impingement plate is much higher when it is impinged upon by a swirling flame.

CHAPTER 9

CONCLUSIONS AND RECOMMENDATIONS

9.1 CONCLUSIONS

Heat transfer characteristics of impinging flame jets have been investigated by many previous researchers. Different methods were applied to enhance the combustion efficiency and hence the heat transfer performance of the flame jets. Swirl has been successfully adopted in the large-scale industrial combustors utilizing turbulent diffusion flame jets to extend the flame stability as well as to enhance the combustion efficiency. However, the application of swirl to the small-scale premixed gas-fired impinging flame jets under low Reynolds numbers has not yet been reported.

The present study is conducted to fill the gap by studying the flow and heat transfer characteristics of the premixed butane/air circular impinging flame jets with induced swirl. An essentially experimental approach has been adopted. Swirl is induced by balancing the axial flow and tangential flow of working fluids into the conical chamber of the burner, where the tangential flow is admitted into the burner through two symmetrical tangential inlets. The local heat flux distributions on the copper impingement plate under different operating conditions are measured and compared. The total heat flux received by the impingement plate is then obtained by integrating the local heat flux of the whole impingement area of the plate. The area-averaged heat flux can also be obtained by dividing the total heat flux by the whole impingement area under consideration.

The major operation parameters including Reynolds number of the air/fuel jet, Swirl number of the air/fuel jet, nozzle-to-plate distance and equivalence ratio of the air/fuel mixture are varied in the experiments, in order to examine their effects on the thermal performance of the swirling impinging flame jet. Butane gas is used as the gaseous fuel for the present investigation.

Two experimental setups, namely I and II, have been used to produce the swirling flame jets, in which different methods to mix and distribute the air and fuel streams into the burner are applied.

In the experiment setup I, the air and fuel streams are admitted into the burner via the tangential and axial inlets, respectively. Thus, ratio between the tangential flow / axial flow which determines the Swirl number is directly linked to the air/fuel ratio (i.e. equivalence ratio). For this particular setup, effects of the Swirl number and equivalence ratio can not be separately assessed but the swirl intensity obtained within the flame stability limit can be rather high. The method used together with the experimental setup I is also referred as the “Geometric Swirl Number Calculation Method” [55 and 56], in which the Swirl number is calculated directly from the tangential and axial flow rates.

In the experiment setup II, the air and fuel are premixed in a premixed chamber and the air/fuel mixture is divided into two separate streams, which are then supplied to the burner via the axial and tangential inlets. Each of these two streams is monitored and measured by a flow meter. The method applied with the experimental setup II can be called the "Smoke Flow Visualization Technique", in which the Swirl number is determined with the aid of the photographs obtained by applying the smoke flow visualization technique.

Experimental results obtained from both experimental setups I and II are discussed and compared with each other, as well as with the findings obtained form the previous work on non-swirling flame jets. Semi-analytical non-dimensional equations are developed with the aid of the present experimental results. These equations provide quick but accurate predictions of the convective heat transfer coefficient, both local and area-averaged, between the swirling impinging flame jet and the impingement plate. In addition, a better understanding of the impinging flame jet with swirl induced can be achieved by comparing the present findings with those obtained with similar impinging flame jets without swirl induced, which have been reported by previous researchers.

In this chapter, conclusions are drawn based on the present study, however, suggestions for possible future work on premixed gas-fired impinging flame jets with swirl induced are also provided.

9.1.1 Work performed with experimental setup I

Photographs of the impinging flame are taken by a digital camera. Effects of Reynolds number, nozzle-to-plate distance, Swirl number and equivalence ratio are examined. The following summaries can be drawn:

1) The flame shape of a swirling impinging flame jet shows a divergence at the flame tip, which is different from the typical conical Bunsen flame without swirl induced. Besides, flow pattern of the combustion gases is slightly changed due to the introduction of swirl.

2) The premixed circular impinging flame jets with swirl induced can produce a more uniform local heat flux distribution around the stagnation point of the impingement plate when compared with the non-swirling counterparts.

3) When Reynolds number is increased, the heat flux received by the impingement plate increases. On the one hand, the air and fuel supplies are increased. On the other hand, the local turbulence is enhanced. The heat flux distribution around the stagnation point is rather uniform and the occurrence of a central cool region at the stagnation point, which is usually obtained with the impinging flame jet without swirl induced, has been avoided.

4) The optimum nozzle-to-plate distance corresponding to the occurrence of a maximum area-averaged heat flux is obtained at H/d = 2.5 in swirling flame jet. The introduction of swirl has obviously reduced the axial component of the flame length which indicates a smaller nozzle-to-plate distance is already sufficient for the fully development of the flame.

5) When the equivalence ratio is increased, not only the air supply is insufficient for the combustion to become complete but the Swirl number is also decreased, which results in the impingement of larger amount of unburned fuel onto the impingement plate surface. The heat transfer rate around the stagnation point decreases, and the thermal characteristics of the flame becomes similar to that of the non-swirling impinging flame.

6) Comparing the present experimental findings with the heating performances of both circular and slot premixed impinging flame jets without swirl, it can be concluded that the swirling flame is able to produce a better heating effect around the stagnation point of the impingement plate. This also suggests the significance to investigate the feasibility in substituting the multiple-jet arrangement of the non-swirling impinging flame jets by swirling flame jets in many domestic and industrial applications.

9.1.2 Work performed with experiment setup II

Smoke flow visualization technique has been applied to aid the understanding of the flow and heat transfer characteristics of the swirling impinging flame in this experimental setup. Effects of the important parameters, including Reynolds number, nozzle-to-plate distance, Swirl number and equivalence ratio, on the local heat flux distribution along the radial direction of the impingement plate and the area-averaged heat flux receiving by the plate are examined. The following summaries can be drawn:

1) The divergence of the flame tip caused by the swirl has enlarged the flame's surface area there, so that the heat flux received by the impingement plate around its stagnation zone becomes more uniform.

2) The heat flux received by the whole impingement plate increases with the increasing Reynolds number, which agrees well with the findings of the studies on non-swirling impinging flame jets. It is noted that for the swirling flame, the area-averaged heat flux experiences a more rapid increase when Re is increased from 1200 to 1500. However, when Re is further increased to 1700, the area-averaged heat flux received by the impingement plate is slightly decreased instead. It may be due to the transition of the flow condition from laminar to transitional, perhaps, it brings an adverse effect to the thermal performance of the flame jet system. Thus, it suggests the importance to investigate the flammable limits of the swirling impinging flame jet.

3) The optimum nozzle-to-plate distance corresponding to the occurrence of a maximum impingement heat transfer is obtained between H/d = 2 and H/d = 2.5. It confirms the findings obtained from the experimental setup I that the mixing of air and fuel, and hence a more rapid combustion can be achieved by the introduction of swirl. It also shows that a better mixing of the air and fuel can be achieved by using the experimental setup II.

4) The central cool core occurs at the stagnation point of an impingement plate, which is the usual characteristics of a premixed gas-fired laminar impinging flame jet system can be avoided by applying a swirling flow.

5) Location of the maximum local heat flux shifts outwards away from the stagnation point as the induced swirl is increased because of the increasing centrifugal force, which brings the active gaseous species towards the wall-jet region. When the swirl intensity is increased, the heat transferred to the impingement plate is first increased because of a better mixing between the air and fuel but is decreased when the Swirl number is becoming too large. It may be attributed to the fact that transition of the flow condition from laminar to transitional is encouraged to take place earlier by the turbulence generating with the swirling flow.

6) The induced swirl enables more ambient air to be entrained into the combustion zone to facilitate a more complete combustion, so that even though the premixed mixture is slightly fuel-rich, the combustion can be more complete than that is occurred in the non-swirling impinging flame jet. When the swirling impinging flame jet is applied, the heating performance is enhanced when the supplied fuel is slightly rich. The flame length is also slightly prolonged when the equivalence ratio is increased, which enlarges the area to be impinged on the impingement plate. As a result, a better heating performance is obtained. It is a definite advantage for the domestic applications, which is usually operated under fuel-rich conditions.

7) Comparing the experimental results obtained from the present study and those from the previous work on non-swirling impinging flame jets shows that the use of swirl is able to enhance the mixing of air and fuel effectively, thus, to facilitate a more complete combustion. It is evident that the axial component of the flame length can be reduced. It is found that the premixed impinging flame jet with swirl induced is able to provide higher heat flux and more uniform heat flux distribution around the stagnation point of the impingement plate. However, it seems that a higher area-averaged heat flux can be obtained at the impingement plate by applying a much higher swirl number, which is associated with the generation of higher turbulence and can only be achieved by using the experimental setup I.

9.1.3 Development of non-dimensional correlations

Non-dimensional heat transfer coefficient, the Nusselt number, is correlated with the major non-dimensional parameters including Prandtl number, Reynolds number, equivalence ratio, nozzle-to-plate distance and Swirl number, by using the multiple regression method. A quick and accurate method is provided for the predictions of the maximum heat flux and the area-averaged heat flux received by the impingement plate from the circular premixed gas-fired impinging flame jet with swirl induced. The non-dimensional equations are developed with the aid of the experimental results obtained with the experimental setup II of the present study.

A better understanding of the swirling impinging flame jets can also be achieved by comparing the predictions with the analytical solutions of the non-swirling impinging flame jets provided by the previous researchers.

For the calculation of maximum local heat flux of the non-swirling impinging flame jet system:

$$Nu_{\max} \cdot \mathrm{Pr}^{-0.4} = 3.1267\,\mathrm{Re}^{0.2334}\,\phi^{0.9738}\left(\frac{H}{d}\right)^{-0.7544} S^{e},\left\{\begin{array}{l} 800 \le \mathrm{Re} \le 1500,\ e = 0.3108 \\ 1500 \le \mathrm{Re} \le 1700,\ e = -0.1097 \\ 1 \le \phi \le 1.4 \\ 2 \le \dfrac{H}{d} \le 5 \\ 0 \le \dfrac{r}{d} \le 3.5 \\ 0.075 \le S \le 0.171 \end{array}\right\}$$

For the prediction of area-averaged heat flux of the non-swirling impinging flame jet system:

$$\overline{Nu} \cdot \Pr^{-0.4} = 18.647 \,\mathrm{Re}^{0.1035} \phi^{1.164} \left(\frac{H}{d}\right)^{-0.3247} S^{e1}, \left\{ \begin{array}{l} 800 \le \mathrm{Re} \le 1500,\ e1 = 0.2307 \\ 1500 \le \mathrm{Re} \le 1700,\ e1 = -0.3078 \\ 1 \le \phi \le 1.4 \\ 2 \le \dfrac{H}{d} \le 5 \\ 0 \le \dfrac{r}{d} \le 3.5 \\ 0.075 \le S \le 0.171 \end{array} \right\}$$

9.2 RECOMMENDATIONS

The gaseous flow and heat transfer characteristics of the premixed gas-fired impinging flame jet with induced swirl have demonstrated to be very complicated. The situation should become far more difficult to analyze when combustion is also considered. The present experimental study has provided fundamental information about the heat transfer characteristics of a small-scale premixed impinging flame jet with swirl induced. With the aid of the results presented, future works in the following areas are suggested to carry out:

1) The velocity profile at the exit of the burner nozzle should be determined to provide sufficient information for the study of the flame properties and the heat

transfer mechanisms. The influence of introducing swirl to the impinging flame jet on the combustion process and the heat transfer characteristics can then be better understood.

2) It is found in the previous studies on turbulent diffusion flame with swirl induced that the flame stability and hence the flammable limits can be enhanced by the introduction of swirl. The range of flame stability for the small-scale premixed gas-fired swirling impinging flame jet operating under different operating conditions needs to be investigated.

3) Since the heat transfer performance of the swirling impinging flame jet appears to be better especially around the stagnation point region of the impingement plate, it is worth to look into the feasibility of substituting the multiple non-swirling impinging flame jets, which are commonly used in the domestic and industrial applications, by the swirling flame jets.

4) Emissions obtained after combustion should also be influenced by the introduction of swirl. Thus, measurement of the emitted gaseous products including CO, CO_2, NO_X, hydrocarbon and particulates, is necessary for a comprehensive understanding of the effects of inducing swirl to the impinging flame jet.

9.3 Contributions of Present Investigation

The present study creates valuable information and knowledge on the thermal and flow characteristics of the circular premixed butane/air impinging laminar flame jets with induced swirl. The effects of each of the major parameters on the thermal performance of the swirling impinging flame jets are explored, which have not been reported in the literature. These parameters are: Reynolds number of the air/fuel jet, Swirl number of the air/fuel jet, equivalence ratio of the air/fuel mixture and nozzle-to-plate distance.

The feasibility of introducing a swirl to small-scale, low-Reynolds-number and low-pressure thermal or combustion systems utilizing premixed gas-fired impinging flame jets is confirmed. Such finding provides a very good reference for further work on the topic of swirling impinging flame jets.

Development of the semi-analytical non-dimensional equations with the aid of the extensive experimental results enables more user-friendly and accurate quantitative prediction of the heat transfer at the flame and plate interface. The following equations provide reliable quantitative relationships between Nusselt number, Prandtl number, Reynolds number, Swirl number, equivalence ratio and nozzle-to-plate distance. The following equations are for the calculation of maximum Nusselt number and area-averaged Nusselt number, respectively:

$$Nu_{\max}\cdot \Pr^{-0.4} = 3.1267\,\mathrm{Re}^{0.233}\,\phi^{0.974}\left(\frac{H}{d}\right)^{-0.754} S^{e}, \left\{\begin{array}{l} 800 \le \mathrm{Re} \le 1500,\ e = 0.311 \\ 1500 \le \mathrm{Re} \le 1700,\ e = -0.11 \\ 1 \le \phi \le 1.4 \\ 2 \le \dfrac{H}{d} \le 5 \\ 0 \le \dfrac{r}{d} \le 3.5 \\ 0.075 \le S \le 0.171 \end{array}\right\}$$

$$\overline{Nu}\cdot \Pr^{-0.4} = 18.647\,\mathrm{Re}^{0.104}\,\phi^{1.164}\left(\frac{H}{d}\right)^{-0.325} S^{e1}, \left\{\begin{array}{l} 800 \le \mathrm{Re} \le 1500,\ e1 = 0.231 \\ 1500 \le \mathrm{Re} \le 1700,\ e1 = -0.308 \\ 1 \le \phi \le 1.4 \\ 2 \le \dfrac{H}{d} \le 5 \\ 0 \le \dfrac{r}{d} \le 3.5 \\ 0.075 \le S \le 0.171 \end{array}\right\}$$

As a conclusion, the present investigations have made very significant contributions in exploring the science of this problem. In addition, several publications have been emerged from the present findings.

REFERENCES

1. Kreith, F. and Sonju, O. K., The decay of a turbulent swirl in a pipe, J. Fluid Mech., 22: 257-271, 1965.

2. Chang, F. and Dhir, V. K., Mechanisms of heat transfer enhancement and slow decay of swirl in tubes using tangential injection, Int. J. Heat Fluid Flow, 16: 78-87, 1995.

3. Huang, B., Douglas, W. J. M. and Mujumdar, A. S., Heat transfer under a laminar, swirling impinging jet – a numerical study, Proceedings of the 6^{th} International Heat Transfer Conference, 5: 311-316, Washington, DC, 1978.

4. Tangirala, V., Chen, R. H. and Driscoll, J. F., Effect of heat release and swirl on the recirculation within swirl-stabilized flames, Combust. Sci. and Tech., 51: 75-95, 1987.

5. Feikema, D., Chen, R. H. and Driscoll, J. F., Enhancement of flame blowout limits by the use of swirl, Combust. Sci. and Tech., 80: 183-195, 1990.

6. Feikema, D., Chen, R. H. and Driscoll, J. F., Blowout of non-premixed flames: maximum coaxial air velocities achievable, with and without swirl, Combust. Sci. and Tech., 86: 347-358, 1991.

7. Huang, L. and El-genk, M. S., Heat transfer and flow visualization experiments of swirling, multi-channel, and conventional impinging jets, Int. J. Heat Mass Transfer, 44 (3): 583-600, 1998.

8. Baukal, C. E., Heat transfer from flames impinging normal to a plane surface, PhD Thesis, Univ. Penn, 1996.

9. Dong, L. L., Leung, C. W. and Cheung, C. S., Heat transfer from an impinging premixed butane/air slot flame jet, Int. J. Heat Mass Transfer, 45: 979-992, 2002.

10. Dong, L. L., Leung, C. W. and Cheung, C. S., Heat transfer and wall pressure characteristics of a twin premixed butane/air flame jets, Int. J. Heat Mass Transfer, 47: 489-500, 2004

11. Dong, L. L., Leung, C. W. and Cheung, C. S., Heat transfer of a row of three butane/air flame jets impinging on a flat plate, Int. J. Heat Mass Transfer, 46: 113-125, 2003.

12. Dong, L. L., Leung, C. W. and Cheung, C. S., Heat transfer characteristics of premixed butane/air flame jet impinging on an inclined flat surface, Heat and Mass Transfer, 39: 19-26, 2002.

13. Masri, A. R., Kalt, P. A. M. and Barlow, R. S., The compositional structure of swirl-stabilized turbulent non-premixed flames, Combust. Flame, 137: 1-37, 2004.

14. Kwok, L. C., Leung, C. W. and Cheung, C. S., Heat transfer characteristics of slot and round premixed impinging flame jets, Experimental Heat Transfer, 16: 111-137, 2003.

15. Zhao, Q. W., Chan, C. K., and Zhao, H. F., Numerical simulation of open swirl-stabilized premixed combustion, Fuel, 83: 1615-1623, 2004.

16. Yilmaz, M., Comakli, O., Yapiei, S. and Sara, N., Heat transfer and friction characteristics in decaying swirl flow generated by different radial guide vane swirl generators, Energy Conv. Manag. 44: 283-300, 2003.

17. Viskanta, R., Convective and radiative flame jet impingement heat transfer, The 9th International Symposium on Transport Phenomena in Thermal-Fluids Engineering, 46-60, 1996.

18. Milson, A. and Chiger, N. A., Studies of methane and methane-air flames impinging on a cold plate, Combust. Flame, 21: 295-305, 1973.

19. Milson, A., Impinging jet flames, PhD Thesis, Univ. Sheffield, 1972.

20. Fairweather, M., Kiham, J. K. and Nawaz, S., Stagnation point heat transfer from laminar high temperature methane flames, Int. J. Heat Fluid Flow, 5: 21-27, 1984.

21. Hustad, J. E. and Sonju, O. K., Heat transfer to pipes submerged in turbulent jet diffusion flames, Heat Transfer in Radiating and Combusting Systems, Proceedings: 474-490, Oct. 1990.

22. Viskanta, R., Heat transfer to impinging isothermal gas and flame jets, Exper. Therm. Fluid Sci., 6: 111-134, 1993.

23. Fells, I. and Harber, J. H., An investigation into heat transfer from unseeded propane-air flames augmented with D.C. electrical power, Combust. Flame, 12 (6): 587-596, 1968.

24. Baukal, C. E., and Gebhart, B., A review of flame impingement heat transfer studies – Part 1: Experimental conditions, Combust. Sci. Tech., 104: 339-357, 1995.

25. Giedt, W. H., Cobb, L. L. and Russ, E. J., Effect of hydrogen recombination on turbulent flow heat transfer, ASME Paper-60-WA-256, New York, 1996.

26. Baukal, C. E. and Gebhart, B., Surface condition effects on flame impingement heat transfer, Exper. Therm. Fluid Sci., 15: 323-335, 1997.

27. Rigby, J. R. and Webb, B. W., An experimental investigation of diffusion flame jet impingement heat transfer, Proceedings of the ASME/JSME Thermal Engineering Joint Conference, 3: 117-126, 1995.

28. Dhir, V. K. and Chang, F., Heat transfer enhancement using tangential injection, ASHRAE Trans., 98: 383-390, 1992.

29. Razgaitis, R. and Holman, J. P., A survey of heat transfer in confined swirl flows, Heat Mass Trans. Proceed. 2: 831-866, 1976.

30. Shuja, S. Z., Yilbas, B. S. and Rashid, M., Confined swirling jet impingement onto an adiabatic wall, Int. J. Heat Mass Transfer, 46: 2947-2955, 2003.

31. Owsenek, B. L., Cziesla, T., Mitra, N. K. and Biswas, G., Numerical investigation of heat transfer in impinging axial and radial jets with superimposed swirl, Int. J. Heat Mass Transfer, 40 (1): 141-147, 1997.

32. Van der Meer, T. H., Stagnation point heat transfer from turbulent low Reynolds number jets and flame jets, Exper. Therm. Fluid Sci., 4: 115-126, 1991.

33. Kilham, J. K. and Purvis, M. R. I., Heat transfer from hydrocarbon-oxygen flames, Combust. Flame, 16: 47-54, 1971.

34. Conolly, R. and Davies, R. M., A study of convective heat transfer from flames, Int. J. Heat Mass Transfer, 15: 2155-2172, 1972.

35. Hargrave, G. K. and Kilham, J. K., The effect of turbulence intensity on convective heat transfer from premixed methane-air flames, Institution of Chemical Engineering Symposium Series, 2: 1025-1034, 1984.

36. Sibulkin, M., Heat transfer near the forward stagnation point at a body of revolution, J. Aero. Sci., 19: 570-571, 1952.

37. Baukal, C. E. and Gebhart, B., A review of semi-analytical solutions for flame impingement heat transfer, Int. J. Heat Mass Transfer, 39 (14): 2989-3002, 1996.

38. Fay, J. A. and Riddell, F. R., Theory of stagnation point heat transfer in dissociated air, J. Aero. Sci., 25: 73-85, 1958.

39. Rosner, D. E., Convective heat transfer with chemical reaction, Aeron. Res. Lab. Rept. ARL 99, Part 1, AD269816, 1961.

40. Baukal, C. E. and Gebhart, B., A review of flame impingement heat transfer studies – Part 2: Experimental conditions, Combust. Sci. Tech., 104: 359-385, 1995.

41. Dong, L. L., Studies of single and multiple impinging hydrocarbon flame jets, PhD Thesis, The Hong Kong Polytechnic University, 2002.

42. Buhr, E., Haupt, G. and Kremer, H., Heat transfer from impinging turbulent jet flames to plane surfaces, Combustion Institute European Symposium 1973, Academic Press, New York, 607-612, 1973.

43. Kremer, H., Buhr, E. and Haupt, R., Heat transfer from turbulent free-jet flames to plane surfaces, Heat Transfer in Flames, Washington, DC: Scripta Book Co., 463-472, 1974.

44. Bradley, D. and Matthews, K. J., Measurement of high gas temperatures with fine wire thermocouples, J. Mech. Engr. Sci., 10: 299-305, 1968.

45. Coghe, A., Solero, G. and Scribano, G., Recirculation phenomena in a natural gas swirl combustor, Exper. Therm. Fluid Sci., 28: 709-714, 2004.

46. Khezzar, L., Velocity measurements in the near field of a radial swirler, Exper. Therm. Fluid Sci., 16: 230-236, 1998.

47. Syred, N. and Beer, J. M., Combustion in swirling flows: a review, Combust. Flame, 23: 143-201, 1974.

48. Guillaume, D. W. and La Rue, J. C., Combustion enhancement using induced swirl, Exper. in Fluids, 20: 59-60, 1995.

49. Chan, C. K., Lau, K. S. and Chin, W. K., Freely propagating open premixed turbulent flames stabilized by swirl, 24th International Symposium on Combustion, Pittsburgh, 511-518, 1992.

50. Noui-Mehidi, M. N., Salem, A., Legentilhomme, P. and Legrand, J., Apex angle effects on the swirling flow between cones induced by means of a tangential inlet, Int. J. Heat Fluid Flow, 20: 405-413, 1999.

51. Baukal, C.E. and Gebhart, B., Heat transfer from oxygen-enhance/natural gas flames impinging normal to a plane surface, Int. J. Heat Mass Transfer, 40: 2539-2547, 1998.

52. Kilham, J. K., Energy transfer from flame gases to solids, Gas Research Board Community, No. GRB 47: 733-740, 1949.

53. Zhao, Z., Wong, T. T. and Leung, C. W., Impinging pre-mixed butane/air circular laminar flame jet – influence of impingement plate on heat transfer characteristics, Int. J. Heat Mass Transfer, 47: 5021-5031, 2004.

54. Katoka, K., Optimal nozzle-to-plate spacing for convective heat transfer in nonisothermal, variable-density impinging jets, Drying Technology, 3: 235-254, 1985.

55. Hargrave, G. K., Fairweather, M. and Kilham, J. K., Forced convective heat transfer from premixed flames-part 1: flame structure, Int. J. Heat Fluid Flow, 8: 55-63, 1987.

56. Beer, J.M. and Chigier, N.A., Impinging jet flames, Combust. Flame, 12(6): 575-586, 1968.

57. Kwok, L. C., Studies of the premixed butane/air impinging flame jets, MPhil Thesis, The Hong Kong Polytechnic University, 2004

58. Hoogendoorn, C. J., The effect of turbulence on heat transfer at a stagnation point, Int. J. Heat Mass Transfer, 20: 1333-1338, 1977.

59. Claypore, T. C. and Syred, N., Effect of swirl burner aerodynamics on NO_X formation, 18th International Symposium on Combustion, Pittsburgh, 81-89, 1981.

60. Ikoku, C. U., Natural Gas Production Engineering, New York: Wiley, 1984.

61. Kline, S. J. and McClintock, F. A., Describing uncertainties in single sample experiments, Mech. Eng., 75: 3-8, 1953.

62. Zhang, D. and Hill, P. G., Effect of swirl on combustion in a short cylindrical chamber, Combust. Flame, 106: 318-332, 1996.